NASA-CR-193085

LOW BANDWIDTH ROBUST CONTROLLERS FOR FLIGHT
NASA Grant NCC 2-711

June 1991 - December 1992

Final Report

by

Dr. Daniel J. Biezad
Principal Investigator
(805) 756-5126

and

Hwei-Lan Chou
Graduate Student

Aeronautical Engineering Department
California Polytechnic State University
San Luis Obispo, CA 93407

presented to

Mr. Glenn Gilyard
NASA Technical Officer
(805) 258-3724

May 1993

Propulsion and Performance Branch, D-2112
XRP PO 273, NASA Dryden
Edwards, CA 93523

Table of Contents

List of Figures

List of Tables

PREFACE

The statements and conclusions of this report are those of the authors and not necessarily those of the California Polytechnic State University, San Luis Obispo. The evaluations described in this document are based solely on the results of tests conducted by the authors during this project.

This report does not constitute a standard, regulation or specification. The mention of commerical products, their source, or their use in connection with materials reported herein is not to be construed as either an actual or implied endorsement of such products.

ACKNOWLEDGEMENTS

The authors gratefully acknowledge the sponsored research by NASA, and in particular acknowledge and thank Mr. Glenn Gilyard and Mr. Bill Burcham for their technical support, guidance, and encouragement throughout this project.

The material in this report was prepared and written by Professor Daniel Biezad and Graduate Student Hwei-Lan Chou; and edited by ARDFA Program Assistant Sue Dotson.

SYNOPSIS

This final report for NASA Grant NCC 2-711 cover reporting period June 1992 through December 1992. The report analyzes the longitudinal and lateral flying qualities of Propulsive-Only Flight Control (POFC) for a Boeing 720 aircraft model. Using Quantitative Feedback Theory (QFT), performance results from compensators are documented and analyzed. This report is also the first draft of a graduate thesis to be presented by Hwei-Lan Chou. The final thesis document will be presented to NASA when completed later this year.

The latest landing metrics, related to bandwidth criteria and based on the Neal-Smith approach to flying qualities prediction, were used in developing the performance criteria for the controllers. The compensator designs were tested on the NASA simulator and exhibited adequate performance for piloted flight. There was no significant impact of QFT on the performance of POFC in either the longitudinal or lateral modes of flight. This was attributed to the physical limits of thrust available and the engine rate of response, both of which severely limited the available bandwidth of the closed-loop system.

Abstract

Through throttle manipulations, engine thrust can be used for emergency flight control for multi-engine aircraft. Previous study by NASA Dryden has shown the use of throttles for emergency flight control to be very difficult. In general, manual fly-by-throttle is extremely difficult - with landing almost impossible, but control augmentation makes runway landings feasible. Flight path control using throttles-only to achieve safe emergency landing for a large jet transport airplane, Boeing 720, was investigated using Quantitative Feedback Theory (QFT). Results were compared to an augmented control developed in a previous simulation study. The control augmentation corrected the unsatisfactory open-loop characteristics by increasing system bandwidth and damping, but increasing the control bandwidth substantially proved very difficult. The augmented pitch control is robust under no or moderate turbulence. The augmented roll control is sensitive to configuration changes.

1. Introduction

Through throttle manipulations, engine thrust was found useful in providing some controllability for multi-engine aircraft in emergency situations with severe or complete flight control system failures (such as hydraulic system failures). Aircraft flight control systems are extremely reliable. Current generation aircraft utilize multiple and independent control surfaces, hydraulics, sensors, control computers, and control cables to achieve a high level of control system redundancy and reliability. Although rare, severe flight control system failures do occur.

NASA Dryden has studied the use of throttles for emergency flight control for a range of airplanes[1-5]. Many multi-engine airplanes exhibited some degree of useful control capability with the throttles. In general, flying an aircraft in manual mode using throttles-only requires a tremendous pilot workload and landing is considered extremely difficult to almost impossible. Control augmentation, using feedbacks and direct coupling of the throttle command to stick/thumbwheel motion, has greatly improved flying qualities, and ground simulation landings can be achieved.

The primary aim of this current study on Throttles-Only Flight Control (**TOFC**) is to develop an augmented flight path control using throttles-only to achieve safe emergency landings. Application of TOFC on a large four-engine jet transport airplane, Boeing 720 (**B-720**) (Figure 1), is investigated. An augmented B-720 TOFC, developed and implemented on a high fidelity B-720 flight simulator (Figure 2) by NASA Dryden[2], had obtained good pilot rating by increasing the control bandwidth and the phugoid and Dutch-roll damping[2].

This report presents an alternative control design technique based on Quantitative Feedback Theory (QFT) to further improve the Dutch-roll damping and to increase the control bandwidth for better handling qualities. The control design uses a linearized B-720 model derived from perturbations of the full non-linear equations of motion about trim at an approach and landing flight condition.

A robust controller is highly desirable for systems with plant parameter uncertainty (such as an aircraft undergoing configuration changes). The QFT technique[6-9] was chosen because it allowed designers to specify a desired close-loop response and a performance specification, and then built a controller to meet the specification. Most of all, the technique can incorporate plant parameter uncertainty and plant disturbances into the control system design by converting them into design constraints and then design a controller to have the system satisfy the imposed constraints. The controller thus designed guarantees robust performance over full range of the plant uncertainty while keeping the disturbance effect to the system minimum.

The desired performance specification may not always be achieved within the given control actuation and rate limits. However, the transparency of the QFT technique throughout the design process preserves many of the insights which are lost

in several of the modern control techniques and thus provides control designers with valuable information about the system under investigation. QFT also provides a quantitative relationship between the amount of uncertainty and feedback (i.e. the magnitude of feedback is determined in proportion to the amount of uncertainty, therefore, reduces the possibility of overdesign).

In this report, the strategy of flight control using throttles-only is introduced. The fidelity of the linear B-720 model is examined. An overview of QFT with step-by-step procedures is provided, and its application on the design of an augmented flight path control using throttles-only for approach and landing of B-720 is presented in a summary fashion. Control design results using QFT are compared to the augmented control developed in a previous simulation study.

Nomenclature, Abbreviations, and Acronyms

(a)	short form of (s+a)
c.g.	center of gravity
$C_{\ell\beta}$	non dimensional yaw-roll coupling derivative
C_{mu}	non dimensional velocity-pitch coupling derivative
D.R.	Dutch-roll
G_{in}^{out}	transfer functions
K_q	pitch rate feedback gain
K_γ	flight path angle feedback gain
K_β	sideslip angle feedback gain
K_ϕ	bank angle feedback gain
q	pitch rate (deg/sec)
QFT	Quantitative Feedback Theory
s.p.	short period
TOFC	Throttle-Only Flight Control
z	thrust (lbs)
δ	engine rpm
δ_{Tc}	stick input (full deflection=1 unit)
γ	flight path angle (deg)
θ	pitch angle (deg)
β	angle of sideslip (deg)
φ	bank angle (deg)
ω_i	natural frequency
ζ	damping ratio
[ζ, w_n]	short form for $s^2 + 2\zeta\omega_n s + \omega_n^2$

2. Strategy of Throttles-Only Flight Control

The propulsion system of a multi-engine aircraft can be used for heading and flight path control. Differential throttles is applied to control roll through yaw, and symmetric throttles is applied to control pitch. Speed control by throttles becomes ineffective when control systems fail. Other means may be used to change the airplane speed as described in below. Throttles are coupled to stick/thumbwheel for easier and more conventional control handling.

2.1 Pitch Control

Symmetric throttles induces a phugoid mode and a speed change, which in turn generates a pitching moment change through speed stability effects-C_{mu}. This is the primary source of pitch control. Pitch control may also be generated by other factors such as pitching moment change due to thrust line offset, flight path angle change due to the vertical component of thrust, and an instant pitching moment change generated by engines mounted at different vertical levels, as in the case of B-720.

2.2 Yaw-Roll Control

Differential thrust generates sideslip, which in turn generates rolling moment changes through wing dihedral and sweep effect-C_{l_β}. Roll is controlled by applying differential throttles to achieve the desired bank angle and thus to make turns and heading changes.

2.3 Speed Control

Retrimming speed by the use of throttles becomes ineffective when primary control surfaces are locked due to control systems failure. When control system failure occurs at speeds other than landing speed, retrimming to an acceptable landing speed may be accomplished by using other techniques such as lowering flaps (assuming the electrically controlled flaps are operative), extending landing gears, moving cg. aft, varying stabilizer deflection, or varying the speed between the low and high mounted engines.

2.4 Couple Throttle Command to Stick/Thumbwheel Motion

Direct coupling of the throttle command to stick/thumbwheel motion has eased the pilot's handling of control. The airplane can be controlled in a conventional fashion, such as pitch up with stick forward or pitch down with stick aft.

3. B-720 Linear Model

The B-720 linear model is derived from perturbations of the full nonlinear equation of motion about trim and is completely decoupled in longitudinal and lateral dynamics. All control states and inputs are perturbed independently at the steady state of a desired trim condition. The inputs are thrust from each engine. There are four configurations given for the study of approach and landing of B-720 TOFC. The state-space representation of the linear model of these configurations are listed in Appendix A. Of the four configurations shown, configuration 1 is the nominal configuration for baseline design.

The fidelity of the linear model was examined by comparing the open-loop response of the linear model with the nonlinear model as shown in Figures 3 and 4. The longitudinal response of the linear model was about 30% less in magnitude than the nonlinear model, and was, therefore, modified by a correction factor of 1.3 (Figure 3). The longitudinal linear model after modification closely portraits the longitudinal nonlinear model (Figure 5). Linear design analysis utilized a computer control package "Program CC" to assist the design[10].

The lateral response depicted in Figure 4 shows that the linear model would closely follow the nonlinear model as long as the small perturbation assumption is not violated, i.e. the command input should be of a small magnitude and a short duration. Figures 3 and 4 also illustrate that for the nonlinear model, a flight path angle command would induce little coupling in roll/yaw, while a bank angle command would induce pronounced pitch coupling. Coupling between longitudinal and lateral modes is completely absent for the linear model.

4. Engines and Bare Airframe System Analysis

4.1 Engines

Spool-up and spool-down engine dynamics for the B-720 engine are shown in Figure 6a[12]. The empirical transfer function developed is given in short form notation by

$$G^{Z(lbs)}_{\delta_{Tc(\%)}} = \frac{275}{(.55)(5)}$$

This equation is illustrated in Figure 6b over low frequency ranges up to 1.0 rad/sec.

4.2 Bare Airframe

It is apparent from the engine Bode diagram in Figure 6b illustrates that severe bandwidth attenuation would occur beyond frequencies of 1 rad/sec. Therefore, it may not be possible to increase the closed-loop bandwidth beyond 1 rad/sec within the range of available thrust. This can be seen in the pitch rate "q" to thrust "z" transfer function, $G_{\delta_{Tc(\%)}}^{q(deg/sec)}$ (refer to Appendix A), of the bare airframe shown in Figure 7. The full-order transfer function $G_{\delta_{Tc(\%)}}^{q(deg/sec)}$ shows that 80 dB of gain must be added to yield a crossover frequency beyond 1 rad/sec. This corresponds to 10,000 lbs of full thrust from each engine, which is not practical for approach and landing.

A low order fit to $G_{\delta_{Tc(\%)}}^{q(deg/sec)}$ is also depicted in Figure 7 and is very accurate near the phugoid frequency. Piloted flight of the unaugmented aircraft was consistently a level 3 [2]. The main difficulties were the lightly damped phugoid and the low bandwidth throttle control.

The accuracy of the low order fit near the phugoid frequency means that, to a first order approximation[12], the phugoid frequency and damping are found from the following equation:

$$2\zeta\omega_n = -X_u + \frac{M_u(X_\alpha - g)}{M_\alpha}$$

$$\omega_n^2 = \frac{-g(Z_u - \frac{M_u}{M_\alpha}Z_\alpha)}{U_o}$$

Conventional transport aircraft can be shown to be roughly proportional to M_u.

It should be strongly noted here for the classic case of M_u=0 and for negative values of M_u (Mach tuck) that the aircraft cannot be practically flown with throttle alone unless rotational control in pitch is added and difficulties will also be encountered as M_α becomes small (aft c.g. location). Both of these cases require the addition of an effective rotational controller about the pitch axis. This may be achieved by using differential inboard and outboard thrust, provided the inboard engines are a different distance from the aircraft xy-plane than the outboard engines. These configuration characteristics determine the innate capability for throttles-only piloted control.

5. Overview of Quantitative Feedback Theory

QFT is a frequency domain control technique that uses a fairly straightforward and transparent design approach[6-9]. To apply QFT, systems are usually modeled in a unit feedback form (Figure 8) where all blocks may present scalar (SISO) or matrix (MIMO) system transfer functions. For MIMO systems, a m x m MIMO system can be converted into a m^2 - equivalent multi-input single-output (MISO) loops (Figure 9). QFT techniques allow designers to specify a desired performance specification with performance tolerance and then incorporate the tolerance with the plant uncertainty and system disturbances to form the design constraints: the performance bounds and the U contour (Figures 10, 11 and 12).

The design constraints are then placed on a Nichols Chart together with the nominal plant transfer function, P_o. A controller will be selected to reshape P_o to form L_o (the nominal open-loop transfer function) as to have L_o satisfying all the design constraints of performance bounds and U contour (Figure 13). By having L_o satisfy all the design constraints, if possible within the given control actuation and rate limits, the system is guaranteed robust over the full range of plant uncertainty. However, the system may not completely meet the performance specification (Figure 14). A prefilter is usually required to further reshape the system to fully meet the specification. The prefilter design is implemented on a Bode plot.

The basic design procedures of the QFT technique for minimum phase systems are accomplished by the following four steps:

1) Model the system in a unit feedback form to apply QFT. A m x m MIMO system can be converted into a m^2-equivalent MISO system and the coupling between loops can be considered disturbance input (Figures 8 and 9).

2) Specify the desired close-loop frequency response performance specification. Figure 10 shows the construction of a desired close-loop performance specification with an upper bound, B_u; a lower bound, B_L; a tolerance, δ_R; and a maximum peak magnitude, M_m.

   The tolerance, δ_R, is specified to obtain robust performance, and the maximum M_m is specified to obtain a desired system damping. The upper bound is generally synthesized by an underdamped second order close-loop transfer function (T.F.), $T_u(s)$ and the lower bound by an overdamped close-loop T.F., $T_L(s)$ with figures of merit such as settling time, rise time, peak overshoot or damping ratio, and natural frequency, etc.

   A desired disturbance performance specification (Figure 11) needs only an upper bound to confine the disturbances. The objective of the technique is to design a controller such that the variation of the response due to plant uncertainty lies within the specified boundaries and the effect of disturbance is minimized, that is to have:

$$B_L(\omega) \le |T_R(j\omega)| \le B_U(\omega)$$

$$|T_{D1}(j\omega)| \le |M_D(j\omega)|$$

$$|T_{D2}(j\omega)| \le |M_D(j\omega)|$$

3) Convert the performance tolerance, δ_R, and the maximum M_m, onto Nichols Chart to form the design constraints: the performance bounds, $B_o(j\omega_i)$, and the U contour.

   i) Performance bounds are curves on the Nichols Chart that are determined by matching the magnitude of the range of plant uncertainty with the magnitude of the performance tolerance, δ_R. Therefore, satisfying this constraint guarantees the variation of the system response due to plant uncertainties will be no greater than δ_R. There is a performance bound for each frequency.

   ii) On the Nichols Chart, the U contour is a M-circle that has the magnitude of M_m, with part of the circle stretched for uncertainty at high frequencies (same as the length V shown in Figure 12). By having the open-loop response not penetrating the U contour, the system's damping will be guaranteed no less than the damping correlating to M_m. The construction of a U contour is shown in Figure 12.

4) Reshape the nominal plant transfer function, P_o. Gain/pole/zero compensation may be placed on P_o to reshape it to satisfy the design constraints. After reshaping, P_o becomes L_o, and the compensation chosen forms the controller, G_c, as can be depicted from the relationship:

$$L_o = P_o * G_c$$

   To satisfy the design constraints, L_o should not penetrate the U contour, while each frequency ω_i on L_o should be kept on and above its corresponding $B_o(j\omega_i)$. The U contour , the performance bounds and the optimal L_o of an example problem are shown in Figure 13.

5) After reshaping, the system is guaranteed robust over the full range of plant uncertainty, i.e. $\delta_T(jw_i) \le \delta_R(jw_i)$ (Figure 14). However, the system may not have met the performance specifications completely. A prefilter is usually required to further reshape the system to fully meet the specification.

6. Quantitative Feedback Theory Control Design

A QFT computer control package was used to assist the QFT design[8]. The program is to be used for minimum-phase plants only, i.e., the plants should have no zeros in the right half s-plane, therefore, only the gain curve of the desired performance will be specified and satisfied. For nonminimum-phase plant, the phase of the desired close-loop performance shall also be specified and satisfied.

6.1 System Modeling

The block diagrams of flight-path-angle control and bank-angle control are presented in Figures 15 and 16. The inner pitch-rate (q) loop and sideslip-angle (β) loop were first closed with $G_{e_\phi}^{\delta_{T_c}}=1$, $K_q=60$ and $G_{e_\beta}^{\delta_{T_c}}=10$, $K_\beta=4$, respectively, which were the heuristic settings chosen by investigating the properties of the inner loop. Tables 1 and 2 summarize the investigation:

Table 1. Investigation of Longitudinal Feedback Parameter

Feedback Parameter	Phugoid Mode	
	ζ	ω_n
q	Increase (Require high gain)	No change
γ	No change	Increase

Table 2. Investigation of Lateral Feedback Parameter

Feedback Parameter	Lateral Phugoid		Dutch Roll	
	ζ	ω_n	ζ	ω_n
p	Increase	Increase	Decrease	No change
r	Small increase	No change	Small increase	No change
β	Small decrease	Small increase	Increase	No change
φ	Increase	Increase	Small increase	No change

To apply QFT, with the inner loop closed, the outer loops are rearranged in a unit feedback form as shown in Figures 17 and 18.

6.2 Performance Specification

To obtain good handling qualities, the close-loop response for each of the γ- and φ- loops, which are also the pilot control open-loops, should have the following characteristics:

1) A bandwidth, $\omega_{\omega B}$, ~ 2 rad/sec for landing of a transport aircraft[11].

2) A k/s gain curve slope (-20 dB/decade) around the crossover frequency, ω_c[12].

A desired close-loop specification was synthesized based upon these two requirements, and is shown in Figure 19, which has a k/s slope near $\omega_c \sim 1.5$ rad/sec (with $\omega_{\omega B} \sim 2$ rad/sec) and a corner frequency, $\omega_{corner} \sim 0.8$ rad/sec.

The desired close-loop specification is synthesized in the following four steps:

1) Synthesize the initial B_U and B_L. B_U is usually modeled by an underdamped simple second order close-loop T.F.,

$$T_u(s)=\frac{\varpi_n^2}{s^2+2\varsigma\varpi_n s+\varpi_n^2},$$

while B_L modeled by an overdamped simple second order close-loop T.F.,

$$T_L(s)=\frac{k}{(s+\sigma_1)(s+\sigma_2)}, \text{ where} \sigma_1 \text{ and } \sigma_2 \le \varpi_n.$$

With a desired performance specification of $\varsigma=.6$ and $\varpi_n=.8$ rad/sec, this yields:

$$T_u(s)=\frac{.64(s+1)}{s^2+.96s+.64} \text{ and } T_L(s)=\frac{.385}{(s+.55)(s+.7)}$$

2) Add a pole to $T_L(s)$ to widen the δ_R at high frequencies. This yields:

$$T_L(s)=\frac{.77}{(s+.55)(s+.7)(s+2)}$$

This is required by the Bode derived theorem which states that $\int_0^\infty L_m S_p^T d\varpi = 0$,

i.e. the reduction in sensitivity S_p^T at the lower frequencies must be compensated by an increase in sensitivity at the higher frequencies.

3) Add a zero at 1 rad/sec to increase the gain slope from -40 dB/decade to -20 dB/decade. This yields:

$$T_u(s) = \frac{.64(s+1)}{s^2+.96s+.64} \quad \text{and} \quad T_L(s) = \frac{.77(s+1)}{(s+.55)(s+.7)(s+2)}$$

4) Raise the whole synthesized gain curve until a $\omega_{\omega B}$ ≈ 2 rad/sec is obtained.

The magnitude of B_U, B_L and δ_R at each frequency can thus be obtained and are shown in Table 3.

Table 3. QFT performance specification

Frequency(rad/sec)	0.1	0.3	0.5	0.7	1.0	2.0	5.0
Bu(dB)	17.0	17.0	17.3	16.0	13.0	2.0	-13.0
BL(dB)	16.8	15.0	12.3	9.9	4.6	-7.1	-23.0
δ_R (dB)	0.2	2	5	6.1	8.4	9.1	15.0

6.3 Airplane Parameter Uncertainty

Four configurations are provided for the study of approach and landing of B-720 throttles-only flight control. The flight condition of these configurations are summarized in Table 4. Configuration 1 is the nominal configuration for baseline design.

Table 4. Flight Configurations for B-720 Approach and Landing

Config. Number	Weight (lbs)	Altitude (Ft MSL)	Airspeed (Knots)	Flaps (%)	Gear up/down
1	140,000	4,000	160	0	up
2	140,000	4,000	145	30	up
3	160,000	4,000	175	0	up
4	140,000	4,000	155	30	up

A plant transfer function with parameter uncertainty is usually described in a maximum and minimum format in order to form the plant uncertainty template, which will then be used to determine the performance bounds constraint. An example of a plant with parameter uncertainty described in a maximum and minimum format is shown below:

Example

For a plant transfer function

$G(s) = \frac{Ka}{(s+a)}$, where the parameter variations are: $1 < k < 10$ and $1 < a < 10$

then,

$G(s)$ min. $= \frac{1}{s+1}$ and $G(s)$ max. $= \frac{100}{s+100}$

For γ- and φ- feedback loops, the minimum and maximum values of the transfer functions $G^{\gamma}_{\theta_{in}}$ and $G^{\phi}_{\beta_{in}}$, determined from the four given configurations, are shown below:

For γ-feedback loop:

The $G^{\gamma(deg)}_{\theta_{in}(deg)}$ of the nominal configuration(config. 1) is:

$$G^{\gamma(deg)}_{\theta_{in}(deg)} \text{ config. } 1 = \frac{.01(.203)[.37,\ 3.01]}{(.562)[.624,\ .111][.441,\ 1.57](5.25)}$$

and the min. and max. $G^{\gamma(deg)}_{\theta_{in}(deg)}$ are:

$$G^{\gamma(deg)}_{\theta_{in}(deg)} \text{ min.} = \frac{.0053\ (.162)[.35\ ,\ 3.01]}{(.40)[.42\ ,\ 1.48][.66\ ,\ .01](5.19)}$$

$$G^{\gamma(deg)}_{\theta_{in}(deg)} \text{ max.} = \frac{.01\ \ (.28)[.46,\ 3.43]}{(.58)[.45\ ,\ 1.57][.92\ ,\ .14](5.24)}$$

For φ- feedback loop:

The $G^{\phi(deg)}_{\beta_{in}(deg)}$ of the nominal configuration(config. 1) is:

$$G^{\phi(deg)}_{\beta_{in}(deg)}\ \text{nominal} = \frac{.09\,[.47\ ,\ 3.65]}{(.98)\,[.81\ ,\ .15]\,[.26\ ,\ 1.07]\,(5.02)}$$

and the min. and max. of $G^{\phi(deg)}_{\beta_{in}(deg)}$ are:

$$G^{\phi(deg)}_{\beta_{in}(deg)}\ \text{min.} = \frac{.06\,[.45\ ,\ 3.65]}{(.98)\,[.60\ ,\ .15]\,[.24\ ,\ .93]\,(5.01)}$$

$$G^{\phi(deg)}_{\beta_{in}(deg)}\ \text{max.} = \frac{.09\,[.61\ ,\ 4.33]}{(1.03)\,[1.0\ ,\ .20]\,[.29\ ,\ 1.09]\,(5.02)}$$

The QFT control package, used to assist the design, allows the designer to input plant parameter variations by entering the transfer function's maximum and minimum values for gain, first order poles and zeros, and second order poles and zeros. The program forms the plant uncertainty template with the given maximum and minimum values, then uses its CAD capability to graphically determine the performance bounds required for the design. There are tradeoffs between plant parameter uncertainty and system performances. The wider the spread of the parameter uncertainty, the more restricted the constraints; consequently more compensation is required. Therefore, the performance specification may need to be relaxed when there is not enough control power to provide all the compensation that is required.

6.4 Controller and Prefilter Design

Pole/zero/gain compensation may be required to reshape the plant transfer functions of the γ- and φ- feedback loops, $G^{\gamma}_{\theta_{in}}$ and $G^{\phi}_{\beta_{in}}$, and to satisfy performance bounds and U contour constraints. On a Nichols Chart, adding a gain will raise the transfer function curve, while a zero will bend the curve to the right, and a pole will bend the curve to the left. The compensation chosen forms the controller, G_c. After reshaping $G^{\gamma}_{\theta_{in}}$ and $G^{\phi}_{\beta_{in}}$ become, respectively, $L^{\gamma}_{e\gamma}$ and $L^{\phi}_{e\phi}$ (the open-loop transfer functions of the γ– and φ–loops), where $L^{\gamma}_{e\gamma} = G^{\theta_{in}}_{e\gamma} * G^{\gamma}_{\theta_{in}}$ and $L^{\phi}_{e\phi} = G^{\beta_{in}}_{e\phi} * G^{\phi}_{\beta_{in}}$. Each frequency ω_i on $L^{\gamma}_{e\gamma}$ and $L^{\phi}_{e\phi}$ should be placed on and above its corresponding performance bounds, $B_o(j\omega_i)$, to assure robust performance. In addition, $L^{\gamma}_{e\gamma}$ and $L^{\phi}_{e\phi}$ must not penetrate the U contour in order to obtain the desired damping.

Longitudinal Flight-Path-Angle Control: Transfer function $G^{\gamma}_{\theta_{in}}$ and its performance bounds, $B_o(j\omega_i)$, and U contour are displayed on a Nichols Chart in Figure 21. All frequency points on $G^{\gamma}_{\theta_{in}}$ are below their corresponding $B_o(j\omega_i)$, hence reshaping is

required (Figure 21). A pure gain compensator, $G_c = G_\gamma^{\theta_{in}} = 16$, raises the curve to just touching the U contour (Figure 22). Several lead compensators were tried to further reshape the $G_{\theta_{in}}^{\gamma}$ to satisfy all $B_o(j\omega_i)$ while not penetrating the U contour. The lead compensators tried had increased the bandwidth and robustness; however, they also reduces the output γ to a very small value(e.g., an output γ=2 degree for a full stick input). Therefore, only the pure gain of 16 is chosen as the compensator, this left the $B_o(j\omega_i)$ unsatisfied. The frequency response of the close-loop transfer function, $T_{\gamma_{in}}^{\gamma}$ (where $T_{\gamma_{in}}^{\gamma} = L_{e\gamma}^{\gamma} / (1 + L_{e\gamma}^{\gamma}) = (G_{e\gamma}^{\theta_{in}} * G_{\theta_{in}}^{\gamma}) / (1 + G_{e\gamma}^{\theta_{in}} * G_{\theta_{in}}^{\gamma})$, is shown in Figure 23. It can be seen in Figure 23 that δ_T(the spread between T_{max} and T_{min}) had exceeded the δ_R over the frequency range 0.1 to 0.7 rad/sec as a result of $L_{e\gamma}^{\gamma}$ not satisfying the performance bounds over that frequency range. To have any frequency, ω_i, on $L_{e\gamma}^{\gamma}$ higher than its corresponding $B_o(j\omega_i)$ will result in $\delta_T(j\omega_i) \geq \delta_R(j\omega_i)$, while lower than $B_o(j\omega_i)$ will result in $\delta_T(j\omega_i) \geq \delta_R(j\omega_i)$. As can be depicted in figure 23, further modification is required to fully meet the prescribed specification. A prefilter of a pure gain of 6.5 proved most effective in increasing the bandwidth and met the prescribed specification. The frequency response after the prefilter is applied is shown in Figure 24.

Lateral Bank-Angle Control: Transfer function $G_{\beta_{in}}^{\phi}$ and its performance bounds, $B_o(j\omega_i)$, and U contour are displayed on a Nichols Chart in Figure 25. Notice that $G_{\beta_{in}}^{\phi}$ is not only below all performance bounds $B_o(j\omega_i)$ but it also penetrates the U contour. Therefore, more than just a pure gain is required to reshape $G_{\beta_{in}}^{\phi}$. A controller, $G_{e\phi}^{\beta_{in}} = (s+.15)/(s+1.5)$, was added to $G_{\beta_{in}}^{\phi}$ to reshape it and prevent it from penetrating the U contour, but it was not successful in satisfying all of the $B_o(j\omega_i)$. After reshaping, $L_{e\phi}^{\phi}$ is shown on a Nichols Chart in Figure 26. The frequency plot of the close-loop transfer function, $T_{\phi_{in}}^{\phi}$, where $T_{\phi_{in}}^{\phi} = L_{e\phi}^{\phi} / (1 + L_{e\phi}^{\phi}) = (G_{e\phi}^{\beta_{in}} * G_{\beta_{in}}^{\phi}) / (G_{e\phi}^{\beta_{in}} * G_{\beta_{in}}^{\phi})$, with no prefilter applied yet is shown in Figure 27. A lead compensator of (S+1)/(S+2) is added to haunch up the severely deteriorated curve at frequency over 1 rad/sec and to increase the phase margin. A lag compensator of (S+0.25)/(S+0.15) is added to steepen the gain curve at low frequencies and to provide a smoother k/s curve for good pilot handling qualities. The close-loop response after adding the prefilter is shown in Figure 28 and the prefilter selected is 15(S+0.25)(S+1)/((S+0.15)(S+2)).

7. Results and Discussion

The objective of this study is to improve the handling qualities for the approach and landing of B-720 TOFC by increasing the control bandwidth and the light Dutch-roll damping. The control bandwidth of TOFC depends primarily on the engine response to throttle command, and on the propulsion-induced low-frequency speed and dihedral stability effects, which are configuration-dependent, thus are fixed and unalterable. Therefore, the control engineer's only tools are compensation and feedback.

To improve control bandwidth is very difficult as can be depicted from the pitch rate to thrust bode in Figure 7. Full thrust of 10,000 lbs from each engine is required to yield a crossover frequency just beyond 1 rad/sec. This clearly shows how control bandwidth is limited by the control power (the engine) available.

For flight-path-angle control, pitch rate feedback was effective in increasing phugoid damping while γ feedback was effective in improving frequency of the phugoid mode. For bank-angle control, β feedback was found most effective in increasing Dutch-roll damping while φ feedback is crucial to lateral phugoid damping. Yaw rate feedback, which is effective in damping Dutch-roll when rudder power is available, helps Dutch-roll damping and the lateral phugoid damping very little. Tables 5 and 6 compare the dynamic modes of the bare airframe with the dynamic modes of previous simulation designs, of QFT design and of heuristic design(heuristic compensation will be discussed later on page 19.) Transfer functions of γ to stick and φ to stick for all the four configurations are listed in Appendix A.

Table 5. Longitudinal Mode Comparison

	Density	Phugoid	Short Period	Engine	Pre-filter	$G_{\gamma}^{\theta_{in}}$	$G_{e_\theta}^{\delta_{Tc}}$	K_{γ}	K_q
Bare Airframe	(1.4E-6)	(.04,.13)	(.65,1.4)	(.55)(5)	-	-	-	-	-
Simulation Augmented Control	(4.7E-6)	(.52,.24)	(.52,1.5)	(.4)(5.2)	10	1	10	1	4
QFT Augmented Control	(3.4E-6)	(.62,.32)	(.46,1.6)	(.3)(5.2)	6.5	16	1	1	60

Table 6. Lateral Mode Comparison

		Dutch Roll	Roll	Engine	Pre-filter	$G_{e_\phi}^{\beta_{in}}$	$G_{e_\beta}^{\delta_{Tc}}$	K_ϕ	K_p	K_β	K_r
Bare Airframe	(1.1E-4)	(.12,.99)	(1)	(.55)(5)	-	-	-	-	-	-	-
Simulation Augmented Control	(.73,.35)	(.15,.99)	(1)	(5)	40	1	1	.5	.5	1	-
QFT Augmented Control	(.39)	(.29,1.0)	(1.5)	(.45)(5)	$\frac{2.5(.25)(1)}{(.15)(2)}$	$\frac{(.15)}{(1.5)}$	1	1	-	4	-
Heuristic Augmented Control	(.75,.28)	(.22,1.0)	(.9)	(5)	40	1	1	.15	.5	3	1

For longitudinal control, pure gain compensation was used. Since the short period mode has a frequency around 1.5 rad/sec (which was beyond the frequency that throttles can control) the primary concern was to increase phugoid damping and frequency. The phugoid damping and frequency increased from 0.52 to 0.62 and from 0.24 rad/sec to 0.32 rad/sec, respectively. This increase of response frequency can also be depicted from the flight path angle response shown in Figure 29.

For lateral control, pole/zero compensation was used. The Dutch-roll damping was almost doubled, from 0.15 to 0.29. The simulation augmented control has a lateral phugoid mode [0.73, 0.35] which combines the spiral and the slow engine mode. This was replaced using the QFT design with two real root modes, (0.39) and (0.45), both with higher frequencies, therefore faster responses. The comparison of the responses is shown in Figure 30.

All plots in Figures 21 through 32 were obtained from nonlinear simulation runs at approach and landing conditions with major control surfaces (ailerons, elevator sand rudders) locked while the electrical and mechanical systems, and the landing gear remained operative. Figure 33 through 35 shows the throttle response, and flight-path-angle and bank-angle tracking response to full stick deflection.

Turbulence Response: The response of the flight-path-angle control under intermediate turbulence is presented in Figure 31. Because of gust randomness, more than one simulation run was made to examine the tracking integrity under turbulence.

The bank angle tracking by QFT design does not perform well under intermediate turbulence (Figure 32). This could be caused by the larger K_β gain (K_β=4) being used in the β-feedback loop by QFT design, while a K_β=1 is used for the

simulation designed control. This larger K_β multiplies the gust-induced-sideslip four times before it was fed back to the airplane. This had a dramatic effect on the bank angle output due to 0.2 degree of sideslip angle would generate approximately 10 degrees of bank angle, owing to the large $C_{l\beta}$ of B-720. The sideslip angle (β) feedback is the only parameter that can effectively increase Dutch-roll damping for B-720 TOFC. A compromise seems necessary between lateral bank angle tracking and Dutch-roll damping.

Good Dutch-roll damping is associated with disturbance excitation of the lateral phugoid mode and results in poor tracking of bank angle. Lowering the feedback gain reduces Dutch-roll damping but also decreases the sensitivity of bank angle to disturbances, and thus makes the lateral phugoid mode less troublesome to the pilot when flying in turbulence.

During the investigation, it was found that the β being fed back into the B-720 simulator was the β at the c.g. instead of the β at the nose boom. The nose boom β is actually measured and fed back into a real airplane. The nose boom β was then modeled into the B-720 simulator and the results of the bank angle tracking under turbulence were fairly good. Figure 36 shows the bank-angle tracking under turbulence due to c.g. β, while Figure 37 shows two runs of bank-angle tracking under turbulence due to nose boom β. The β at the nose boom has two more terms caused by lateral and longitudinal offsets from the c.g. The dominant term is a function of roll rate. When this extra term was active in the feedback loop, lateral performance improved. However, there was some question concerning the correctness of the sign of the yaw rate term as implemented in the simulation. The effectiveness of yaw rate feedback for TOFC need to be further investigated.

A augmented control scheme heuristically determined that feedback p,r, β and φ is investigated. The compensation of this control scheme is shown in Table 6. The yaw rate feedback is included in the control to improve bankangle tracking, the roll rate and bank angle feedbacks are included to increase the damping and frequency of the lateral phugoid mode while the β feedback to increase the Dutch-roll damping. The heuristic augmented control has a slightly slower response speed (ω_n=0.28 < ω_n=0.35 of simulation augmented control), but a higher Dutch-roll damping (ζ=.22 > ζ=.147 of simulation augmented control) which has successfully damped the Dutch-roll oscillation as can be seen in Figure 35.

The system response to configuration variations for γ-control and for φ-control are shown in Figures 38 and 39, respectively. The robustness of the flight-path-angle control is improved by QFT as shown in Figure 38. The Dutch-roll oscillation in the original simulation compensation is taken out by QFT compensation; however, the tracking was not improved (Figure 39). Among the three augmented control developed, the heuristically determined augmented control presented the best robust performance

(with fairly good bank-angle tracking and no Dutch-roll oscillation.) Due to time constraints, the heuristic augmented control was not tested on the real-time nonlinear B-720 simulator.

8. Conclusions and Recommendations

Studies by NASA Dryden has shown that throttles can be used for emergency flight control. Manual fly-by-throttle is extremely difficult with landing almost impossible, but with control augmentation, runway landing is feasible.

Flight path control design using throttles-only to achieve safe emergency landing for a transport airplane, Boeing 720, was investigated. Augmented throttles-only flight path control built in a previous simulation study has made successful simulation landings. However, it showed light Dutch-roll damping and low control bandwidth. To increase the control bandwidth substantially proved very difficult. Differential throttles to engines mounted at different vertical levels to generate an instant pitching moment may be an effective way to increase the control bandwidth.

For throttles-only pitch control using QFT, the control bandwidth , tracking and control robustness were improved by QFT. For bank angle control, QFT has improved the Dutch-roll oscillation. However, the lateral phugoid becomes sensitive to configuration changes. A compromise is required between Dutch-roll and lateral phugoid damping given limited control power. Further investigation of the effects of yaw rate feedback is recommended.

References

1. Burcham, F., Fullerton, G., Gilyard, G., Wolf, T., and J. Stewart. "A Preliminary Investigation of the Use of Throttles for Emergency Flight Control." NASA Dryden Document. 1991.

2. Gilyard, G., Conley, J., Le, J., and W. Burcham. "A Simulation Evaluation of a Four-Engine Jet Transport Using Engine Thrust Modulation for Flight Path Control." 27th Joint Propulsion Conference. June 24-26, 1991. Sacramento, CA.

3. Azzano, C.P. "A Preliminary Look at Optimal Multi-Variable Design of Propulsion-Only Flight Controllers for Jet Transport Aircraft." NASA Dryden Technical Report. Sept 21, 1990.

4. Biezad, D.J. "The Propulsive-Only Flight Control Problem," NAECON , Vol. 2. Dayton, Ohio. May 20-24, 1991. 494-500.

5. Biezad, D.J. and C.P. Azzano. "Designing Low Bandwidth Propulsive-Only Flight Controllers." AIAA Guidance, Navigation, and Control Conference Paper No. 91-2628CP. August 12-14, 1991. New Orleans, LA. 267-275.

6. Horowitz, I.M. and M. Sidi. "Synthesis of Feedback Systems with Large Plant Ignorance for Prescribed Time-domain Tolerances." Int. J. Control, Vol. 16. 1972. 287-309.

7. D'Azzo, J.J. and C.H. Houpis. "Linear Control System Analysis and Design Conventional and Modern." McGraw-Hill. 1988.

8. Yaniv, O. "Multiple-Input Single-Output (MISO) User Manual." Tel-Aviv University. 1991.

9. Horowitz, I.M. "Quantitative Feedback Design Theory (QFT)." Vol. 1. QFT Publication. 1992.

10. Thompson, Peter M. "Program CC Version 4 Reference Manual: Volume 1." Systems Technology, Inc. November 1988.

11. Biezad, D.J. and Hwei-Lan Chou. "Pilot-in-the-Loop Analysis of Propulsive-Only Flight Control Systems." NAECON. Dayton, Ohio. May 1992.

12. McRuer, D., Ashkenas, I., and D. Graham. "Aircraft Dynamics and Automatic Control." Princeton University Press. 1973.

13. Sarrafian, S.K. and B.G. Powers. "Application of Frequency Domain Handling Qualities Criteria to the Longitudinal Landing Task." NASA Technical Memorandum. August 1985.

14. MIL-STD-1797A. "Flying Qualities of Piloted Vehicles." Limited Distribution. ASD/ENES. Wright-Patterson AFB, Ohio. January 1990.

15. Gaffney, T. "Pilot in Sioux City Jet Crash Tells Story in Dayton." Dayton Daily News. March 26, 1991. Page 3-A.

16. Leavitt, P. "Crash Settlement." USA Today. March 27, 1991. Page 3-A.

17. Roskam, J. "Airplane Flight Dynamics and Automatic Flight Controls." Roskam Aviation and Engineering Corporation. Ottawa, Kansas. 1979.

18. Blakelock, J. "Automatic Control of Aircraft and Missiles." John Wiley and Sons, Inc. 1965.

FIGURES

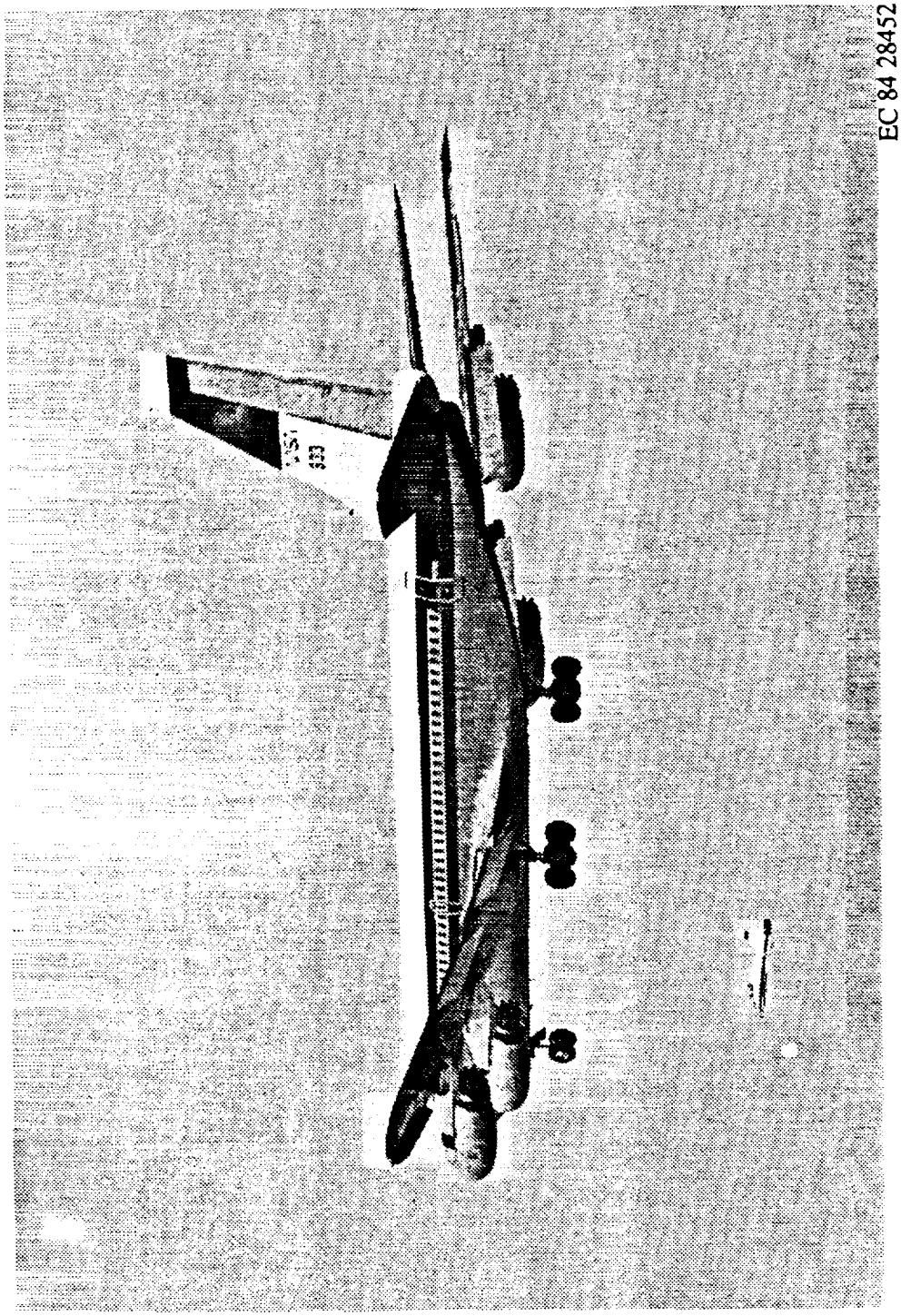

Figure 1. Boeing-720

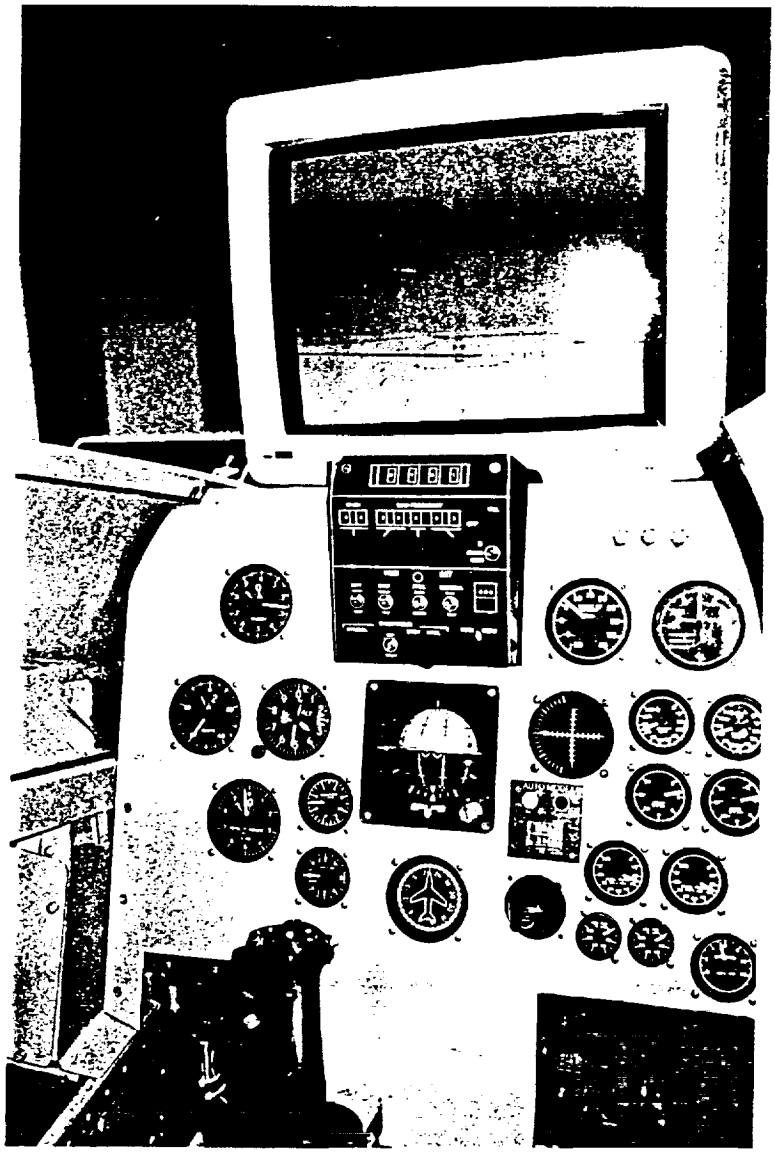

Figure 2. Boeing-720 simulation cockpit

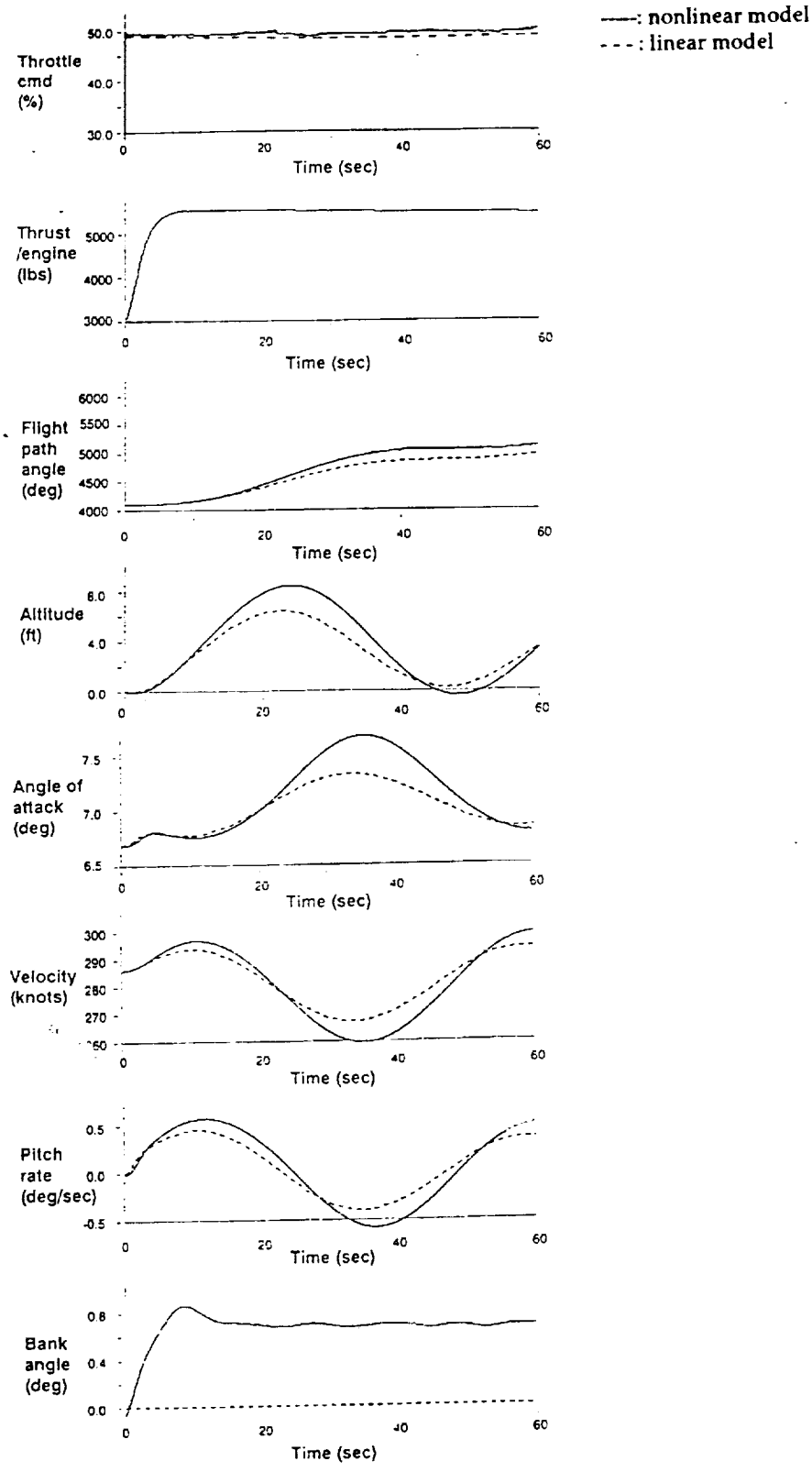

Figure 3. Comparison of the longitudinal open-loop response of the B-720 linear and nonlinear model, 20% step throttle cmd, nominal configuration

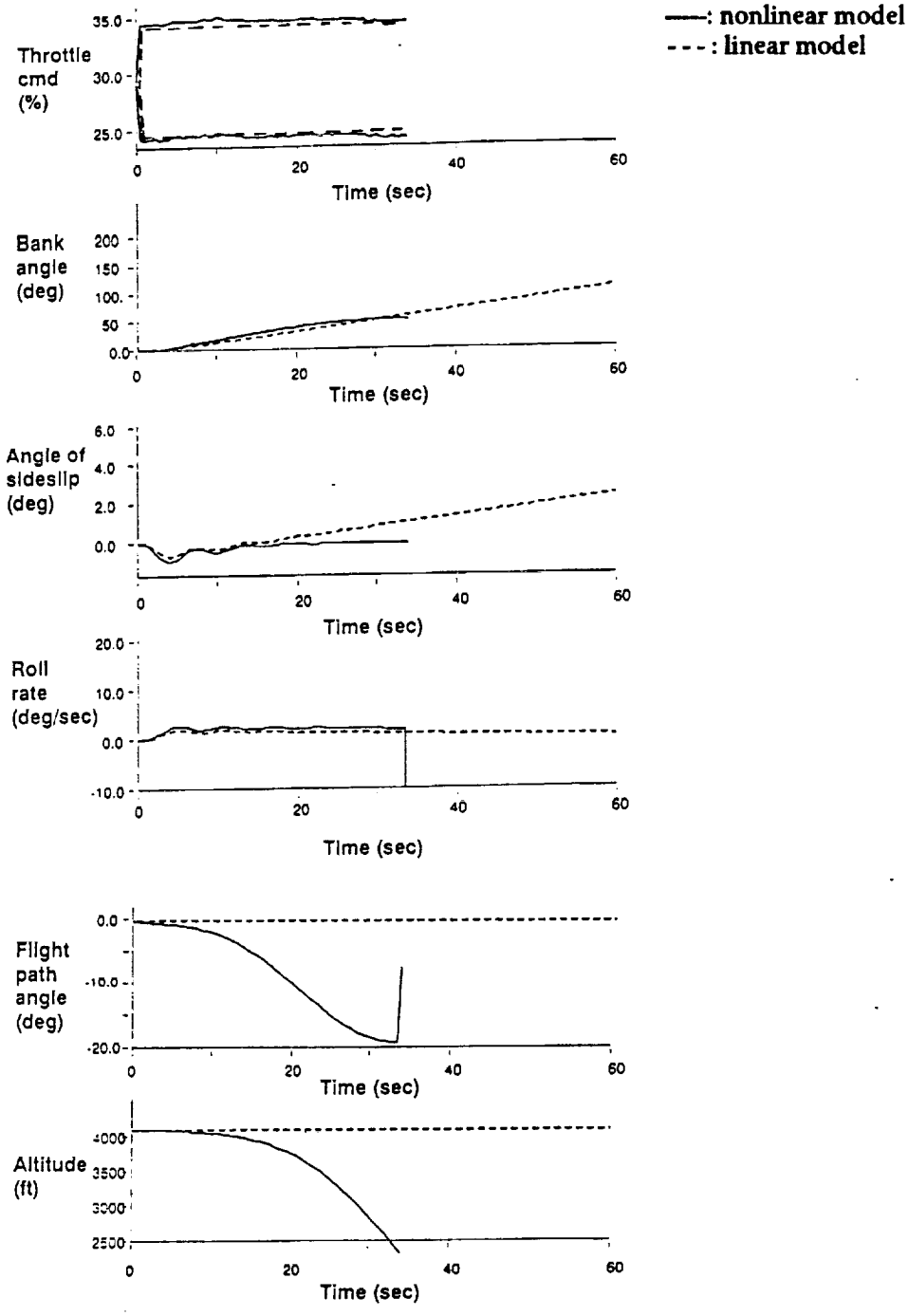

Figure 4. Comparison of the lateral open-loop response of the B-720 linear model and nonlinear model, 5% differential throttle, nominal configuration

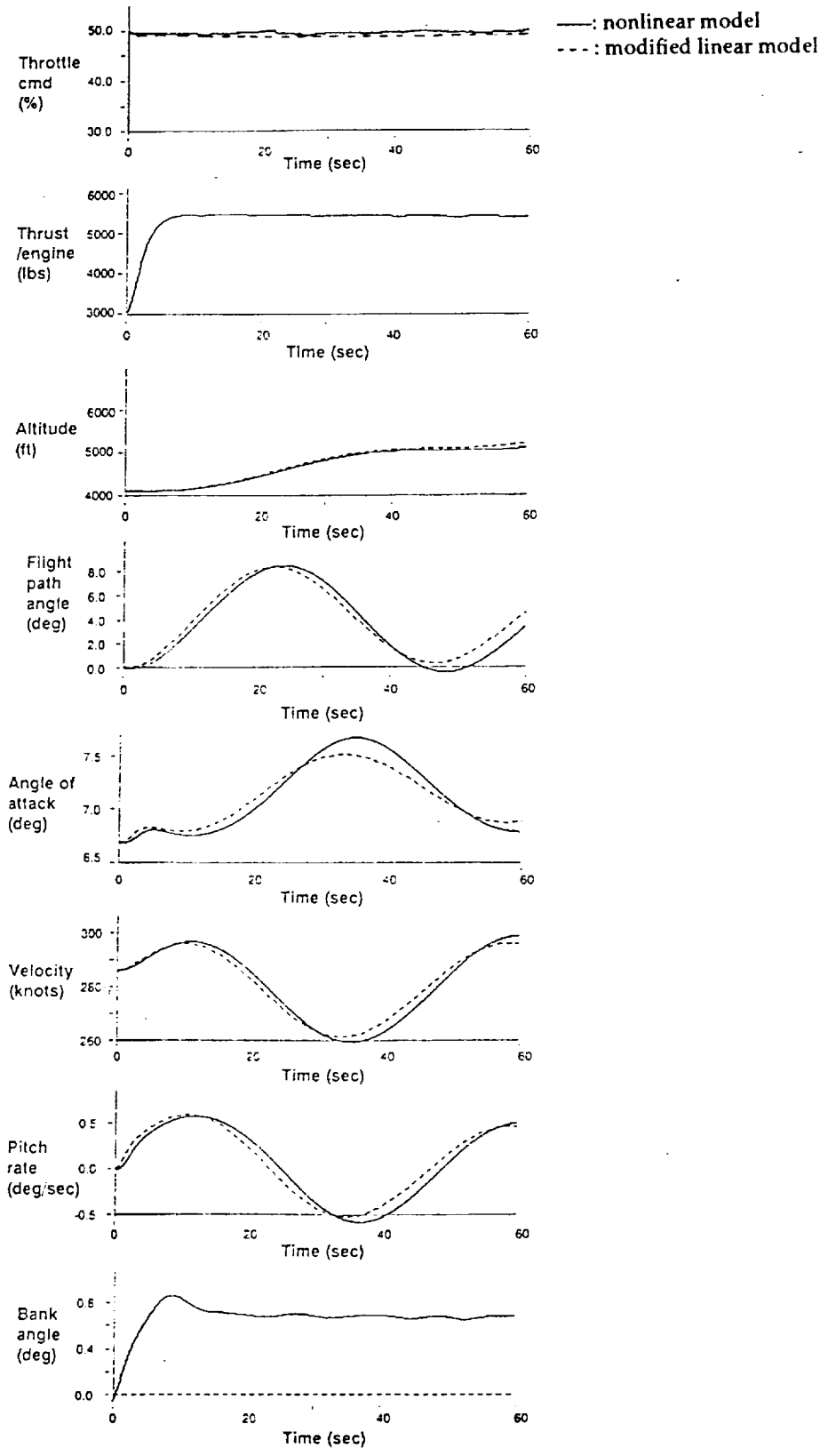

Figure 5. Comparison of the longitudinal open-loop response of the modified B-720 linear and nonlinear model, nominal configuration

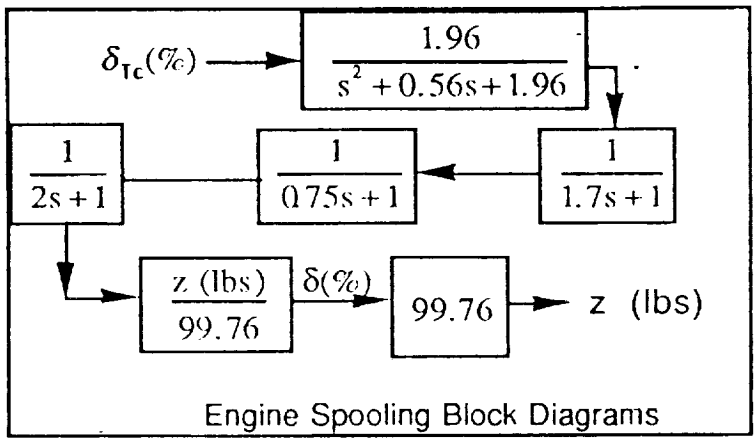

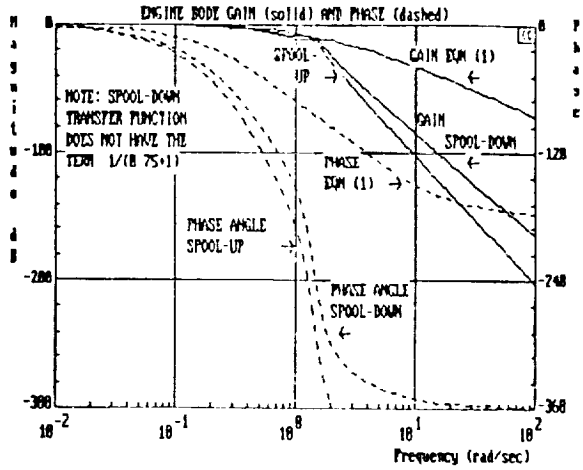

Engine δ to δ_{Tc}

Figure 6. Engine spooling block diagrams and Engine δ to δ_{Tc}

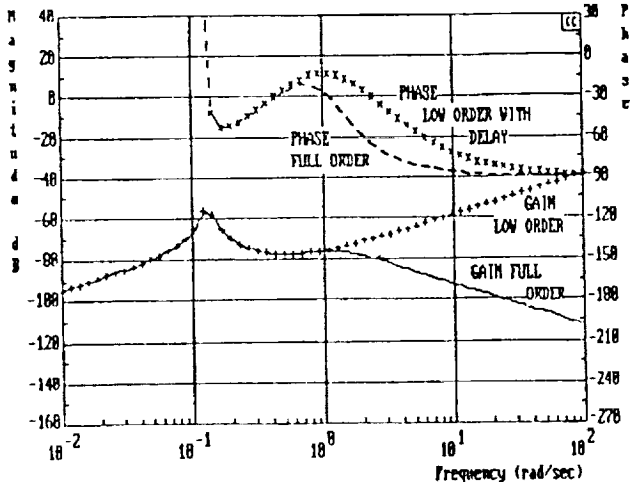

Figure 7. Pitch rate to thrust bode

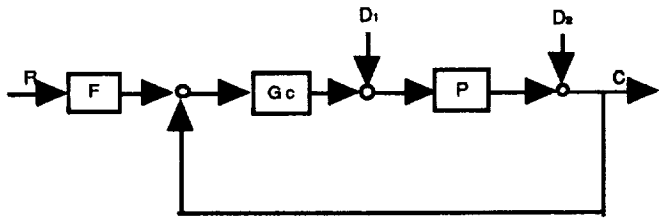

where
R : Command Step Input
D : Disturbance Inputs
C : output
P : Plant
Gc : Compensator
F : Prefilter

The open loop transmission function, L, is defined as:

$L = Gc * P$ and $Lm\ L = Lm\ Gc + Lm\ P$

The close loop transfer functions are:

Tracking: (D1=D2=0) $T_R = \frac{FL}{1+L}$ and $Lm\ T_R = Lm\ F + Lm\ \frac{L}{1+L}$

Disturbance: (R=D2=0) $T_{D1} = \frac{P}{1+L}$

Disturbance: (R=D1=0) $T_{D2} = \frac{1}{1+L}$

Figure 8. QFT unit feedback control structure

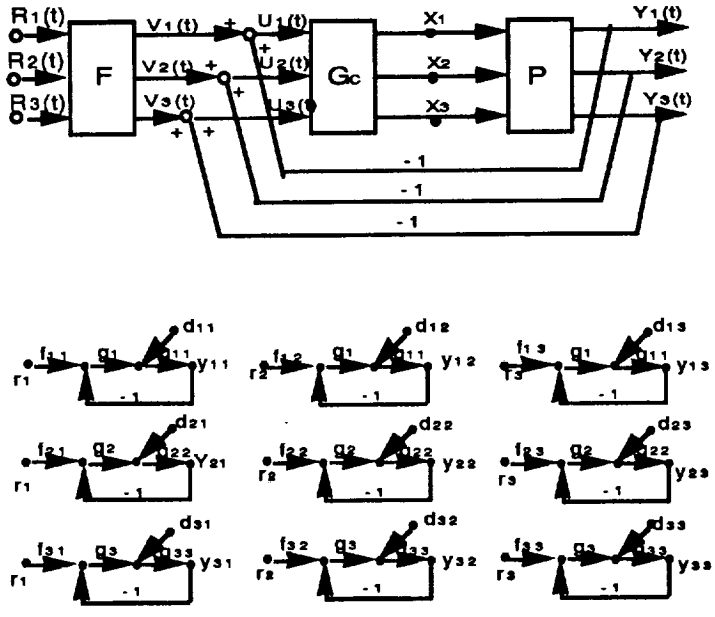

Figure 9. Equivalent MISO systems of a 3x3 MIMO system

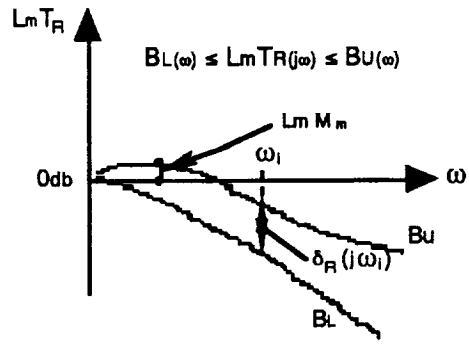

Figure 10. Typical close loop tracking specification

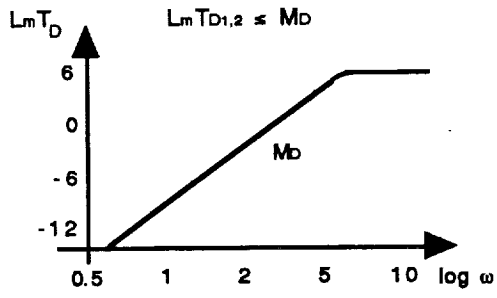

Figure 11. Typical disturbance rejection specification

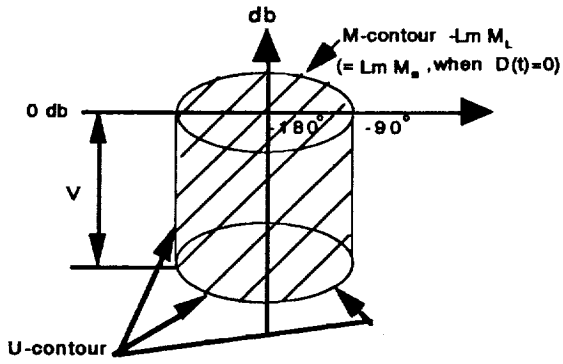

Figure 12. U contour construction

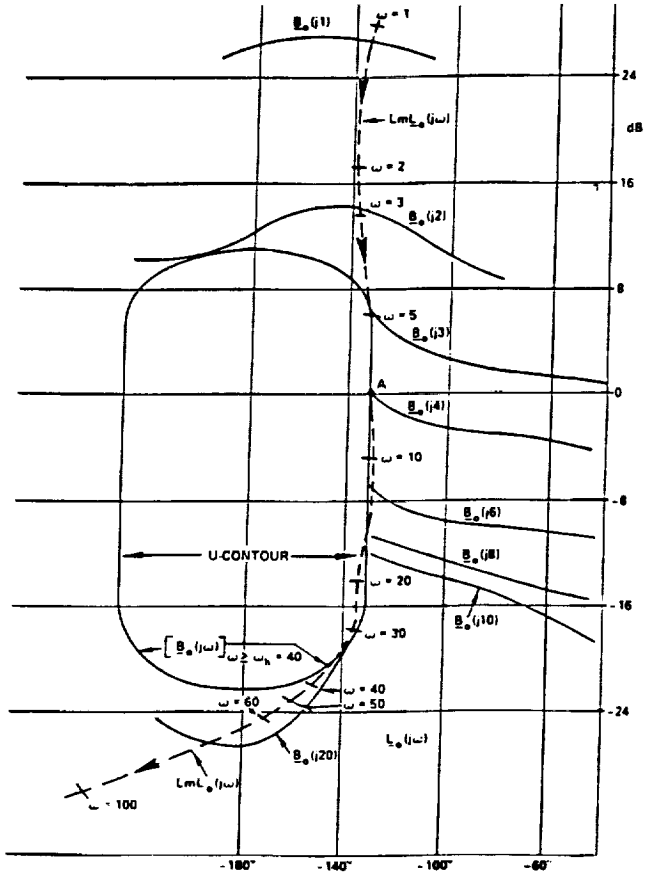

Figure 13. Performance bounds, U contour, and optimal L_0

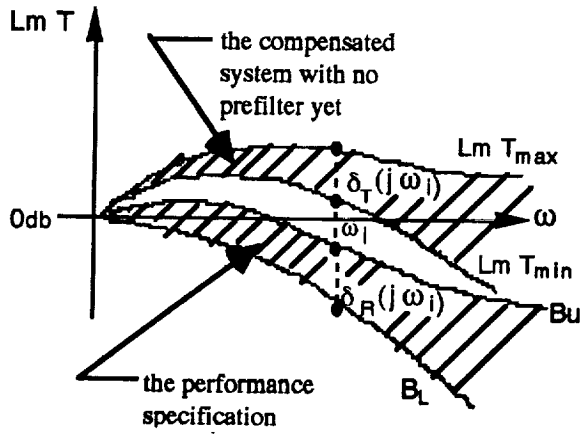

Figure 14. A prefilter is required to fullfill the performance specification

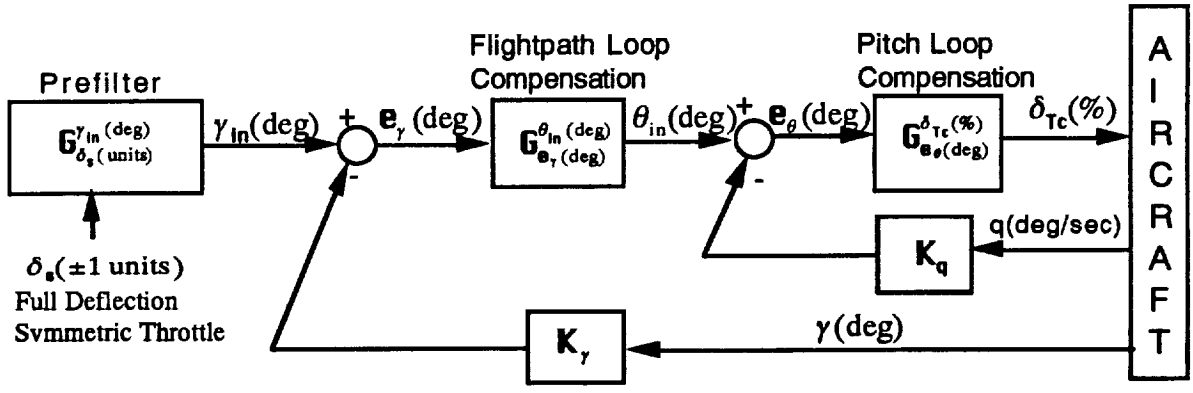

Figure 15. Flight-path-angle control block diagram

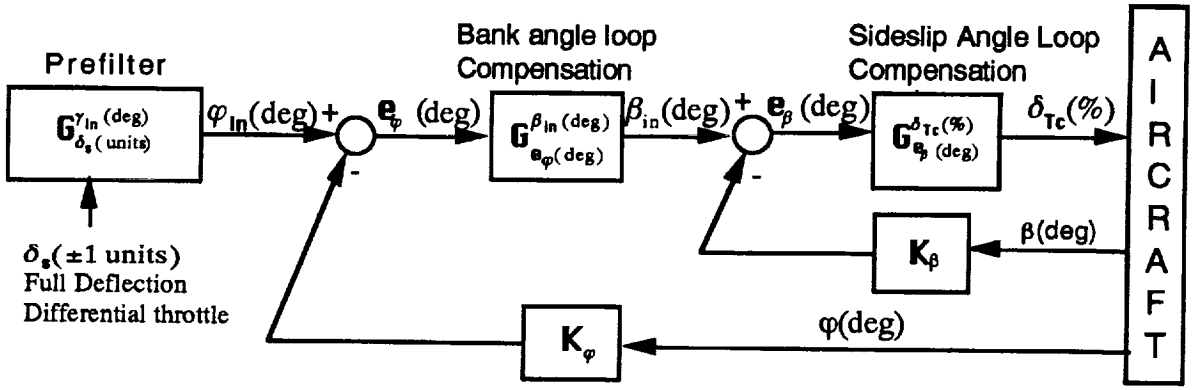

Figure 16. Bank-angle control block diagram

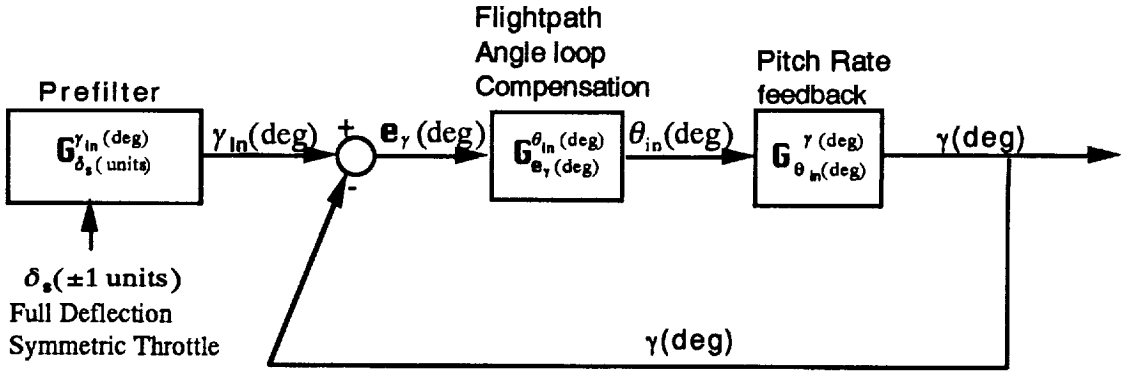

Figure 17. Flight-path-angle control with inner q-loop closed

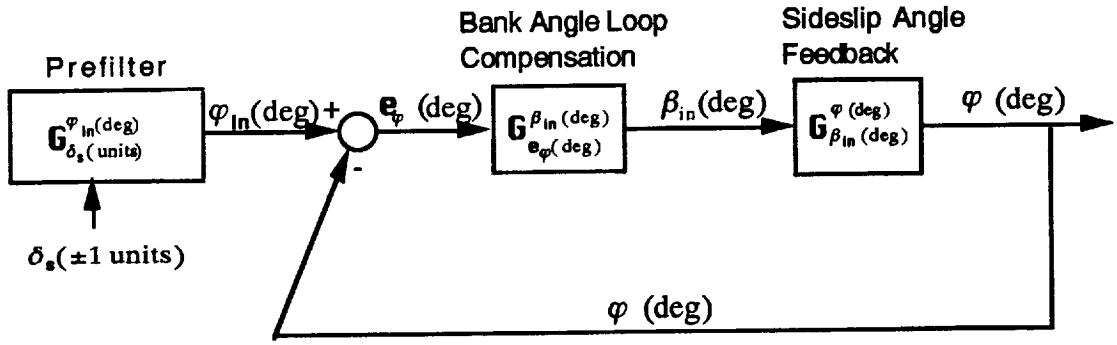

Figure 18. Bank-angle control with inner β-loop closed

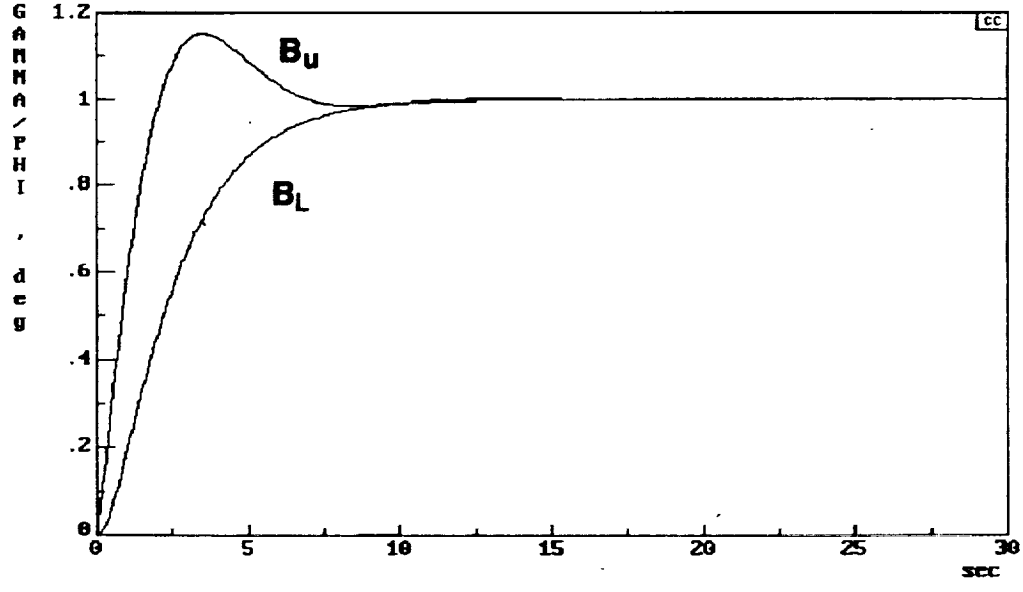

Figure 19. Performance specification in time domain for approach and landing of B-720 TOFC

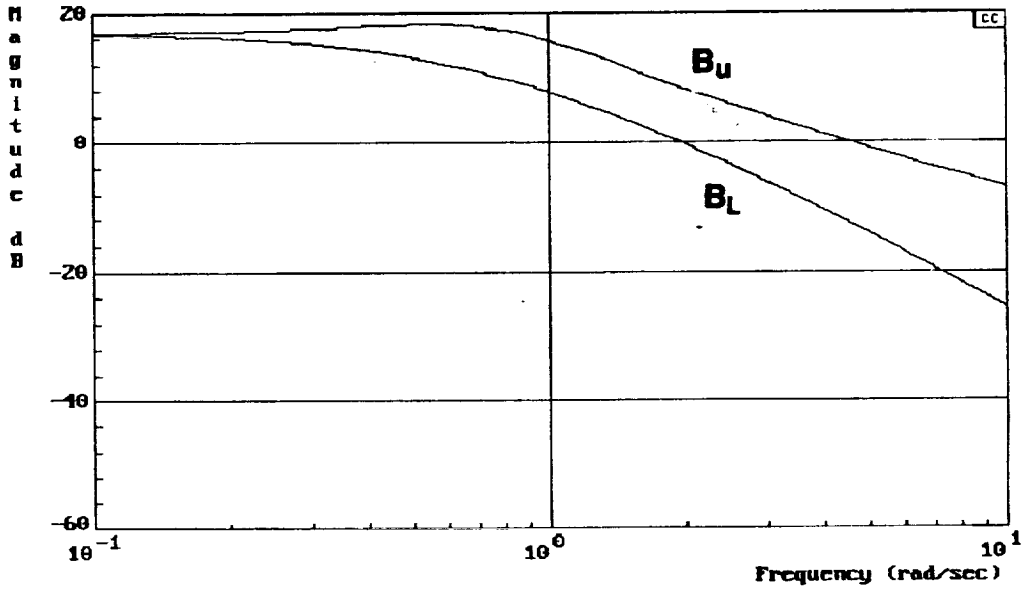

Figure 20. Performance specification in frequency domain for approach and landing of B-720 TOFC

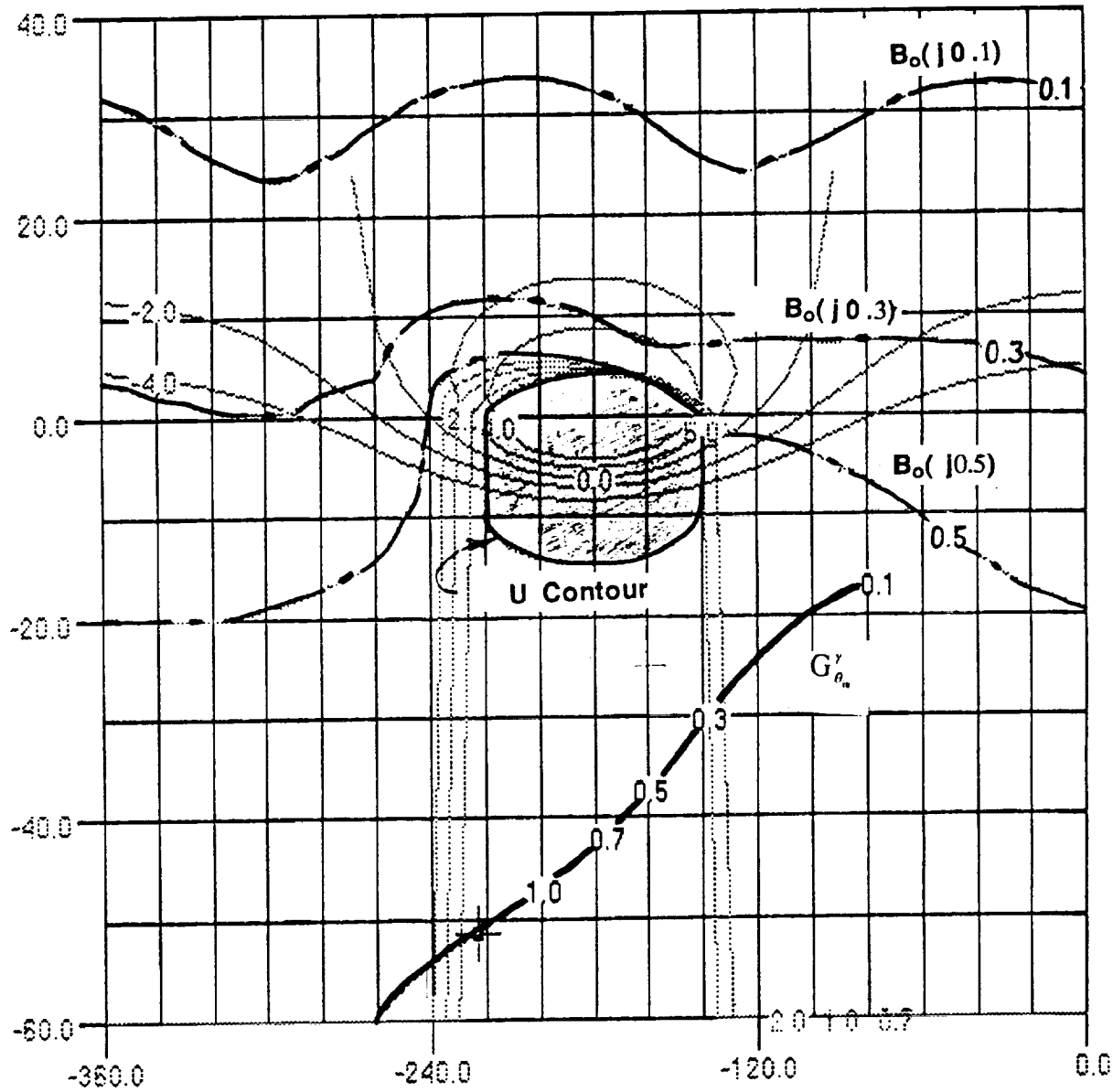

Figure 21. Transfer function $\mathbf{G}^{\gamma}_{\theta_{in}}$, its performance bounds B(jw), and U contour on Nichols Chart

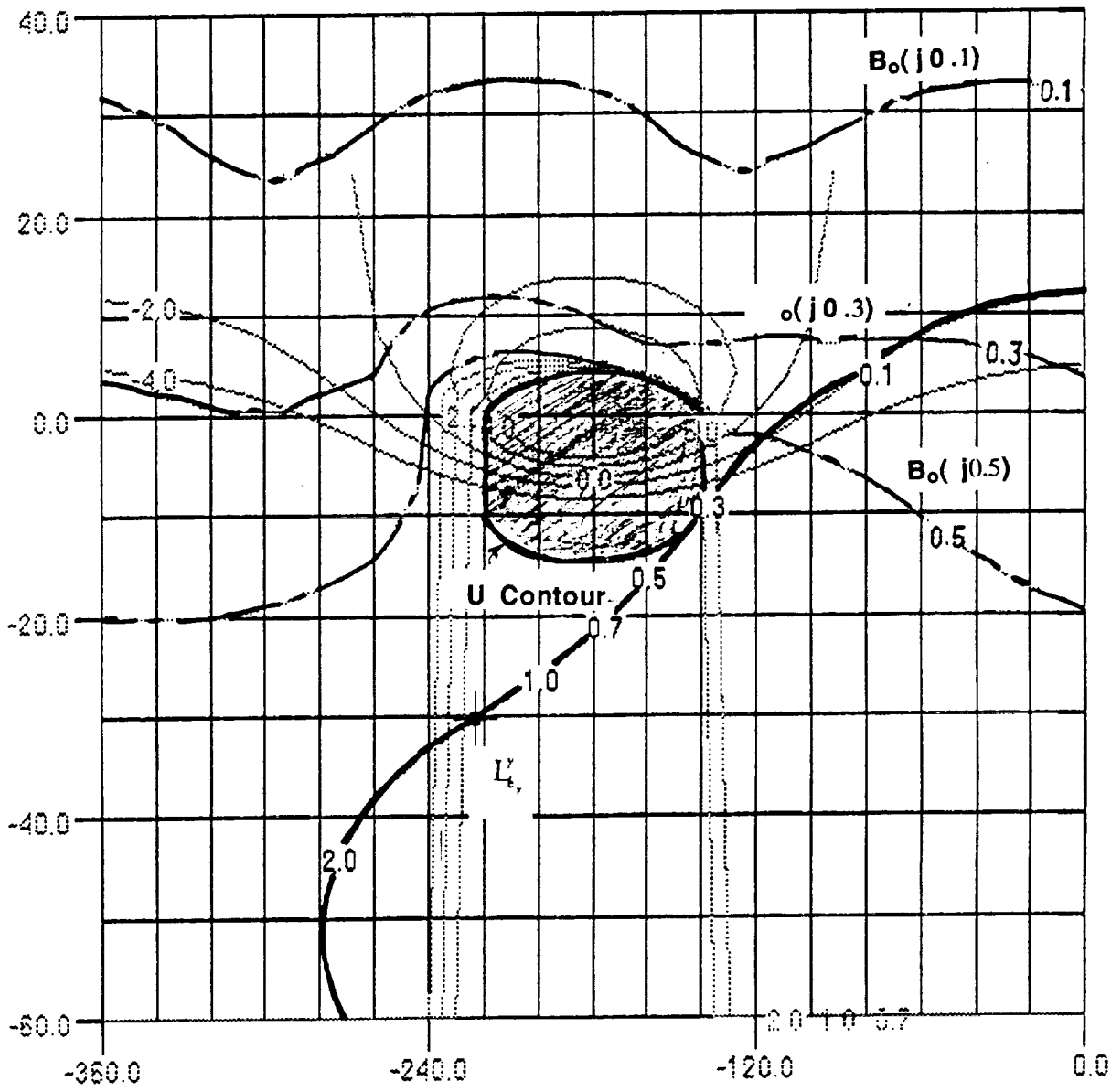

Figure 22. Open-loop transfer function, $\mathbf{L}^{r}_{\theta_{in}}$, on Nichols Chart

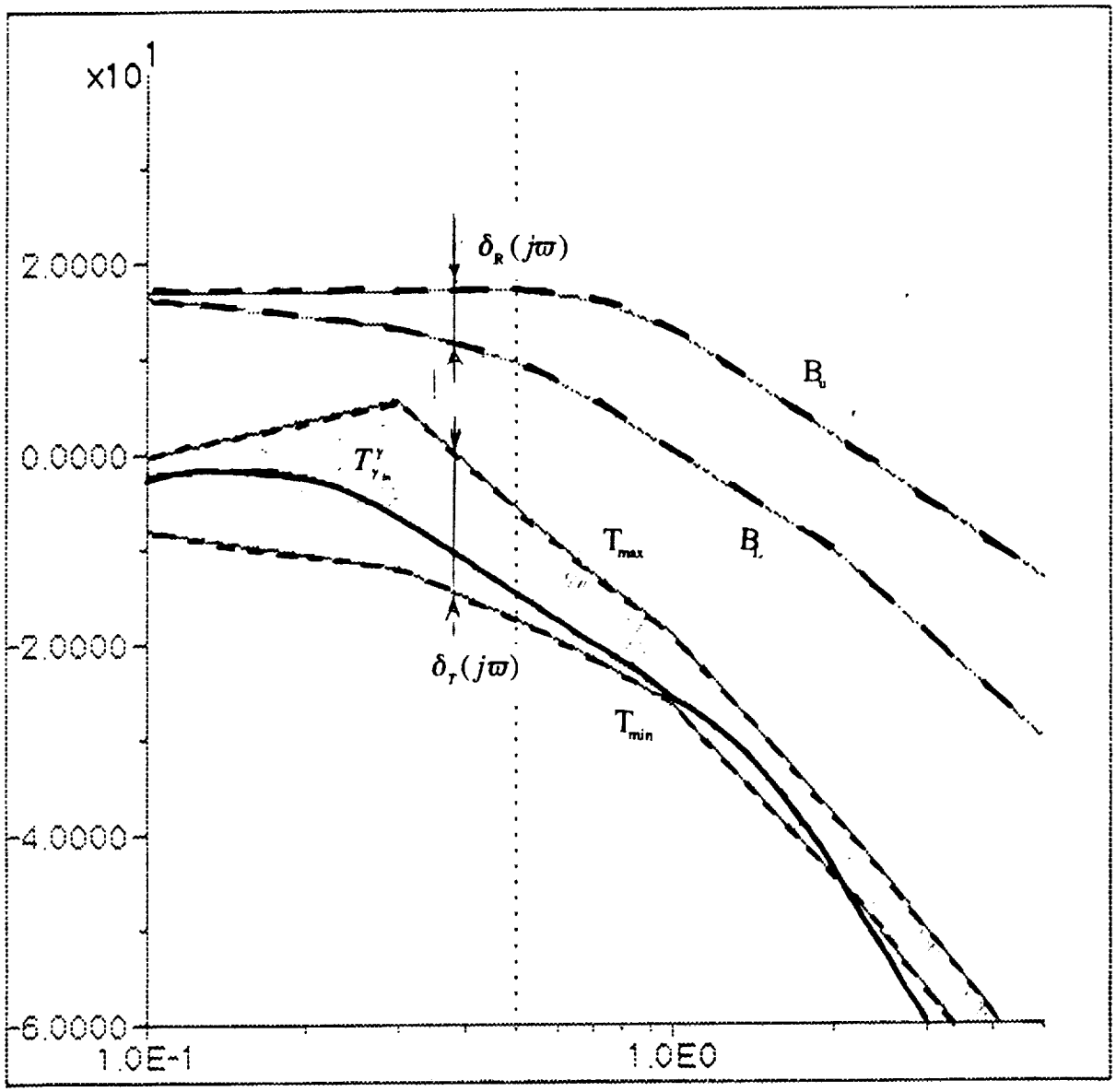

Figure 23. Frequency plot of the close-loop transfer function $\mathbf{T}_{\gamma_{in}}^{\gamma}$ with no prefilter

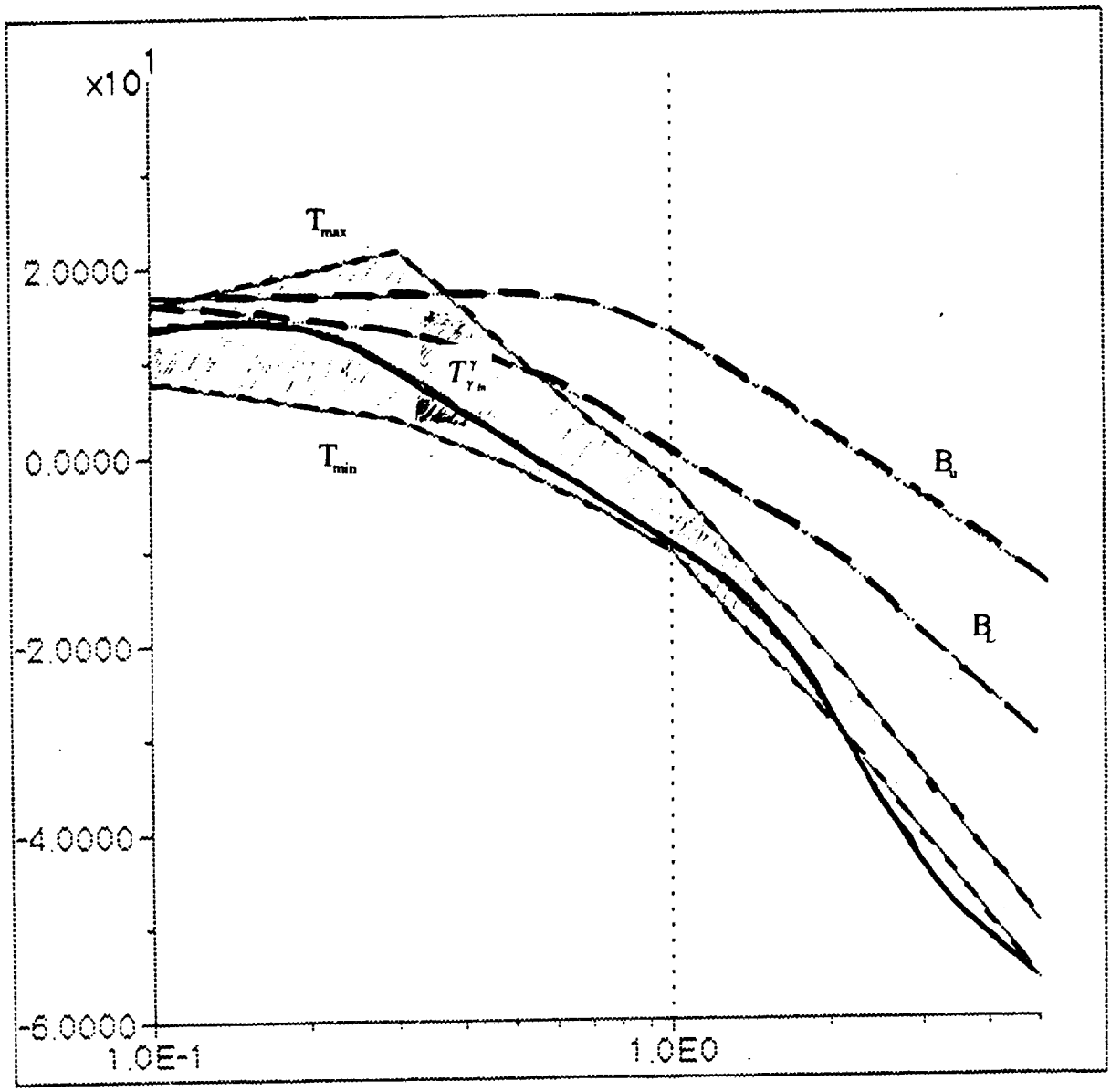

Figure 24. Frequency plot of the close-loop transfer function $\mathbf{T}_{y_{in}}^{y}$ with prefilter

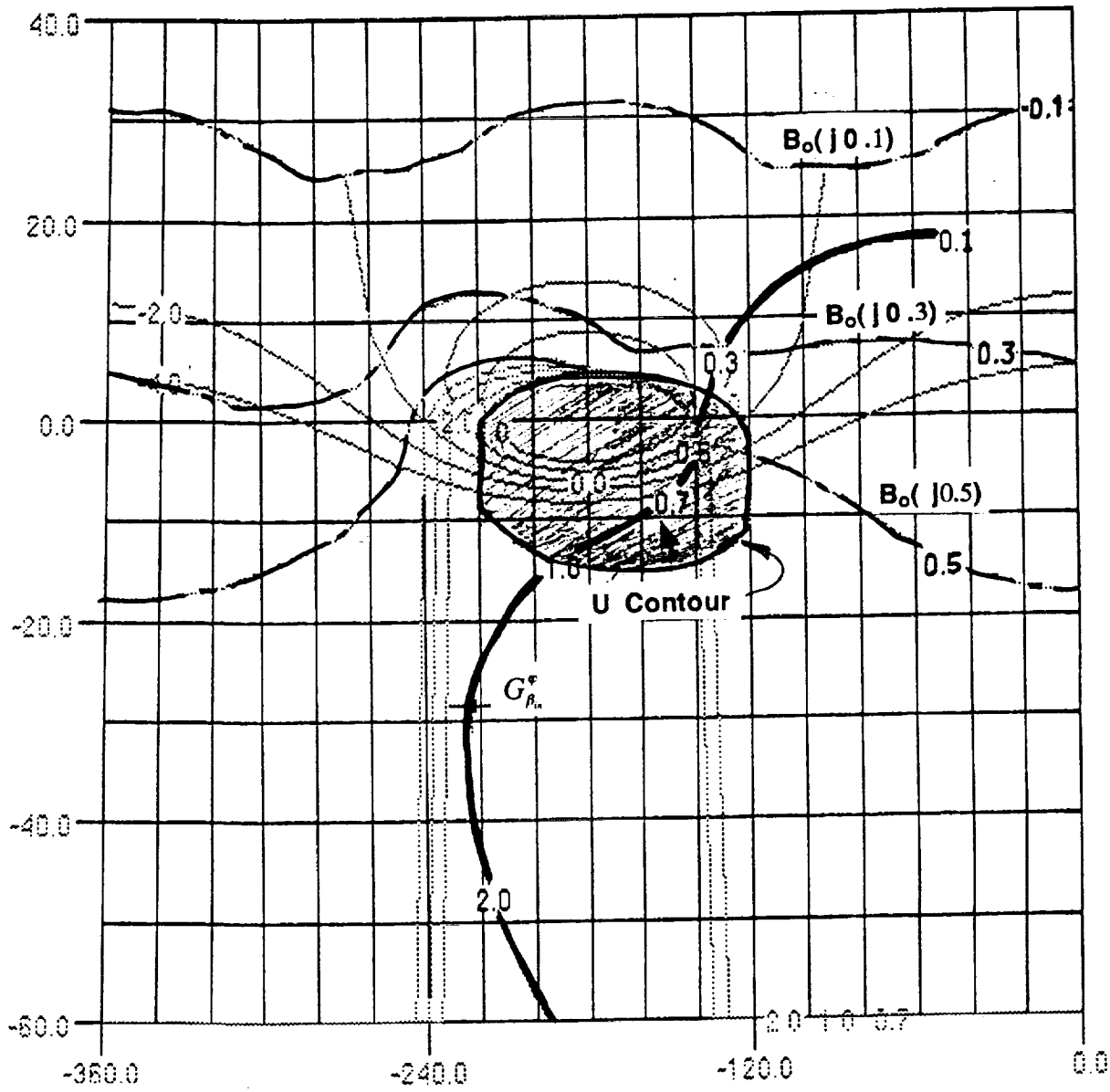

Figure 25. Transfer function $\mathbf{G}^{\phi}_{\beta_{in}}$, its performance bounds B(jw), and U contour on Nichols Chart

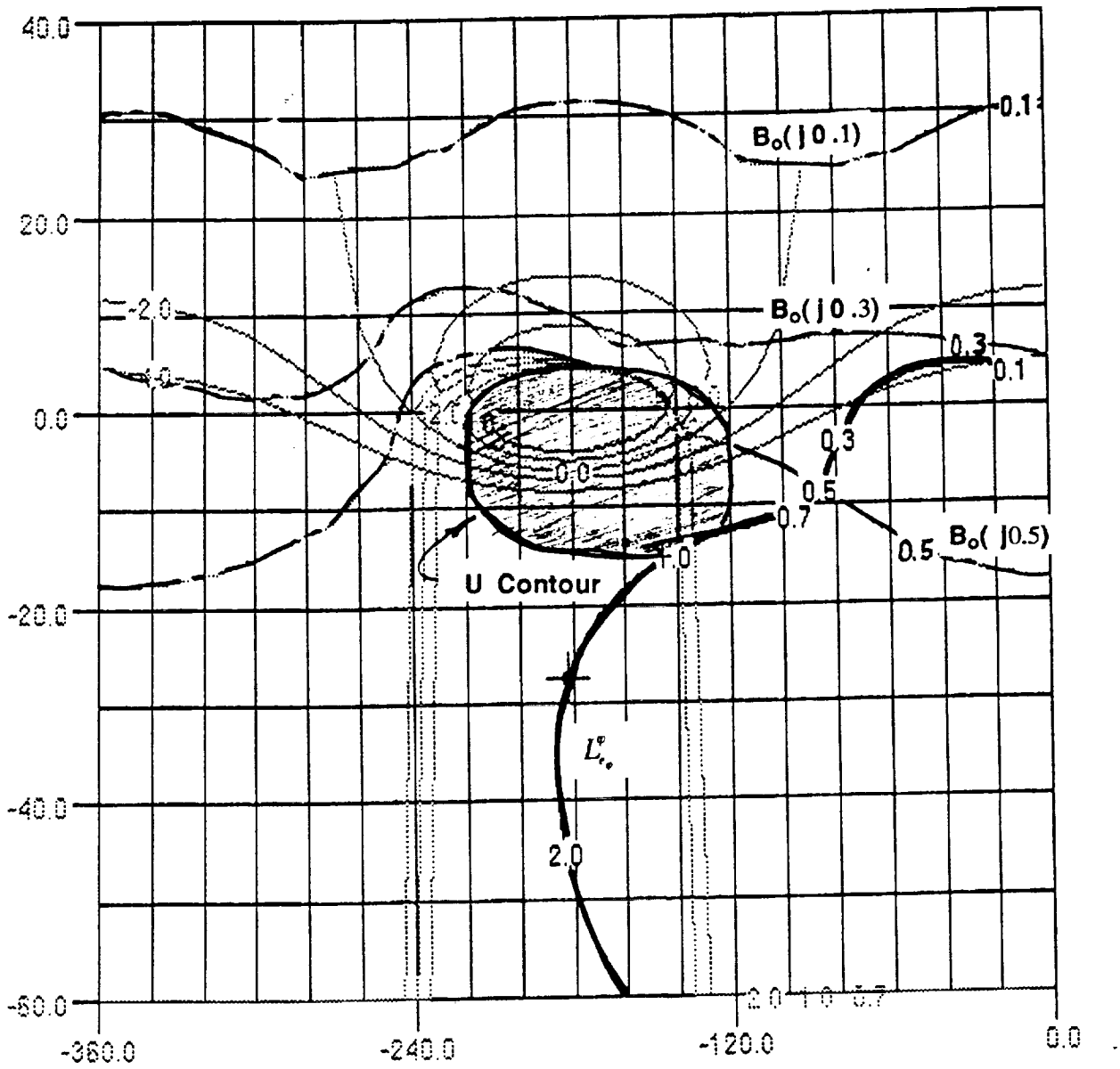

Figure 26. Open-loop transfer function, $L^{\phi}_{e\phi}$, on Nichols Chart

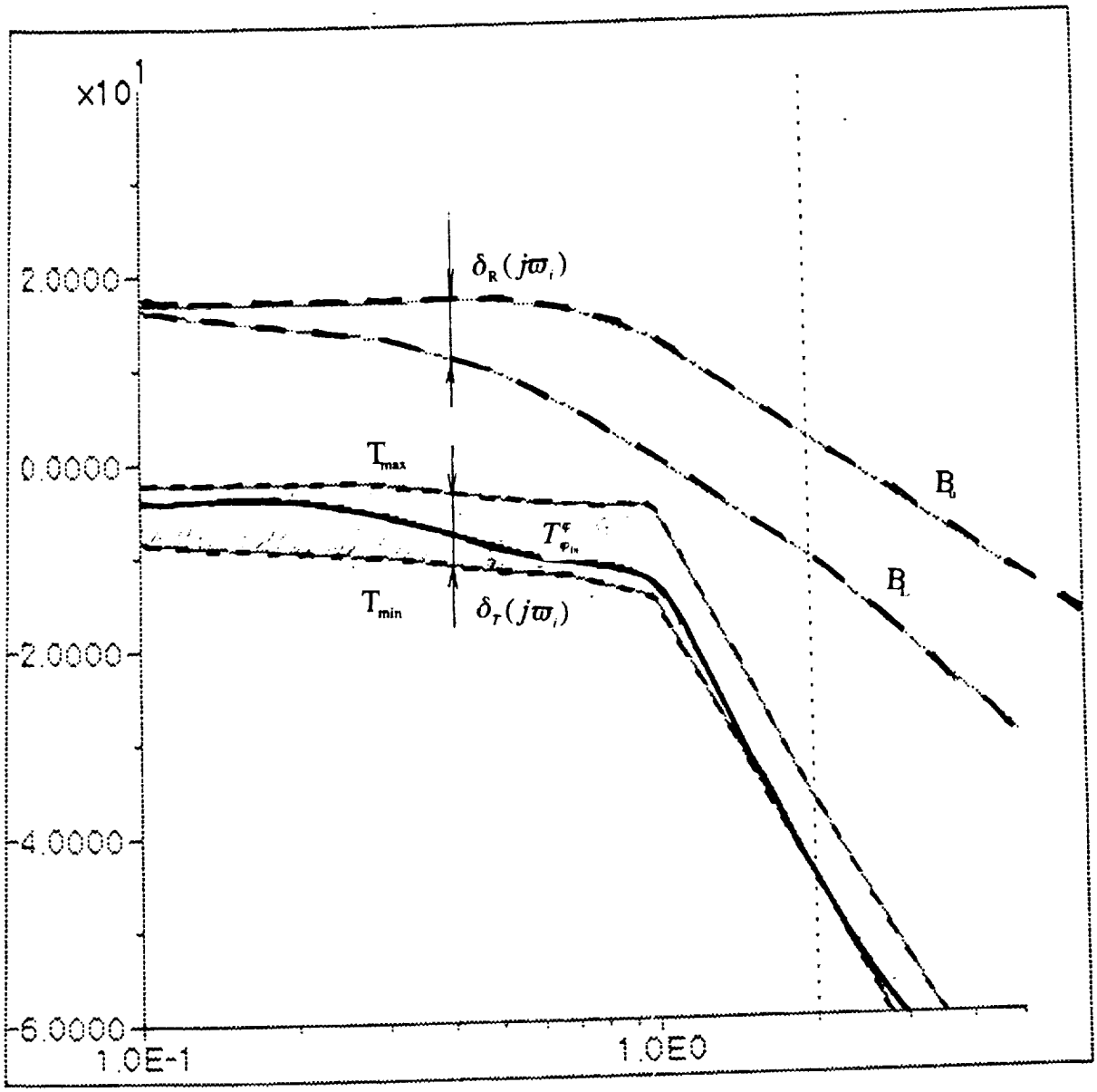

Figure 27. Frequency plot of the close-loop transfer function $\mathbf{T}^{\phi}_{\phi_{in}}$ with no prefilter

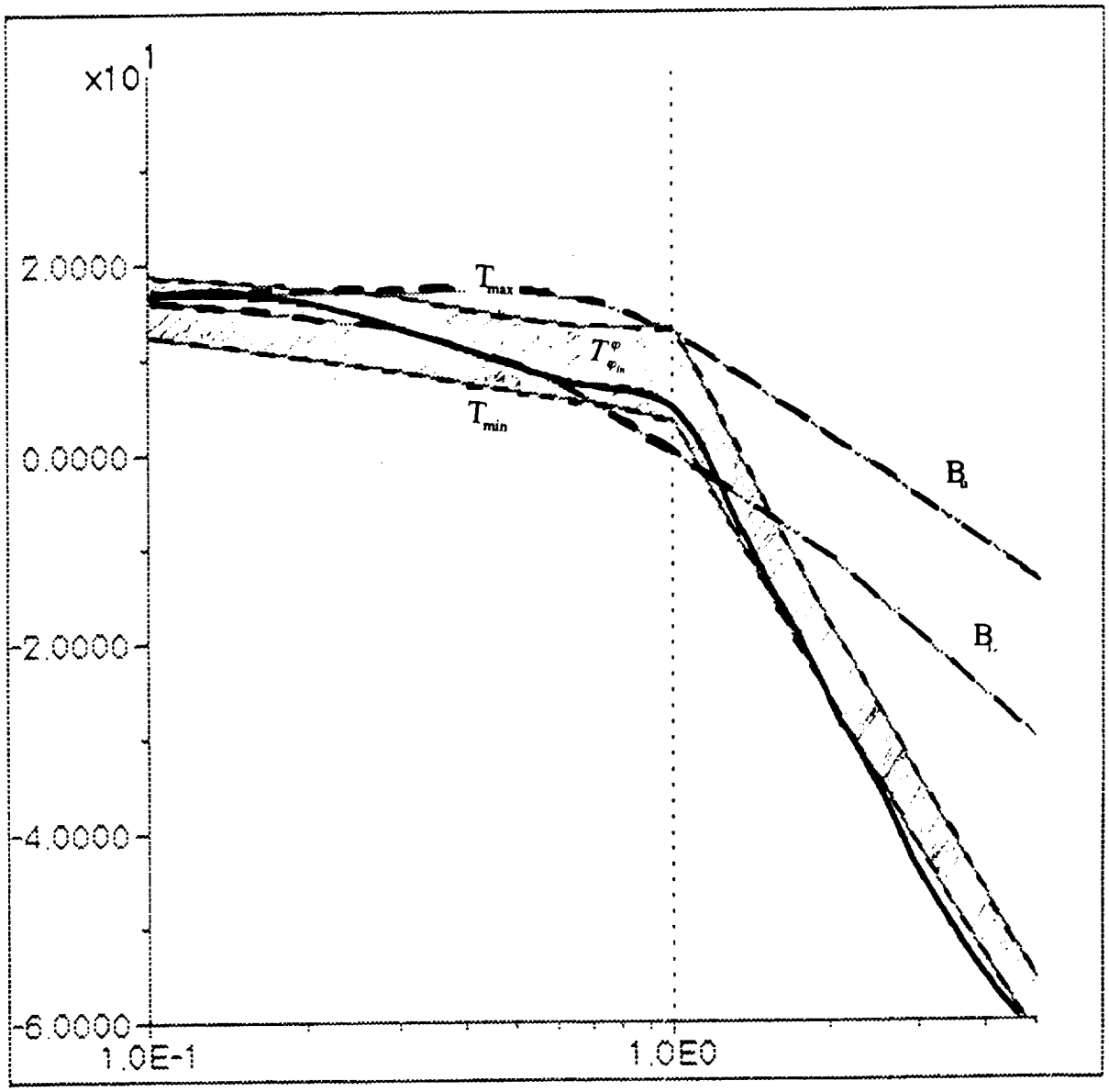

Figure 28. Frequency plot of the close-loop transfer function $T^{\phi}_{\phi_{in}}$ with prefilter

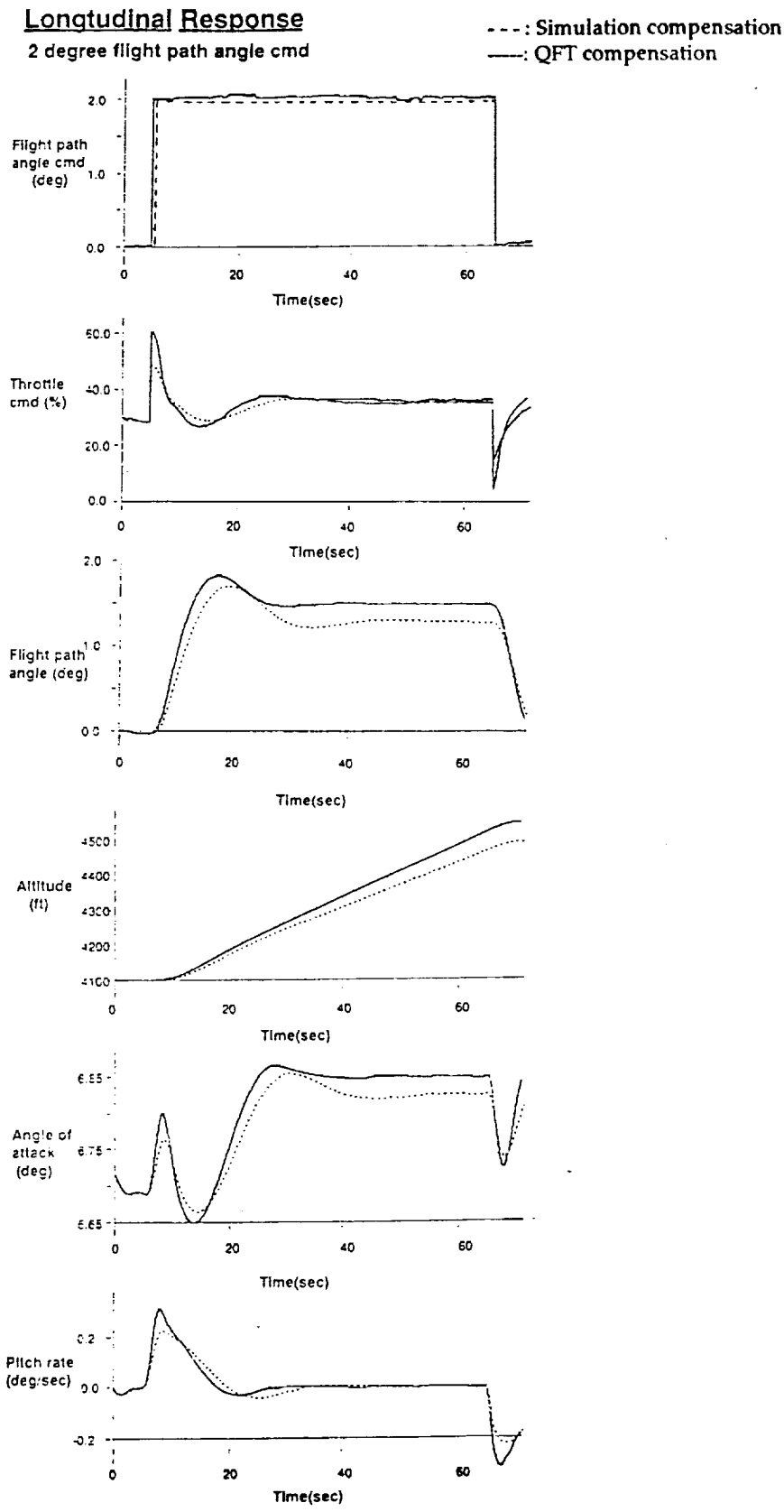

Figure 29. B-720 augmented control, step flight-path-angle response with no turbulence, nominal configuration

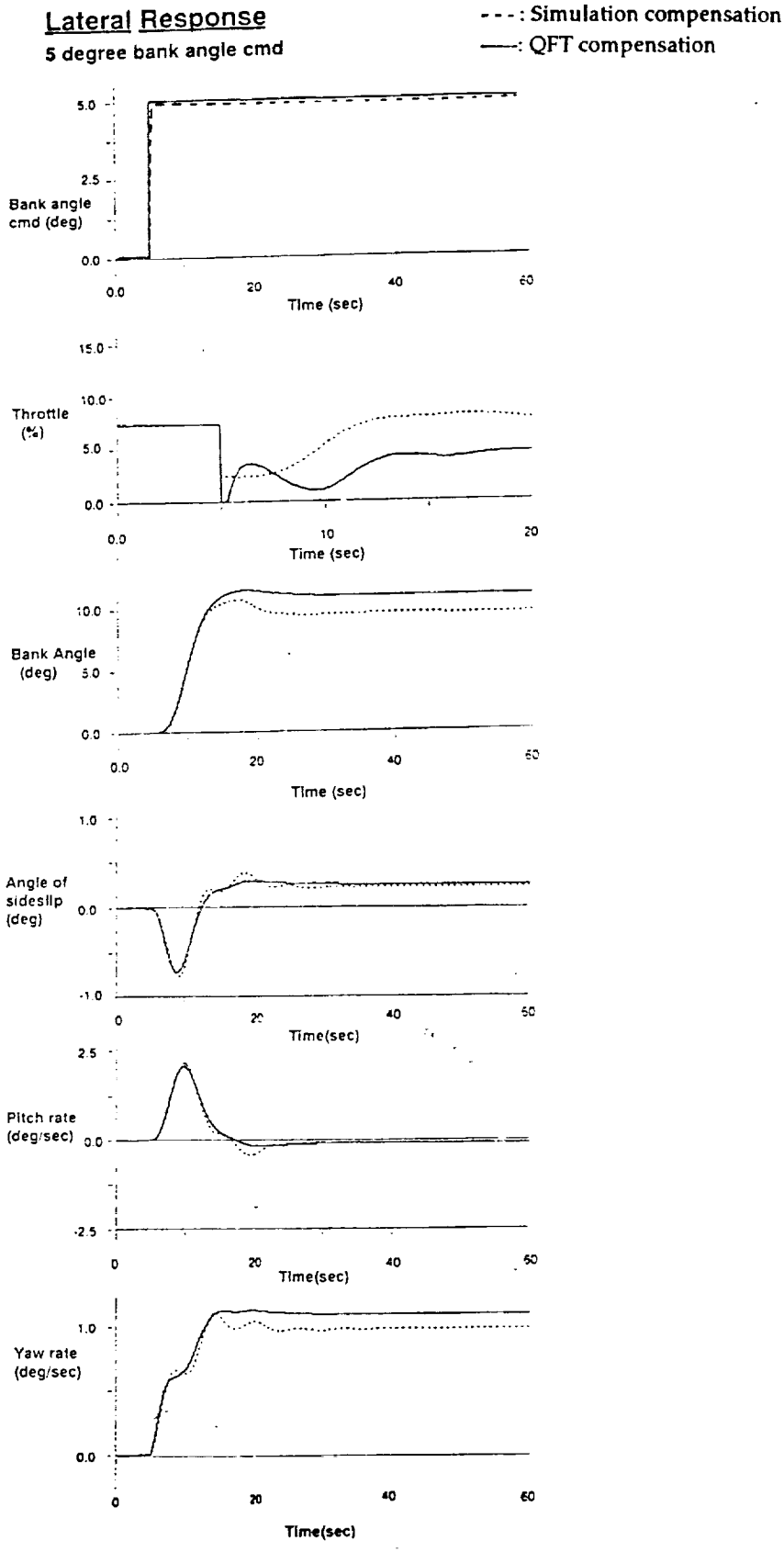

Figure 30. B-720 augmentedcontrol, step bank-angle response with no turbulence, nominal configuration

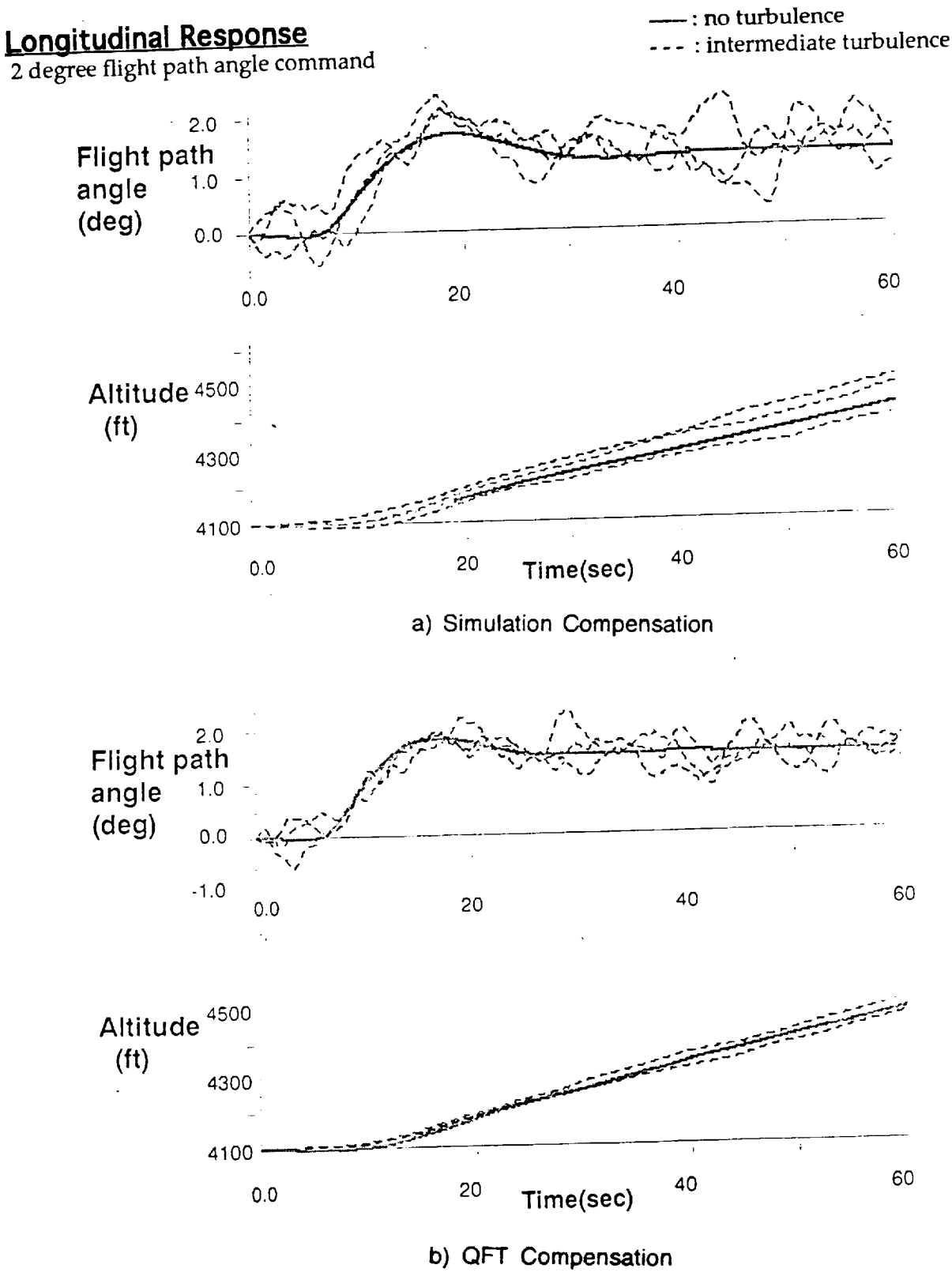

Figure 31. B-720 augmented control, step flight-path-angle response with turbulance, nominal configuration

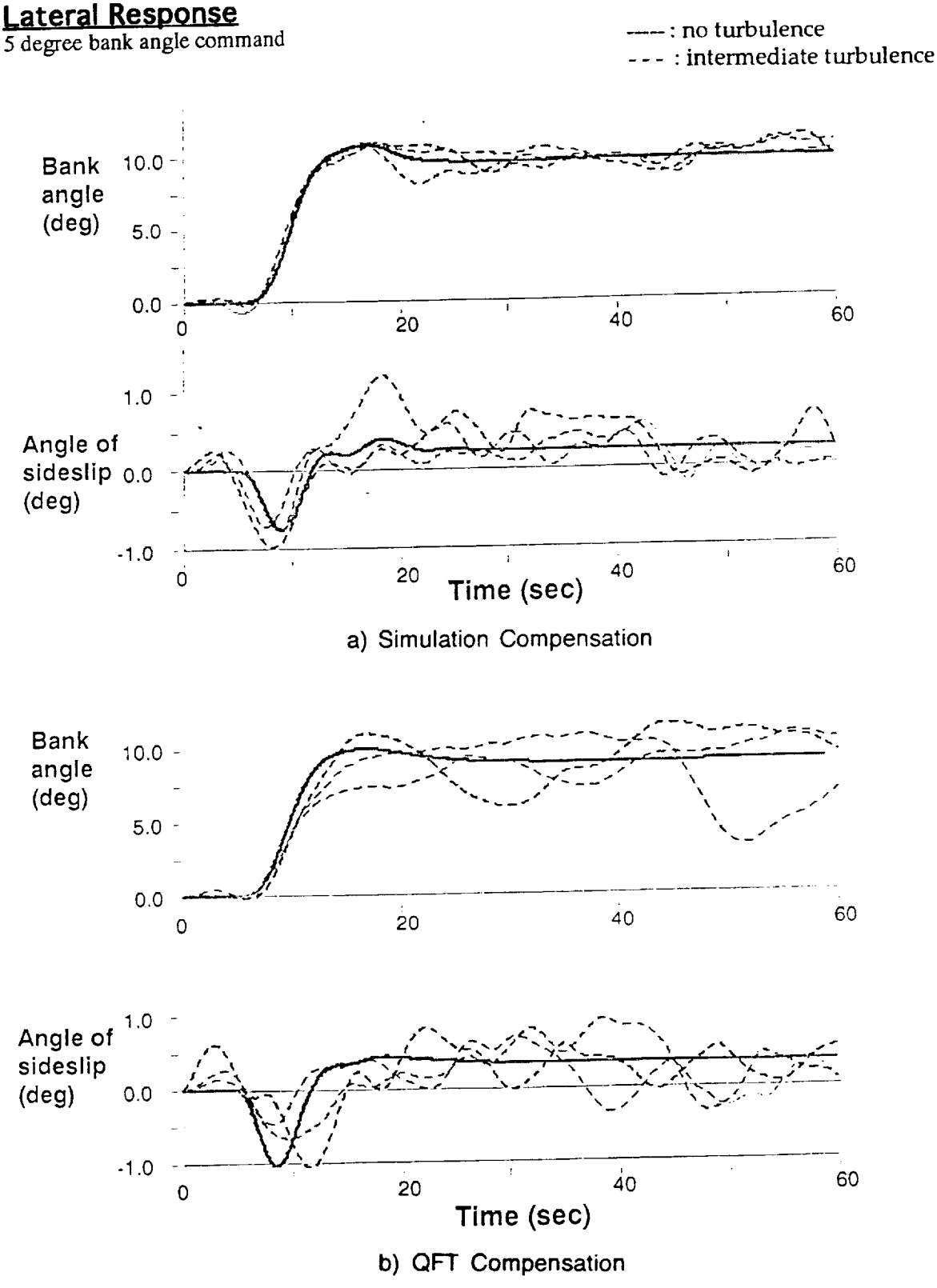

Figure 32. B-720 augmented control, step bank-angle response with turbulance, nominal configuration

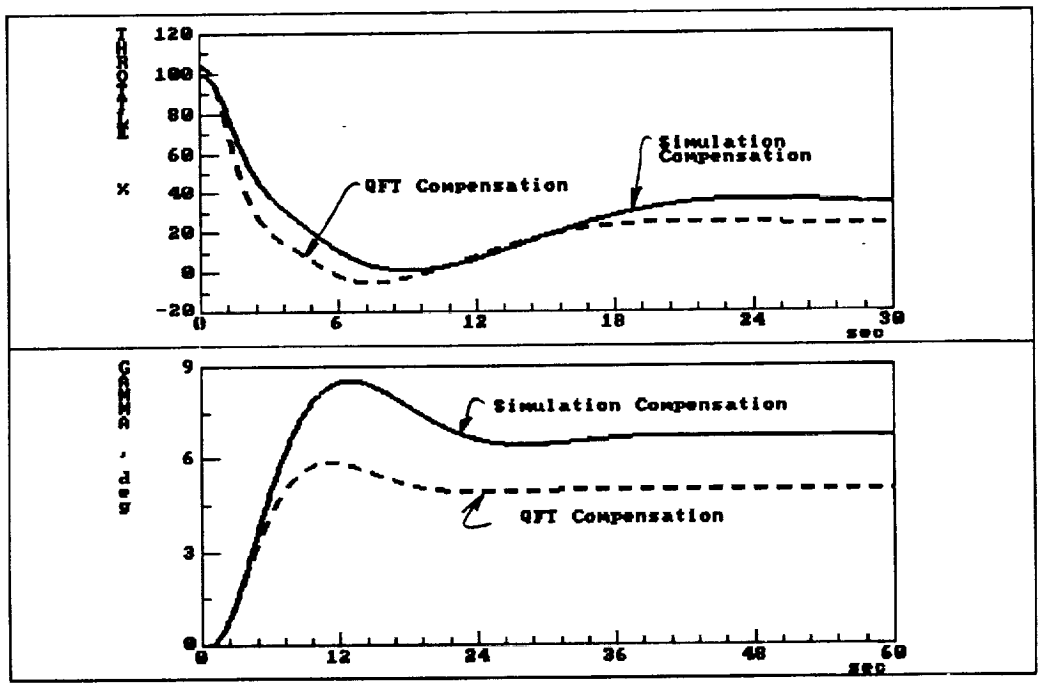

Figure 33. Flight-path-angle and throttle response to full-forward stick deflection, nominal configuration

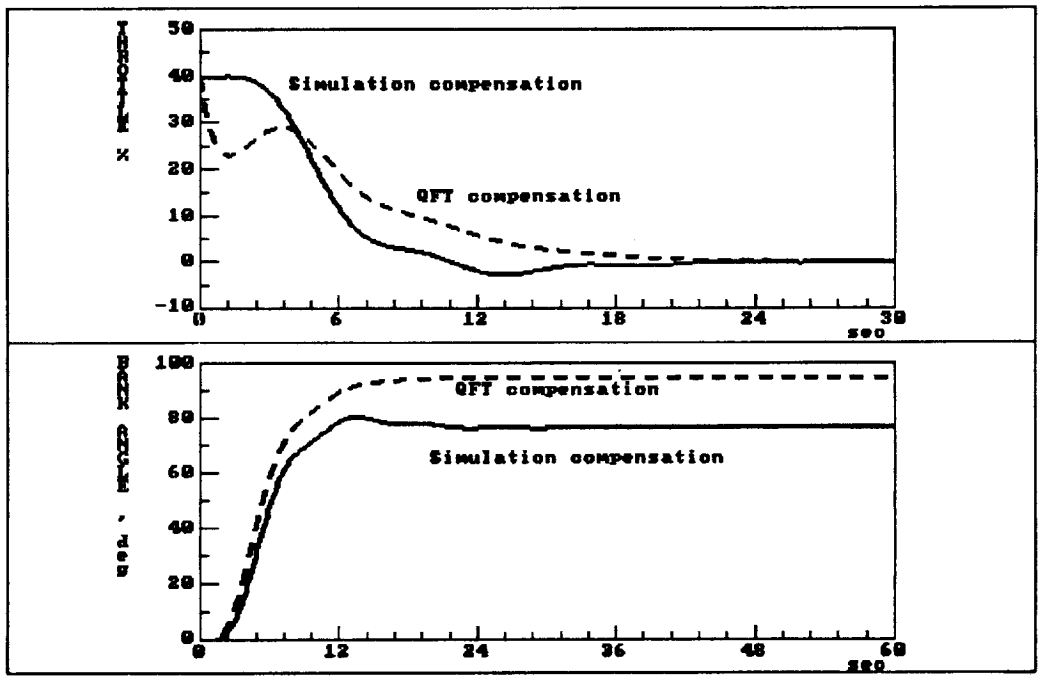

Figure 34. Bank-angle and throttle response to full-right stick deflection - QFT compensation, nominal configuration

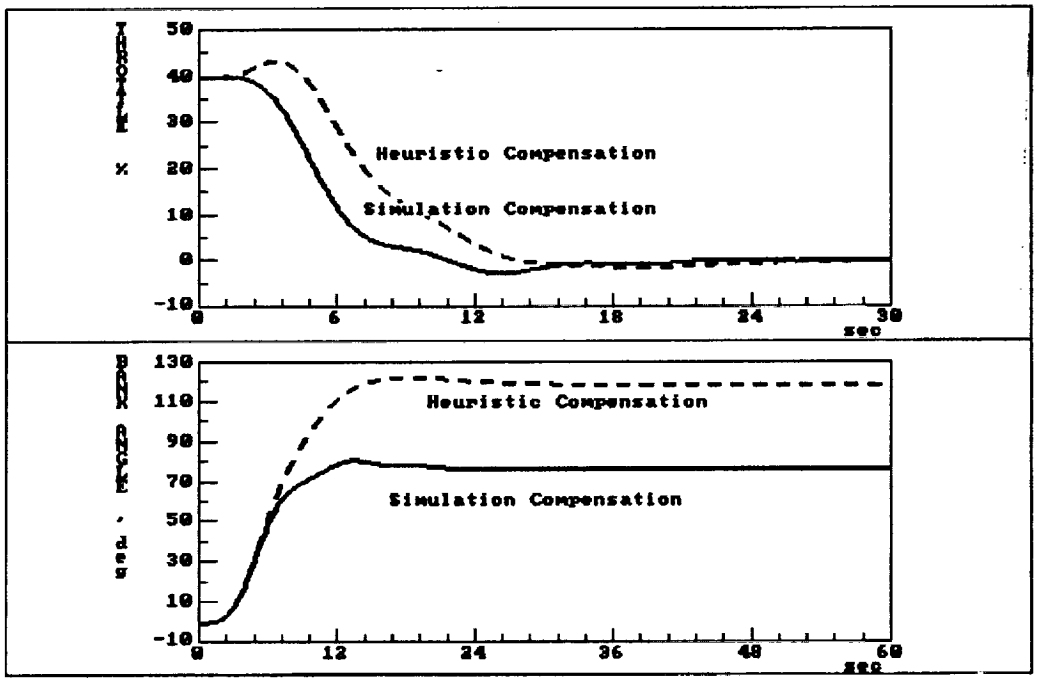

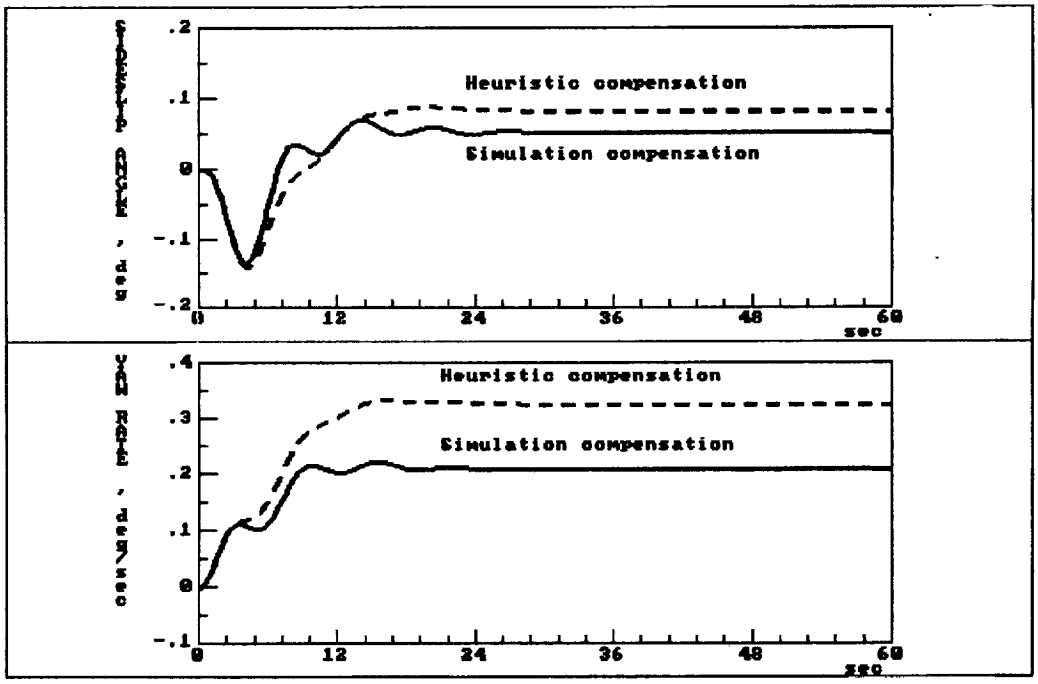

Figure 35. Response to full-right stick deflection - Heuristic compensation, nominal configuration

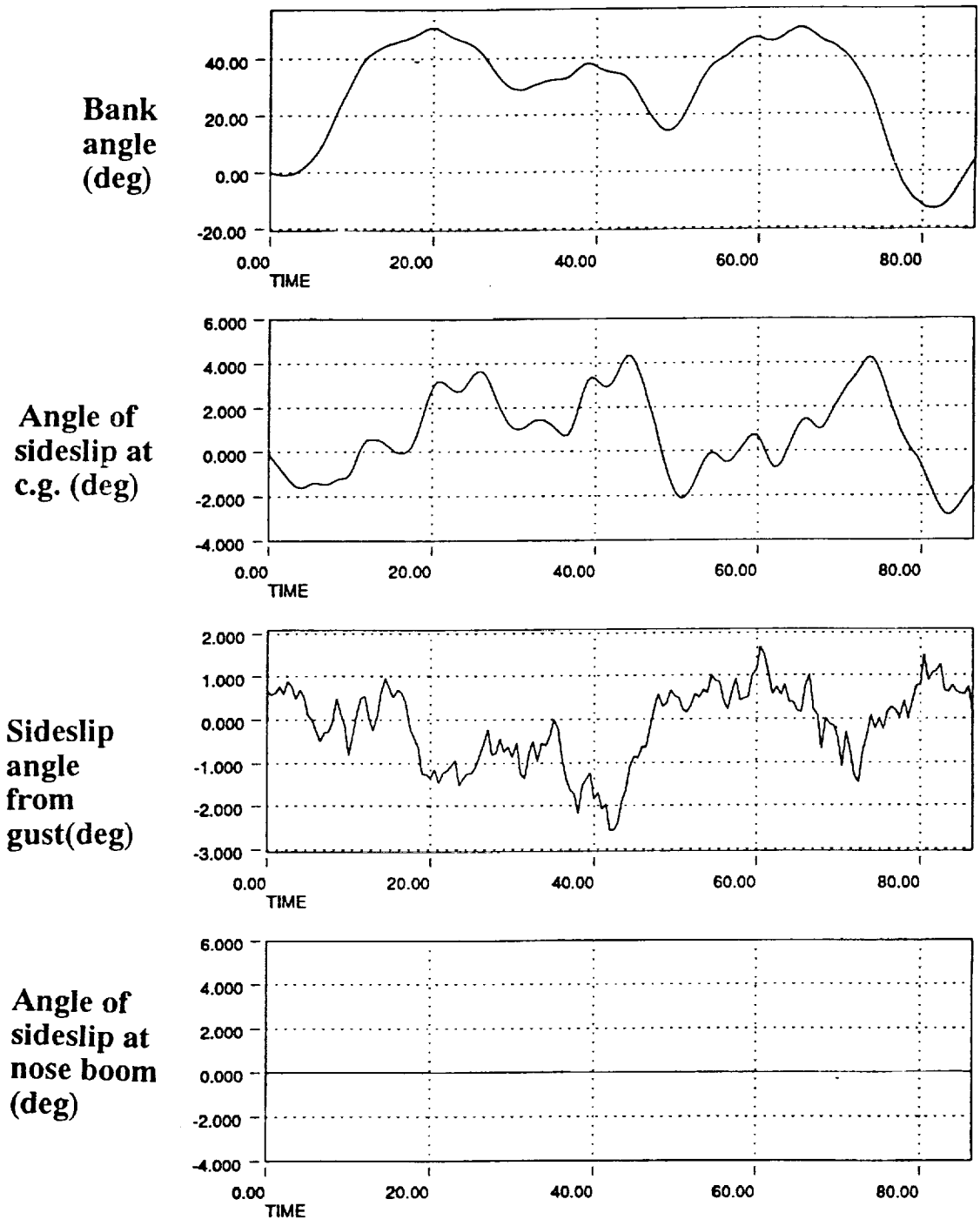

Figure 36. Bank-angle response under turbulance due to c.g. β

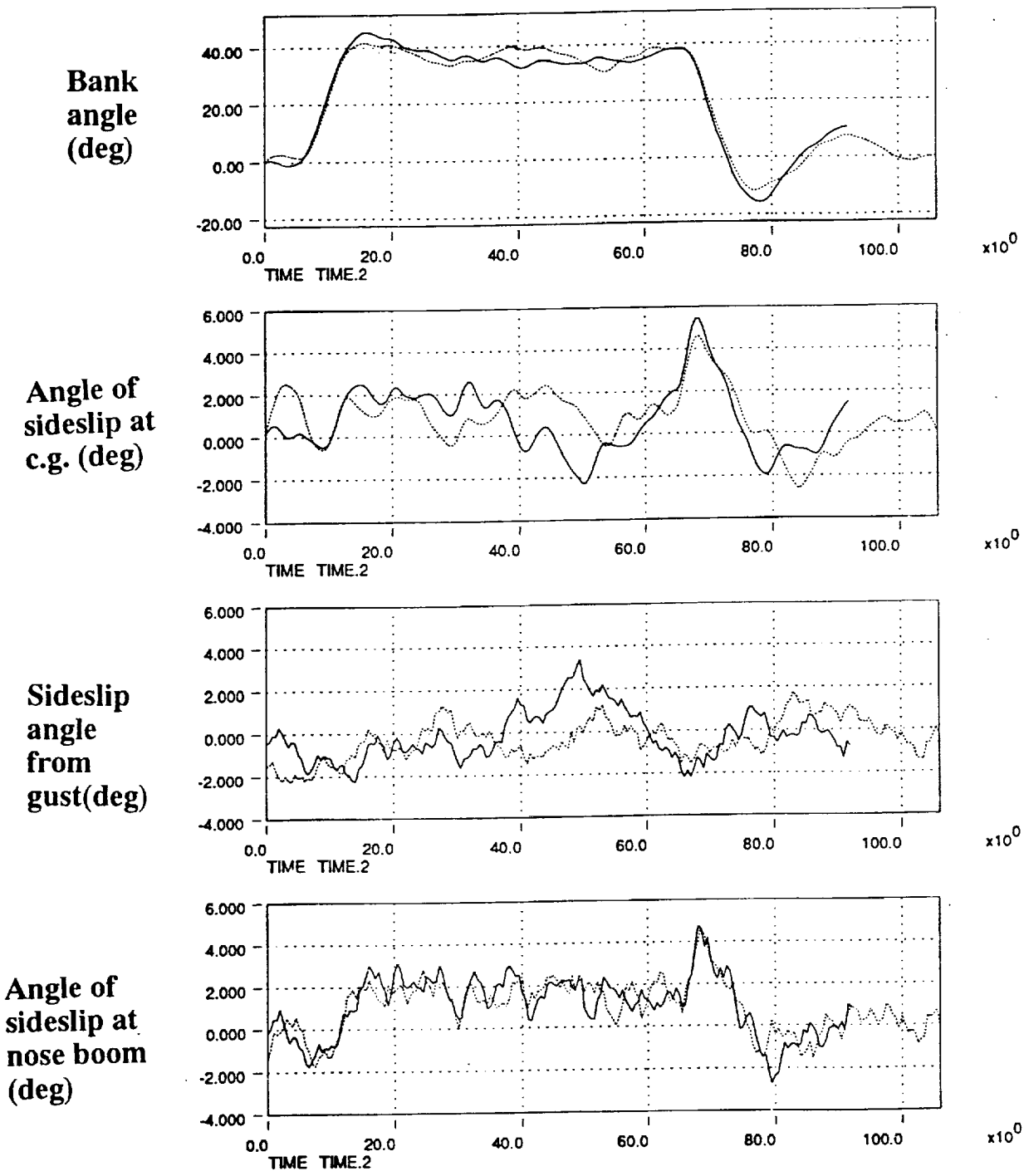

Figure 37. Bank-angle response under turbulence due to nose boom β

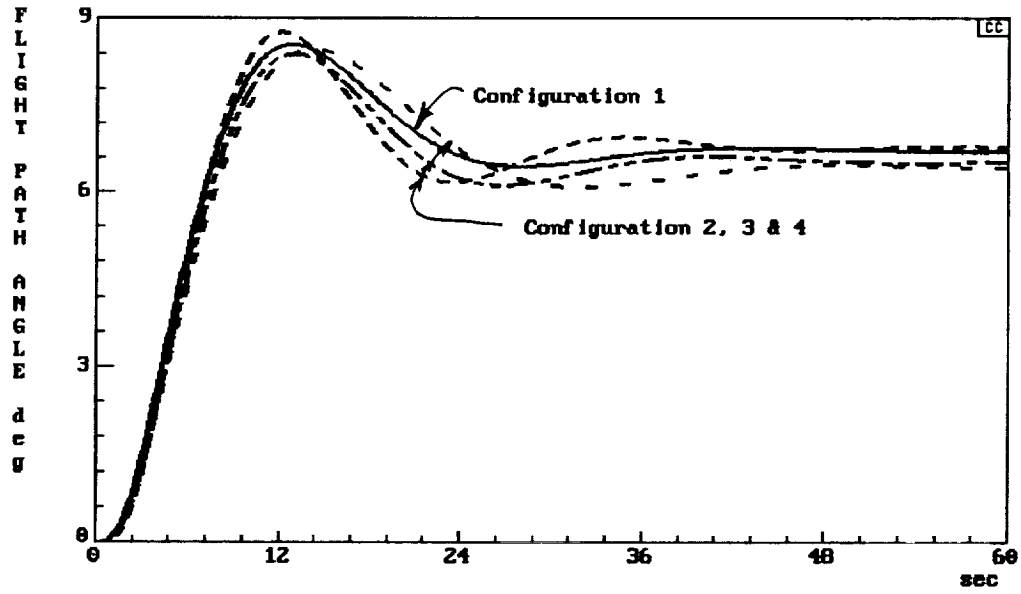

a) Simulation Compensation

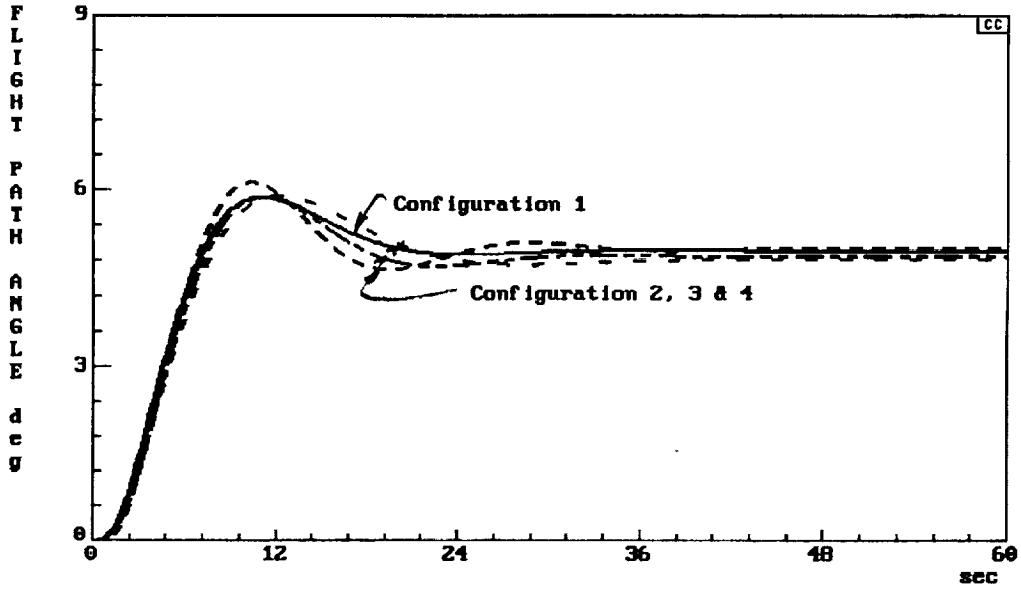

b) QFT Compensation

Figure 38. Robustness of the flight-path-angle control

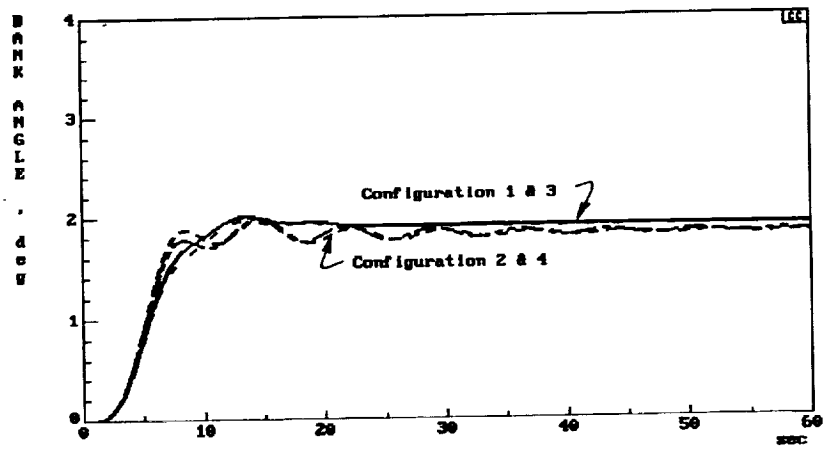

a) Simulation Compensation

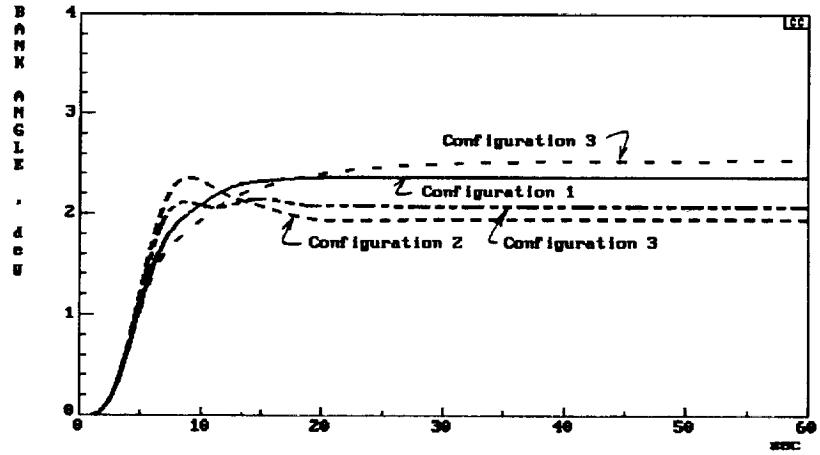

b) QFT Compensation

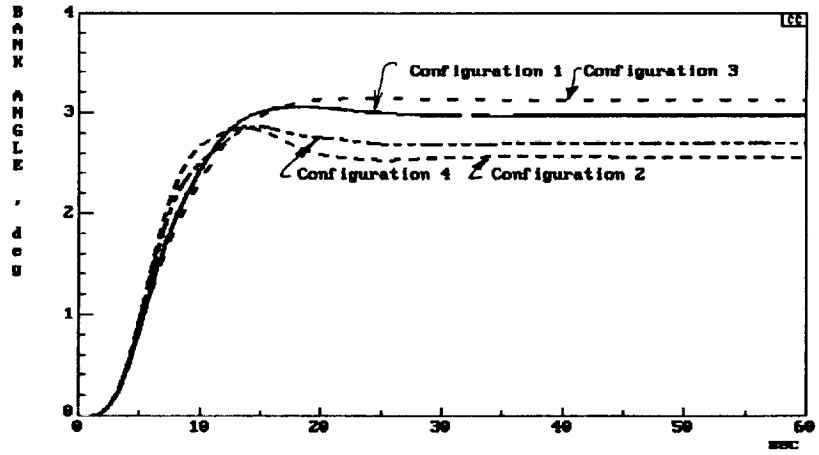

c) Heuristic compensation

Figure 39. Robustness of the bank-angle control

APPENDIX A: B-720 CONFIGURATIONS

The B-720 piloted simulation can be represented by the following block diagram:

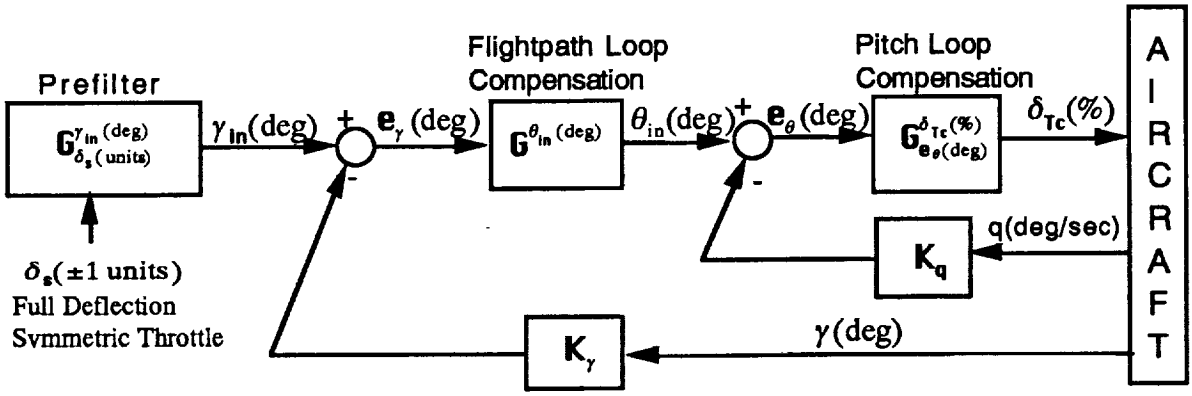

Flightpath Angle Control Simulation

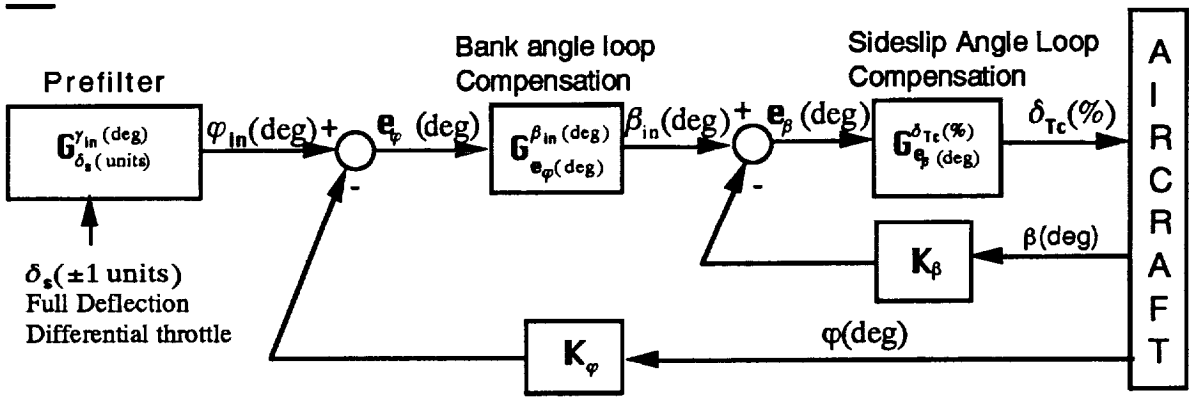

Bank Angle Control Simulation

The "AIRCRAFT" in the box above represents both the engine and the bare airframe dynamics. The engine is approximated by a transfer function, G_{eng}, and the bare airframe dynamics are represented mathematically by a single quadruple, $P_{a/c}$, shown as follows:

Longitudinal Dynamics

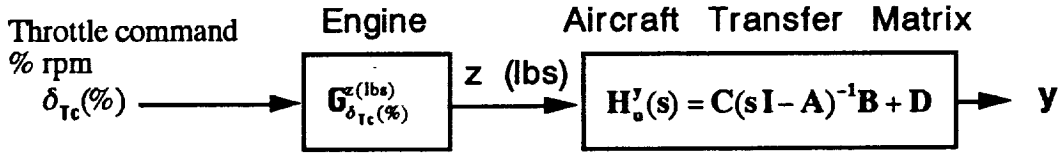

$$\mathbf{P}_{a/c} = \begin{bmatrix} \dot{x} \\ y \end{bmatrix} = \left[\begin{array}{c|c} A & B \\ \hline C & D \end{array}\right] \overset{\text{throttle inputs equal}}{=} \left[\begin{array}{c|c} A & B_1(\text{column}) \\ \hline C & D = 0 \end{array}\right]$$

$$\mathbf{x} = [q(\text{deg/sec}) \mid \alpha(\text{deg}) \mid v(\text{kts}) \mid \theta(\text{deg}) \mid h(\text{ft})]'$$

$$\mathbf{y} = [n_{\text{pilot g's}} \mid n_{\text{fcs g's}} \mid q \mid \alpha \mid v \mid \theta \mid h \mid \gamma(\text{deg})]'$$

$$\mathbf{u} = [z_{\text{outbd left}}(\text{lbs}) \mid z_{\text{inbd left}}(\text{lbs}) \mid z_{\text{inbd right}}(\text{lbs}) \mid z_{\text{outbd right}}(\text{lbs})]'$$

$\mathbf{u}_1 = z(\text{lbs})$ [used when all throttles have same command]

Lateral Dynamics

$$\begin{bmatrix} \dot{x} \\ y \end{bmatrix} = \left[\begin{array}{c|c} A & B \\ \hline C & D \end{array}\right] \begin{bmatrix} x \\ u \end{bmatrix} = \left[\begin{array}{c|c} A & B_2 \\ \hline C & D = 0 \end{array}\right] \begin{bmatrix} x \\ u_2 \end{bmatrix}$$

where

$$\mathbf{P}_{a/c} = \left[\begin{array}{c|c} A & B \\ \hline C & D \end{array}\right] \quad \text{.....for four engine inputs, u}$$

$$= \left[\begin{array}{c|c} A & B_2 \\ \hline C & D = 0 \end{array}\right] \quad \text{.....for one total engine input, } u_2$$

$$\mathbf{x} = [p(\text{deg/sec}) \mid r(\text{deg/sec}) \mid \beta(\text{deg}) \mid \phi(\text{deg})]'$$

$$\mathbf{y} = [A_{Y_{c.g.}} \mid p(\text{deg/sec}) \mid r(\text{deg/sec}) \mid \beta(\text{deg}) \mid \phi(\text{deg})]'$$

$$\mathbf{u} = [z_{\text{outbd left}}(\text{lbs}) \mid z_{\text{inbd left}}(\text{lbs}) \mid z_{\text{inbd right}}(\text{lbs}) \mid z_{\text{outbd right}}(\text{lbs})]'$$

$$\mathbf{u}_2 = [z(\text{lbs})]', \quad \text{where } z = z_{\text{outbd left}} + z_{\text{inbd left}} + (-z_{\text{inbd right}}) + (-z_{\text{outbd right}})$$

The B matrix has four columns, each column is to be multiplied by the thrust input from each engine that is given in matrix u. If symmetric throttle is given (assume all four throttles are given the same command), the **B** matrix in longitudinal dynamics becomes a single column. Each row value in this column matrix $\mathbf{B_1}$ is equal to the sum of the corresponding row elements in

the full order **B** matrix representing four engines. If differential throttle is given (i.e., the left engines and right engines are given same amount of command but in opposite directions), the **B** matrix in lateral dynamics becomes another single column matrix, $\mathbf{B_2}$. Each row element in $\mathbf{B_2}$ is the sum of the positive value of columns 1 and 2, and the negative value of columns 3 and 4 of each row in **B**. The open-loop configuration then becomes **P=Pa/c*Peng**, where **Peng** is the quadruple form of the engine transfer function, $G^{z(lbs)}_{\delta_{lc}(\%)}$. The quadruples for four different configurations were obtained as described in reference.

Flight conditions for each configuration are summarized in the following table.

Configuration Summary

Config. Number	Weight (lbs)	Altitude (Ft MSL)	Airspeed (Knots)	Flaps (%)	Gear up/down
1	140,000	4,000	160	0	up
2	140,000	4,000	145	30	up
3	160,000	4,000	175	0	up
4	140,000	4,000	155	30	up

The transfer functions were obtained from the quadruples using System Technology's Program CC. These aircraft transfer functions are listed here with each respective row of numbers designating the corresponding configuration transfer function values. The nominal configuration, number 1, is represented by values in each row 1 below.

Longitudinal Transfer Functions

$$N^{q(deg/sec)}_{z(lbs)} = N^{q(deg/sec)}_{z(lbs)} / \Delta_{long}$$

$$N^{\gamma(deg)}_{z(lbs)} = N^{\gamma(deg)}_{z(lbs)} / \Delta_{long}$$

$$N^{q(deg/sec)}_{z(lbs)} = \begin{array}{|cccc|} \hline 2.36E-04 & (0) & (-1.17E-05) & (0.40) \quad (0.61) \\ \hline 2.33E-04 & (0) & (1.4E-06) & (0.635 , \ 0.563) \\ \hline 1.976E-04 & (0) & (0.292) & (0.644) \\ \hline 1.955E-04 & (0) & (2.68E-06) & (0.819 , \ 0.508) \\ \hline \end{array}$$

$$N_{z(lbs)}^{\gamma(deg)} = \begin{array}{|c|c|c|c|c|} \hline 2.796E-05 & (0) & (0.203) & (0.370\ , & 3.008) \\ \hline -1.819E-05 & (0) & (0.364) & (2.255) & (-4.452) \\ \hline 2.130E-05 & (0.167) & (0.351\ , & 3.038) & \\ \hline 1.470E-05 & (0) & (0.261) & (0.460\ , 3.426) & \\ \hline \end{array}$$

$$\Delta_{long} = \begin{array}{|c|c|c|c|} \hline (1.438E-05) & (3.918E-02\ , & 0.130) & (0.652\ , \ 1.382) \\ \hline (1.101E-05) & (7.423E-02\ , & 0.147) & (0.596\ , \ 1.375) \\ \hline (3.949E-02\ , & 0.118) & (0.649\ , & 1.301) \\ \hline (1.878E-05) & (7.190E-02\ , & 0.138) & (0.588\ , \ 1.279) \\ \hline \end{array}$$

Lateral Transfer Functions

$$N_{z(lbs)}^{\beta(deg)} = N_{z(lbs)}^{\beta(deg)} / \Delta_{lat}, \qquad N_{z(lbs)}^{\beta(deg)} = \begin{array}{|c|c|c|} \hline -1.58E-03 & (-.0805) & (.927) \\ \hline -1.59E-03 & (-.0922) & (.904) \\ \hline -1.43E-03 & (-.0723) & (.981) \\ \hline -1.44E-03 & (-.0879) & (.940) \\ \hline \end{array}$$

$$N_{z(lbs)}^{\phi(deg)} = N_{z(lbs)}^{\phi(deg)} / \Delta_{lat}, \qquad N_{z(lbs)}^{\phi(deg)} = \begin{array}{|c|c|} \hline 3.19E-04 & (.468\ , 3.65) \\ \hline 2.15E-04 & (.611\ , 4.17) \\ \hline 2.89E-04 & (.447\ , 3.96) \\ \hline 2.04E-04 & (.593\ , 4.33) \\ \hline \end{array}$$

$$\Delta_{lat} = \begin{array}{|c|c|c|} \hline (.0001) & (1.01) & (.116\ , 1.05) \\ \hline (.006) & (1.05) & (.067\ , 0.93) \\ \hline (.0028) & (1.06) & (.114\ , 1.08) \\ \hline (.0065) & (1.09) & (.060\ , .944) \\ \hline \end{array}$$

The engine transfer function for all configurations is given in short form notation by:

$$G_{\delta_{th}(\%)}^{z(lbs)} = \frac{275}{(0.55)(5)}$$

Configuration Storage Table for Quadruples

*Pxxxx.4U : Quadruple with four engine inputs

*Pxxxx.1U : Quadruple with one total engine input

Dynamics	Config. Number	Quadruple **Pa/c**	Quadruple **Pa/c*Peng**
Longitudinal	1 1	P1000.4U P1000.1U	- P100
Longitudinal	2 2	P2000.4U P2000.1U	- P200
Longitudinal	3 3	P3000.4U P3000.1U	- P300
Longitudinal	4 4	P4000.4U P4000.1U	- P400
Lateral	1 1	P5000.4U P5000.1U	- P500
Lateral	2 2	P6000.4U P6000.1U	- P600
Lateral	3 3	P7000.4U P7000.1U	- P700
Lateral	4 4	P8000.4U P8000.1U	- P800

APPENDIX B: PAPERS PRODUCED IN SUPPORT OF THIS GRANT

1. Biezad, D.J. and C.P. Azzano. "Designing Low Bandwidth Propulsive-Only Flight Controllers." AIAA Guidance, Navigation, and Control Conference Paper No. 91-2628CP. New Orleans, LA. August 12-14, 1991. 267-275.

2. Biezad, D.J. "The Propulsive-Only Flight Control Problem." National Aerospace Electronics Conference, Vol. 2. Dayton, OH. May 20-24, 1991. 494-500.

3. Biezad, D.J. and H.L. Chou. "Pilot-in-the-Loop Analysis of Propulsive-Only Flight Control Systems." NAECON, Vol. 2. Dayton, OH. 482-488.

4. Biezad, D.J. and H.L. Chou. "Application of QFT to the Problem of Failed In-Flight Controllers During Approach and Landing of a B-720 Aircraft." To be presented at NAECON 93. Dayton, OH. May 24-28, 1993.

DESIGNING LOW BANDWIDTH PROPULSIVE-ONLY FLIGHT CONTROLLERS

Daniel J. Biezad*
Cal Poly State University
San Luis Obispo, California

Christopher P. Azzano
Lieutenant, United States Air Force

Abstract

Results from an investigation of using engine commands to control flight attitude are described. In-flight operation with simulated failed flight controls is reviewed and ground simulations of piloted propulsive-only control to touchdown are analyzed. A design of an optimal control law to assist the pilot is presented. Recommendations are made for more robust design and implementation. Results to date indicate that simple and effective augmented control can be achieved in a wide variety of failed configurations.

Nomenclature

α	perturbed angle of attack (deg)
β	perturbed sideslip (deg)
γ	perturbed flight path angle (deg)
ϕ	perturbed bank angle (deg)
Γ_{cmd}	glide slope commanded (deg)
ε	glide path deviation angle (deg)
λ	lateral path deviation (deg)
e_T	perturbed throttle (%)
d	deviation above glide path (ft)
h	altitude change--down (ft)
p	roll rate (deg / sec)
q	pitch rate (deg / sec)
r	yaw rate (deg / sec)
K_x	feedback gain for x
G_{in}^{out}	transfer function (s)

Introduction

Propulsive controls which assist conventional control surfaces in the attitude control of aircraft have been recognized as important enhancements of combat aircraft maneuverability[1]. In commercial operations such maneuverability is seldom required, but in the event of hydraulic failure of controls or damage to control surfaces, the engines of a large commercial aircraft are usually capable of attitude control. Recent flight control failures on commercial aircraft, although extremely rare, have shown that piloted aircraft can remain controllable in-flight by the skillful application of thrust.[2,3] The extreme difficulty of this task, however, combined with pilot stress, cannot be expected to result in a successful landing.

An investigation of propulsive-only flight control by NASA Dryden[4,5] has shown it to be feasible for a wide variety of aircraft types and failure configurations. The list of aircraft flown include the Lear 24, Cessna 152, Piper PA-30, and the F-15 (single-engine aircraft required that the rudder be used in addition to the throttle). None of the in-flight tests were flown to touchdown. Pilot ratings were categorized by controlled axis and by task. Typically, longitudinal axis control was rated Level 2 for the approach and Level 3 for runway landing. Lateral axis control was rated Level 2 for both approach and landing. The pilot learning curve in all cases was rapid.

Although controlled flight was always possible, pilots could not safely and predictably maneuver with the throttles alone. There may be sufficient control power available (presuming the throttles are advanced from idle), but the typically long time constants and couplings between dynamic modes make piloted flight precarious for demanding tasks such as landing. Training may alleviate the gross misapplication of throttles but will not guarantee safe landings.

A pilot-assist mode which automatically moves the throttles in order to control attitude is a potential solution. Such a mode would be activated by the pilot in the event of complete or partial failure of the high bandwidth pitch and roll controls. This presumes that the engine power settings and aircraft geometry provide controllability under a variety of aircraft

*Associate Professor, Aerospace Engineering
Member AIAA

configurations, failure modes, and power settings.

Because of the long time constants of the engines relative to those of the contol surface actuators, low-bandwidth control will be most effective for the long-period dynamic modes of the aircraft. This implies the basic airframe with failed controls should exhibit minimal stability handling qualities in flight[6].

This paper will concentrate on the major considerations in designing a propulsion-only flight control system (POFCS). The empirical results of ground simulations using a Boeing 720 will be reviewed,[7] and finally an optimal linear design of the POFCS will be presented.[8] The paper concludes with some recommendations for future work.

Ground Simulation

Fixed-base simulations of a Boeing 720 aircraft were performed at NASA Dryden to investigate throttles-only control. The Boeing 720 represents a four-engine passenger jet aircraft as shown in Figure 1. Asymetric thrust is available for roll control, but the aircraft has slow responding engines. Pitch control was obtained by simultaneously advancing or retarding the throttles. A view of the simulator scene for approach and landing is shown in Figure 2.

The Boeing 720 has a low wing with 35 degrees of sweep. Gross attitude control in both the longitudinal and lateral axes during the simulation was possible without the use of electric trim.

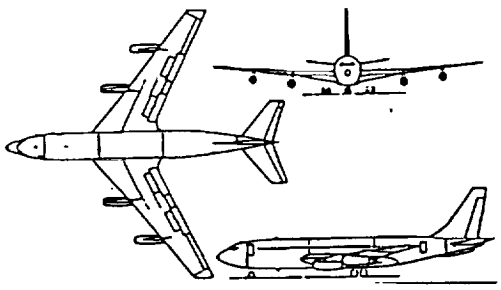

Figure 1. Boeing 720

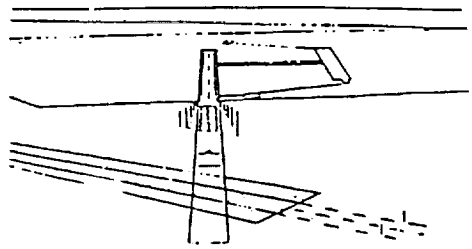

Figure 2. Simulation Visual

Low Bandwidth Control Law

A propulsion-only flight control system (POFCS) must use the control power of the engines, assuming a stable basic airframe, to provide longitudinal and lateral flight path control under a variety of flight control failures throughout the flight envelope.

Pilots must relearn how to generate lead compensation. There are no handling qualities specifications to cover this situation. The pilot may find it difficult to accept watching the throttles move with stick input The control law must allow pilot inputs and pilot-directed configuration changes without exciting large oscillations of the dutch roll or phugoid.

The engine time constants must be fast enough to control any oscillatory mode which could preclude a successful landing. Relatively fast modes, such as the short period, must be stable. In other words, the configuration with failed controls, throughout the flight envelope, must be stabilizable (the uncontrollable poles must be stable).[9]

Boeing 720 Control Law The baseline configuration was gear-up, flaps-up, 10,000 ft pressure altitude, 160 knots, 190,000 lbs. The baseline control law for the four engine jet transport, for both the longitudinal and the lateral axis, was developed by trial and error in the flight simulator at NASA Dryden.[7] The baseline gains corresponding to Figures 3 and 4 were

$$\{K_q, K_\theta, K_\gamma, K_p, K_\phi, K_\beta\} = \{-4, 0, -1, 0.5, 1.0, 0.5\}$$

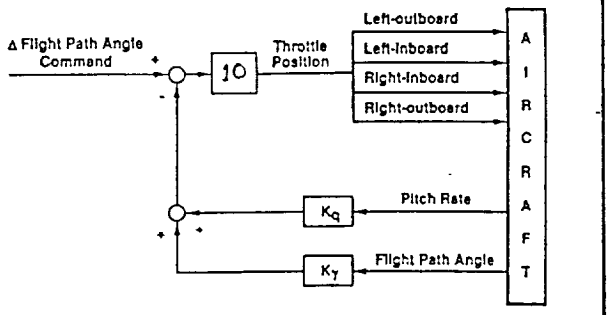

Figure 3. Flight Path Angle Control

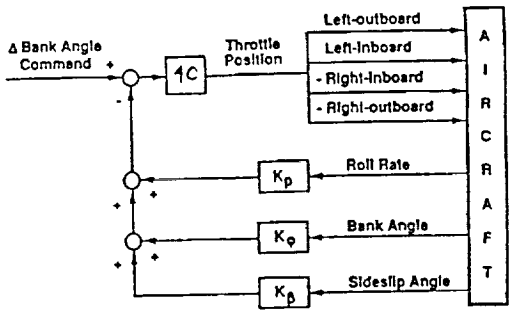

Figure 4. Bank Angle Control

As described in reference 7, ten configurations were then flown with the above set of baseline gains. The worst ratings were for those configurations farthest from the baseline weight of 190,000 lbs. Pilot comments for poorly rated configurations indicated the problem to be severe lateral oscillations that could not be damped predictably by pilot inputs.

Classical Analysis. Linearized models of the longitudinal mode coupled to the glide path by K_ε are shown in Figures 5-7 and may be analyzed in a conventional manner as described by Blakelock.[10] The range to touchdown must be fixed for a linear analysis. Such an analysis shows that the baseline gains chosen are satisfactory longitudinally to ranges within 1000 ft of touchdown.

The lateral mode of coupled flight, however, shows an interesting feature. A two dimensional root locus for the lateral modes of response, varying K_p and K_ϕ , is illustrated in Figure 8. Note the difficulty in selecting these gains using conventional analysis. The lateral response mode has a lateral phugoid in addition to a dutch roll mode. Families of plots of these two pairs of complex roots show that varying either gain pushes one set of roots into the right-half plane. This effect of varying configurations exacerbates this tendency.

Normally, given conventional flight controls, the pilot could compensate for this type of mild and slow instability. Throttles only control, however, even with an augmented system, make such compensation extremely difficult for the pilot. Piloted simulations show that pilots are sensitive to any gain set significantly away from the nominal settings.

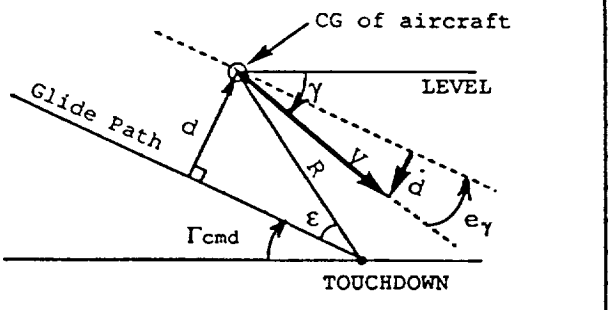

Figure 5. Glide Slope Geometry

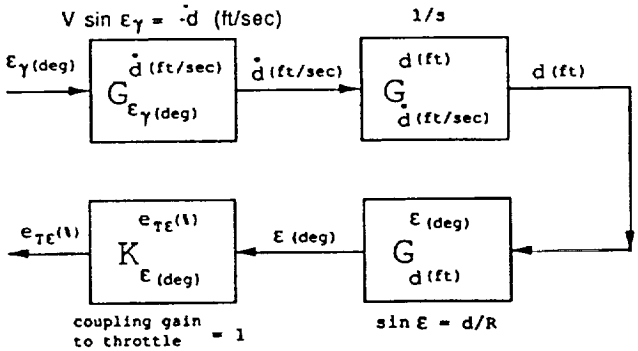

Figure 6. Glide Slope Block Diagram

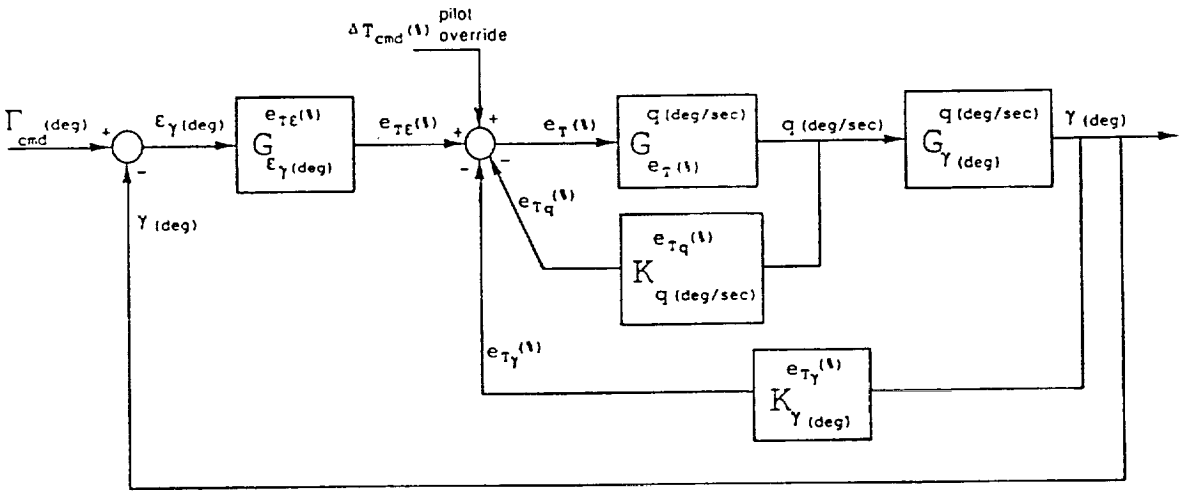

Figure 7. Longitudinal Aircraft Coupled to Glide Path

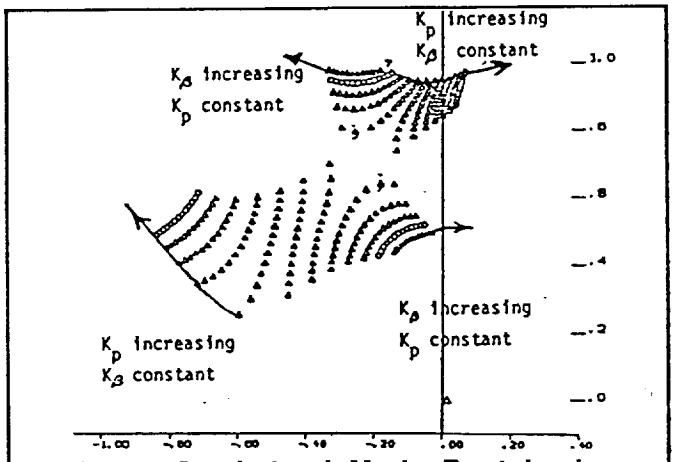

Figure 8. Lateral Mode Root Loci

Optimal Control Law

A Linear Quadratic Regulator (LQR) was developed with modal weights chosen to provide robust behavior.[8] Although this choice results in a complex feedback structure with some loss of insight relative to successive loop closure, the opportunity to use all four engines independently was considered important in a flight control system with such degraded performance. In particular, this provided the capability to control pitch and velocity independently since the thrust lines of the outboard and inboard engines have unequal displacements along the z-body axis. To see this mathematically it is necessary to compare the eigenvalues of the controllability matrix (which is not done here).

Modal Regulator Equations. The regulator consisted of the following feedback control law:

$$\dot{\mathbf{x}}_m = \mathbf{M}^{-1}\mathbf{A}\mathbf{M}\mathbf{x}_m + \mathbf{M}^{-1}\mathbf{B}\mathbf{u} \qquad (1a)$$

$$\mathbf{u} = \mathbf{K}_m\mathbf{x}_m = \mathbf{K}_m\mathbf{M}^{-1}\mathbf{x} \qquad (1b)$$

minimizing

$$J = 1/2\int(\mathbf{x}^T\mathbf{M}^T\mathbf{Q}\mathbf{M}\mathbf{x} + \mathbf{u}^T\mathbf{R}\mathbf{u})dt \qquad (1c)$$

$$\mathbf{Q}_m = \mathbf{M}^T\mathbf{Q}\mathbf{M} \qquad (1d)$$

where the subscript m indicates modal coordinates with modal weights Q_m assigned directly to aircraft dynamic modes such as the phugoid. The state variables for the regulator design are

$$\mathbf{x}^T = [q, \alpha, u, \theta, h, p, q, r, \beta, \phi \quad]^T \qquad (1e)$$

where all units are radians, feet, and seconds, and where the control is given by

$$\mathbf{u} = [\text{four throttles}] \qquad (1f)$$

The LQR design condition was 4,000 ft MSL, 175 KCAS, 160,000 lbs, with gear and flaps up. The plant, throttle control, and feedback matrices for this condition (cg 20.85% MAC) are given in Figure 9.

$$A = \begin{array}{c|ccccc|cccc} q & \alpha & u & \theta & h & p & r & \beta & \phi \\ \hline -.89 & -.98 & .00011 & 0 & 0 & 0 & 0 & 0 & 0 \\ 1 & -.79 & -.00065 & 0 & 0 & 0 & 0 & 0 & 0 \\ 0 & 13 & -.012 & -32 & 0 & 0 & 0 & 0 & 0 \\ 1 & 0 & 0 & 0 & 0 & 0 & 0 & 0 & 0 \\ 0 & -312 & 0 & 312 & 0 & 0 & 0 & 0 & 0 \\ \hline 0 & 0 & 0 & 0 & 0 & -.99 & .55 & -3. & 0 \\ 0 & 0 & 0 & 0 & 0 & -.053 & -.21 & .76 & .0021 \\ 0 & 0 & 0 & 0 & 0 & .11 & -.98 & -.11 & .1 \\ 0 & 0 & 0 & 0 & 0 & 1 & .11 & 0 & 0 \end{array}$$

$$B = 10^{-5} \begin{array}{cccc} \text{Outboard Left (\%)} & \text{Inboard Left (\%)} & \text{Inboard Right (\%)} & \text{Outboard Right (\%)} & \\ \hline 5.1 & 12 & 12 & 5.1 & q \\ -.9 & -.9 & -.9 & -.9 & \alpha \\ 2000 & 2000 & 2000 & 2000 & u \\ 0 & 0 & 0 & 0 & \theta \\ 0 & 0 & 0 & 0 & h \\ 6.8 & 4 & -4 & -6.8 & p \\ 80 & 47 & -47 & -80 & r \\ 0 & 0 & 0 & 0 & \beta \\ 0 & 0 & 0 & 0 & \psi \end{array}$$

$$K = K_m M^{-1} = \text{Feedback Gains (\%)} =$$

q	α	u	θ	h	p	r	β	ϕ	
594	-467	2.6	780	0	93.9	584	91.6	125	Outboard Left
1750	-1290	2.1	2345	0	55.3	344	54.0	73.4	Inboard Left
1750	-1290	2.1	2345	0	-55.3	-344	-54.0	-73.4	Inboard Right
594	-467	2.6	780	0	-93.9	-584	-91.6	-125	Outboard Right

Figure 9. LQR Plant, Control, and Feedback Matrices for Design Configuration

The insight gained by using modal cost weights can effectively be seen by comparing the open and closed-loop responses of sideslip to an initial sideslip of 10 degrees, as shown in Figure 10. One of the penalties of this approach, however, was the normalization of units so that weights in the cost function did not differ by many orders of magnitude.

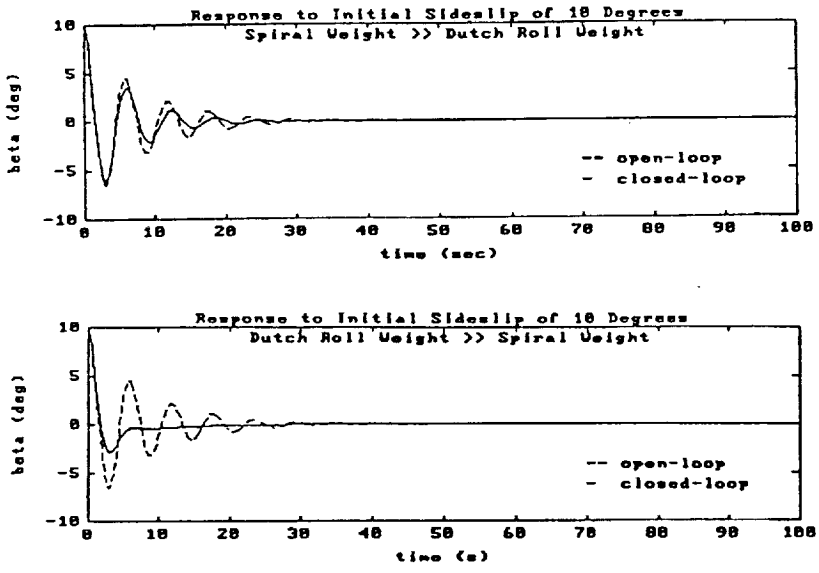

Figure 10. Cost Function Weights Trade-offs (Spiral/Dutch Roll)

Increasing weights on the dynamic modes provided tighter control, but performance suffered when the configurations were altered. This issue of robustness did not exist for the short period or roll modes since they were difficult to realistically excite by the engines, especially when engine lag was taken into account.

The final gain matrix in Figure 9 eliminated state feedbacks for altitude,h, and for the engine model states described in the section below with no adverse effects.

Engine Model. The values in the **B** matrix were obtained from steady-state perturbations in response to thrust. In order to use % throttle position,e_T, and not pounds of thrust in the control **u** of Equation (1f), the **A** matrix was augmented with a second order engine model of the form

$$\begin{bmatrix}\dot{T}\\ \ddot{T}\end{bmatrix}=\begin{bmatrix}0 & 1\\ -\omega^2_n & -2\zeta\omega_n\end{bmatrix}\begin{bmatrix}T\\ \dot{T}\end{bmatrix}+\begin{bmatrix}0\\ K_{T_{ss}}\end{bmatrix}e_T \qquad (2)$$

where ω^2_n=2.5, ζ=.802, and $K_{T_{ss}}$=250. These parameters were chosen to match engine transients at a nominal steady-state throttle setting of 20%. The transfer function form of the engine transient was

$$G^T_{e_T}=\frac{100\cdot 0.55\cdot 5.0}{(s+0.55)(s+5.0)} \qquad (3)$$

The conservative engine model of Equation(2) overestimated the gain $K_{T_{ss}}$ so the controller would not de-stabilize the system by acting on a low authority plant. Equation (3), on the other hand, is accurate for most steady-state conditions on approach.

System Dynamics. The aircraft and engine models were normalized as described above by the factors shown below in Table 1.

Table 1. Normalization Factors

Dimension	Units	Factor
Angle	Radians	.001
Force	Pounds	5906
Distance	Feet	1
Throttle	Percent	0.1

The weights for the dynamic modes given the normalization factors are shown in Table 2.

Table 2. LQR Weights

Mode	Weight	Period (sec)	ζ
Short Period	1	10	0.7
Phugoid	10	57	0.01
Dutch Roll	200	6.1	0.10
Spiral	0.5	68	...
Roll	1	1.2	...

The discrete version[11] of this system at 50 Hz has the open and closed-loop system roots as shown in Figure 11.

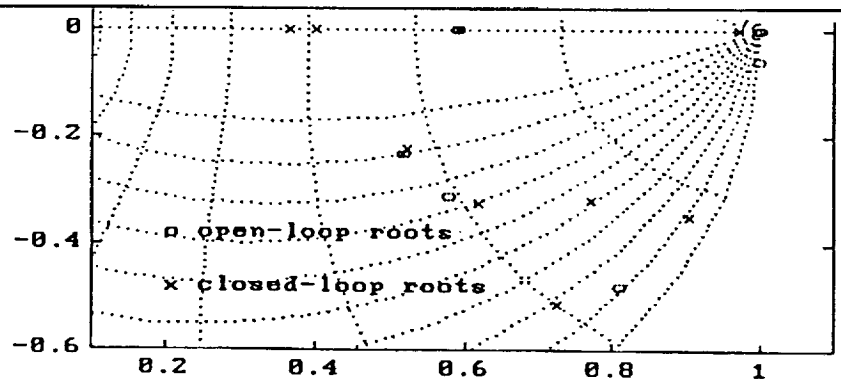

Figure 11. Discrete System Roots at 50 Hz

Pilot Command Interface. A command interface was designed into the LQR loop based on a pseudo rate command for both pitch and roll. This allowed a "batch" test of the linear system prior to implementing the control law on the hi-fidelity nonlinear simulation.

Control authority that would not hinder or "wash out" pilot commands was provided by translating the command into a pseudo rate command. This rate command was digitally integrated over time to determine pitch and bank attitude command. Limiters were also inserted to prevent saturation. Parameter values are shown in Table 3 for the final LQR controller, including pilot interface, of Figure 12.

Table 3. Pilot Interface

Parameter	Value
q_{stick}	0.25
pitch limit	16,000 / gross wt
T_s	0.02
p_{stick}	-0.25
bank limit	$6 \cdot 10^6 / I_{zz}$

Note that the lateral commands take precedence over longitudinal ones, emphasizing the rationale that survivability depends primarily on wings-level flight and touchdown. Also, setting limits as a function of throttle lever position will likely be an impractical implementation. The independent control of velocity and pitch attitude was not accomplished in this investigation.

In general, "batch" linear simulations prior to piloted simulation predicted higher gains for adequate control than were required. Unstable pilot-in-the-loop operation in the nonlinear simulation required that the weights be reduced to those shown in Figure 9. Those gains provided adequate closed-loop performance on the piloted simulator.

Linear system performance did not model the coupled longitudinal and lateral modes, engine nonlinearities, and unequal engine spool-up and spool-down times. The nonlinear simulation also exhibited more Dutch Roll damping. Piloted simulation results follow in the next section.

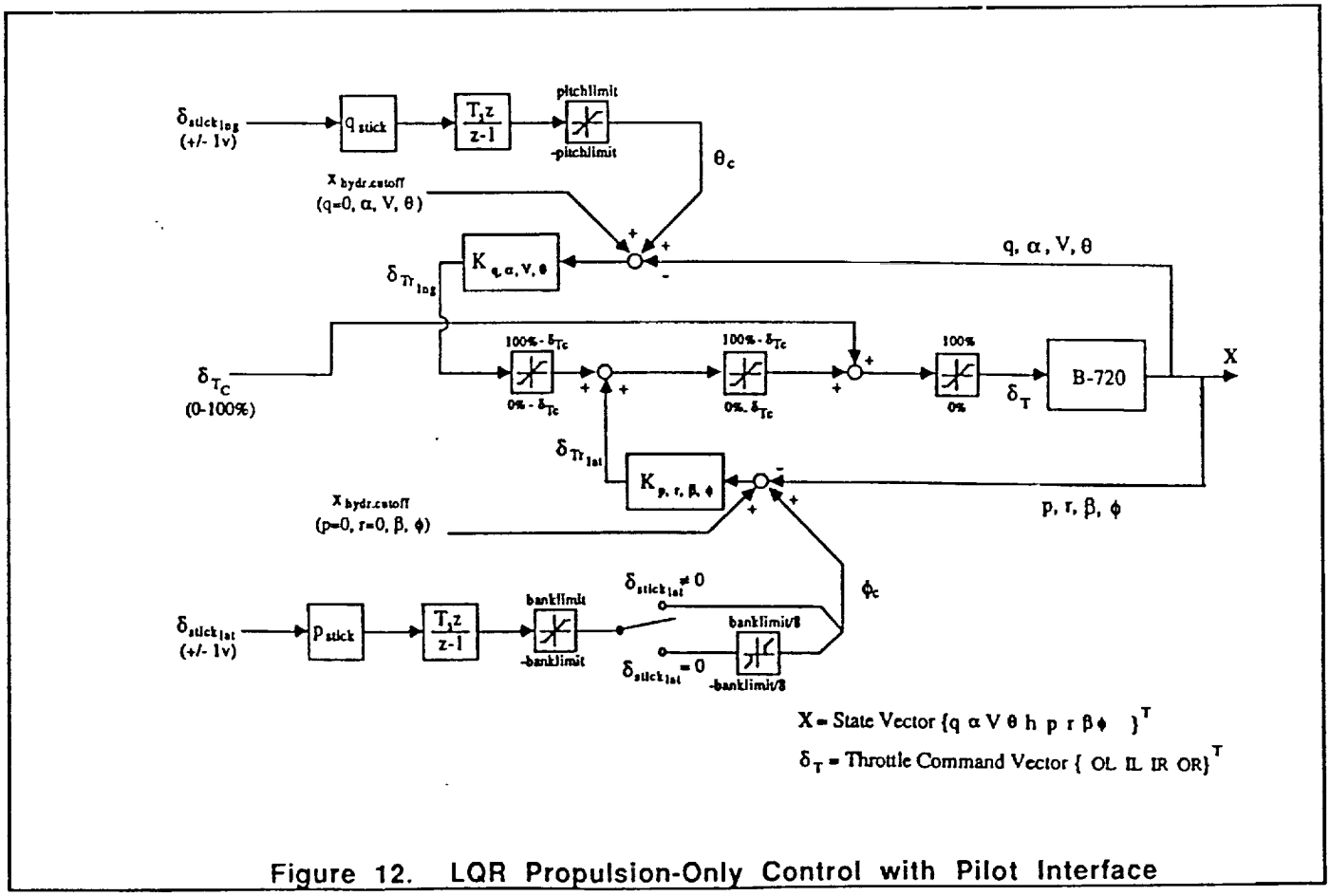

Figure 12. LQR Propulsion-Only Control with Pilot Interface

Piloted Evaluation. The LQR propulsive-only controller of Figure 12 was implemented on a high-fidelity nonlinear simulator at NASA Dryden and evaluated by test pilots. Stick deflection produced thrust commands that were observed on the engine instruments but which did not physically move the throttles.

Pilots were asked to evaluate changes in altitude, velocity, heading, ground track, and flare performance. The LQR implementation did not allow throttles to be physically moved to control velocity since the LQR controller would interpret this as a pitch command. Such motion would also alter the bounds in the limiters shown in Figure 12.

Up-and-away maneuvering did not require excessive pilot workload. The longitudinal implementation, however, made it difficult to fly level, especially when rolling out of turns. Because of the many development changes which occurred during piloted flight, pilot ratings were not documented. In general the aircraft could be considered Level 2. These ratings are similar to those described in this paper's section on the Boeing 720 control law.

The qualitative results of the piloted evaluations are summarized in Table 4. As expected for this type of controller, performance degraded when the LQR control law was implemented on different failure configurations.

Table 4. Qualitative Pilot Evaluation

Task	Pilot Comment
Altitude Change	Holds a rate of climb, but return to level is difficult.
Velocity Change	Somewhat "mysterious"
Heading Change	Holds steady-state turn well, but roll-rate command more intuitive than bank angle command. Difficult to maintain altitude.
Hold Sink Rate	Acceptable after learning curve. Flight path angle command is preferable
Hold Ground Track	Acceptable, but lightly damped roll is somewhat bothersome.
Flare	Too much lag. Will require some practice to determine when to initiate the flare.

Conclusions

Simulations of a Boeing 720 aircraft with failed flight controls show that a propulsion-only flight control system (POFCS) is feasible. Classical analysis using successive loop closure results in simple, effective controllers. Two lightly damped lateral modes,however, can become unstable given minor gain variations or changes in configuration. This suggests that compensation should augment the gains to provide a more robust and stable system.

A LQR augmentation scheme designed using optimal control was flown successfully under pilot control but was not a significant improvement over the gains set by classical analysis. The design implementation employed pseudo rate commands, required limiters, and did not allow the pilot to use the throttles for velocity control independent of pitch.

Despite these limitations it was demonstrated by piloted evaluations that the POFCS concept is feasible and may be implemented as a back-up pilot assist mode when normal flight control has failed. If an optimal controller is employed, an improved pilot interface will be required as well as provisions for velocity control independent of pitch attitude. In particular, the use of differential inboard-outboard thrust should be investigated as a way to uncouple the velocity and pitch modes.

Pilots indicated that improved handling qualities are desired. The wandering bank angle and difficulty in achieving level flight should be rectified. Pitch sensitivity may be reduced by transition to a flight path angle command system.

Research is in progress to investigate the use of compensators for failed flight control configurations. Better performance and more robust behavior for off-design failure conditions are desired. Flight operations which are coupled to the glide path will be analyzed, and the resulting controller is intended to be tested in both ground and inflight simulations.

Acknowledgment

This work was made possible by NASA Grant Number NCC 2-711. Many individuals at the NASA Dryden Flight Research Center provided invaluable assistance, including Bill Burcham, Glenn Gilyard, Gordon Fullerton, Jim Smolka, Joe Conley, and Jeanette Le.

References

1. Wolfe, L.D. and A.E. Fanning, "Advanced Nozzle Technology," AGARD Conference Proceedings CP-241, Fighter Aircraft Design, pp 17-1 to 17-31, Florence, Italy, Oct 1977.

2. Gaffney, T., "Pilot in Sioux City jet crash tells story in Dayton," Dayton Daily News, Mar 26, 1991, page 3-A.

3. Leavitt, P., "Crash Settlement," USA Today, Wed, Mar 27, 1991, page 3-A.

4. Burcham, F., Fullerton, G., Gilyard, G., Conley, J. and J. Stewart, "A Preliminary Look at Propulsion-Enhanced Flight Controls Research," NASA Dryden internal document, 1990.

5. Gilyard, G., Conley, J., Le, J., and W. Burcham, "A Simulation Evaluation of a Four-Engine Jet Transport Using Engine Thrust Modulation for Flight Path Control," 27th Joint Propulsion Conference , June 24-26, 1991, Sacramento, CA.

6. MIL-STD-1797A, "Flying Qualities of Piloted Vehicles", limited distribution, ASD/ENES, Wright-Patterson AFB, Ohio, 30 Jan 1990.

7. Biezad, D.J., "The Propulsive-Only Flight Control Problem," NAECON , Dayton, Ohio, May, 1991.

8. Azzano, C.P., "A Preliminary Look at Optimal Multi-Variable Design of Propulsion-Only Flight Controllers for Jet Transport Aircraft," NASA Dryden TR, Sept 21, 1990.

9. Kwakernaak, H. and R. Sivan, Linear Optimal Control Systems, John Wiley and Sons, 1972.

10. Blakelock, J., Automatic Control of Aircraft and Missiles, John Wiley & Sons, Inc., 1965.

11. Franklin, G.F., and J. D. Powell, Digital Control of Dynamic Systems, Addison-Wesley, Menlo Park, CA, 1986.

The Propulsive-Only Flight Control Problem

by

Daniel J. Biezad

Cal Poly State University
San Luis Obispo, CA 93407

Abstract

Attitude control of aircraft using only the throttles is investigated The long time constants of both the engines and of the aircraft dynamics, together with the coupling between longitudinal and lateral aircraft modes, make piloted flight with failed control surfaces hazardous, especially when attempting to land. This research documents the results of in-flight operation using simulated failed flight controls and ground simulations of piloted propulsive-only control to touchdown. Augmentation control laws to assist the pilot are described using both optimal control and classical feedback methods. Piloted simulation using augmentation shows that simple and effective augmented control can be achieved in a wide variety of failed configurations.

Nomenclature

q	perturbed pitch rate (rad/sec)
α	perturbed angle of attack (rad)
u	perturbed velocity (ft/sec)
θ	perturbed pitch angle (rad)
h	altitude change-down (ft)
γ	perturbed flight path angle (rad)
Γ	glide slope deviation angle (rad)
$K_q, K_\theta, K_\gamma, K_\Gamma$	long. feedback gains
p	perturbed roll rate (rad/sec)
r	perturbed yaw rate (rad/sec)
β	perturbed sideslip (rad)
ϕ	perturbed bank angle (rad)
o	lateral offset angle from runway
$K_\phi, K_\beta, K_p, K_o$	lateral feedback gains
δ_{TR}	perturbed throttle (%)
δ_{TH}	perturbed thrust
δ_{DT}	perturbed differential thrust

Introduction

The failure of hydraulic power to primary flight control systems is an extremely rare occurrence in-flight. Such failures have occurred, however, and their consequences have been especially tragic in commercial operations. In a few of these failures the aircraft remained controllable in-flight by the skillful application of thrust, but the extreme difficulty of this task, combined with the stress of the emergency, did not allow a successful landing.

The fundamental problem is that an aircraft cannot be easily and predictably maneuvered by the pilot with the throttles alone. Although the control power is often sufficient to fly the aircraft, the long time constants and couplings between dynamic modes make pilot control uncertain and precarious for demanding tasks such as landing. Exposure to these situations in training simulations may alleviate the gross misapplication of throttles, but will not eliminate the potential for a serious accident to occur.

A complimentary solution to more training would be the addition of a simple, low cost pilot-assist mode to be activated by the pilot in the event of complete failure of the high bandwidth pitch and roll controls. The goal of such a system would be to provide acceptable flying qualities by driving the throttles through pilot command inputs from the control column. Although the requirements are many for such a system, three factors are worthy of note.

First, the engine power settings and mounting geometry must provide controllability in a mathematical sense for the aircraft equations of motion under a variety of aircraft configurations and failure modes. Second, and possibly the most important factor, the low-bandwidth control system will be coupled with a pilot who will be stressed and anxious under actual emergency conditions. There are no handling qualities requirements to guide the designer here, and even those in military specifications[1] are inapplicable. Third, because of the long time constants of the engines relative to those of the control surface actuators, low-bandwidth control will be most effective for the long-period dynamic modes of the aircraft. This poses a special difficulty for stabilizing the lateral Dutch Roll mode, which may not be a slow mode relative to the engine response.

This paper will concentrate on the development of a practical propulsion-only flight control system (POFCS). The first major issue of controllability due to engine power and geometry will be broadly surveyed in the next section titled "In-Flight Simulations". [2,3] Next, the empirical results of

ground simulations using a Boeing 720 aircraft model with failed flight controls will be presented. The third section will present development issues for the POFCS and highlight the difficulties of achieving a robust, practical design.

In-Flight Simulations

Preliminary investigations of throttle-only aircraft control in-flight have been conducted by NASA Dryden Flight Research Facility. The list of aircraft flown includes the Lear 24, Cessna 152, Piper PA-30, and the F-15. Single-engine aircraft required that the rudder be used in addition to the throttle. None of the in-flight tests were flown to touchdown. Pilot ratings could be categorized by controlled axis and by task. Typically, longitudinal axis control was Level 2 for approach and Level 3 for landing on a runway. Lateral axis control was Level 2 for both approach and landing. The pilot learning curve in all cases was rapid.

F-15 throttles-only. The basic F-15, shown in Figure 1, has a high wing with approximately 45 degrees of sweep and two vertical tails. Although the engines are near the aircraft centerline, flight tests showed roll rates from differential throttles up to 5 deg/sec over a significant part of the flight envelope. Pitch control using throttles alone was available but inadequate below 200 knots.

With yaw augmentation systems off, three test pilots found that differential thrust alone provided good bank angle control as well as roll rate response. With nose up trim, and stick and rudder centered, they were able to exercise crude altitude and heading control.

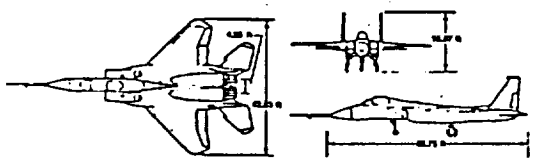

Figure 1. F-15

Lear 24 throttles-only. The twin engine executive jet shown in Figure 2 has a T-tail and fast responding engines. In-flight thrust control of roll rate was effective, reaching 20 deg/sec near 250 knots. Pitch response due to thrust was very poor, due to the high engine location which caused a nose down moment from a thrust increase. The aircraft thus had to be flown using its inherent speed stability, leaving an undamped phugoid and a pitch rate response of approximately 0.2 deg/sec.

Test pilots tried to use bank angle to damp the phugoid with inconsistent results. Only when electric pitch trim was made available could a tractable approach be flown. As with all in-flight tests, no landings were attempted using throttles alone.

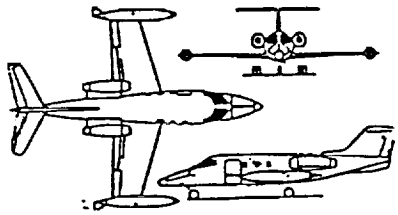

Figure 2. Lear 24

Cessna 152. The single-engine light trainer shown in Figure 3 has a high wing and conventional tail. Rudder was required for directional control, but the throttle provided adequate control of the steady-state speed stability of the aircraft.

Phugoid excitation required damping by pilot application of throttle which was unnatural but easily learned. Pilots stated that they could have landed the aircraft using throttle and rudder alone.

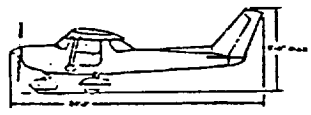

Figure 3. Cessna 152

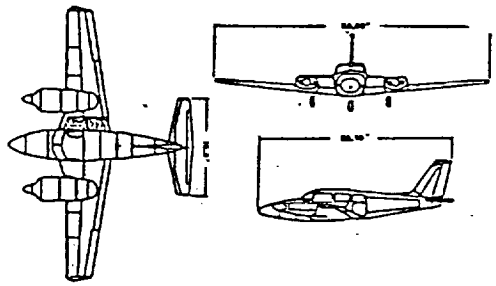

Figure 4. Piper PA-30

Piper PA-30. This twin-engine aircraft shown in Figure 4 has a low wing and conventional tail. The roll control power was considerable but very non-linear, requiring extensive pilot adaptation. Roll rates were observed near 10 deg/sec but bank angle control was very difficult.

Pitch control from throttles-alone came from the inherent speed stability of the aircraft. Pilot damping of the phugoid was difficult and would have made landing under throttles only control dangerous. Providing electric pitch trim alleviated the problem to a great degree, and it was possible for two pilots to simulaneously control flight in this manner.

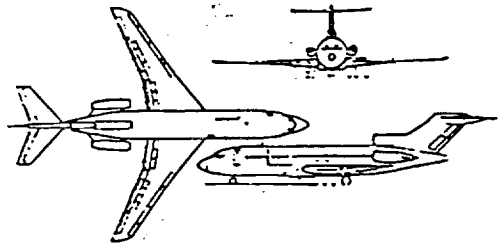

Figure 5. Boeing 727

Ground Simulations

Full six degree-of-freedom simulations of large aircraft were performed at NASA Dryden to investigate throttles-only control. The Boeing 727 and the Boeing 720 represent three- and four-engine variants of passenger jet aircraft as shown in Figures 5 and 6. Although considerable differential thrust exists for roll control, both aircraft have slow responding engines making damping of the dutch roll and phugoid modes difficult. Differential thrust was not used to control pitch attitude. A view of the simulator scene for approach and landing is shown in Figure 7.

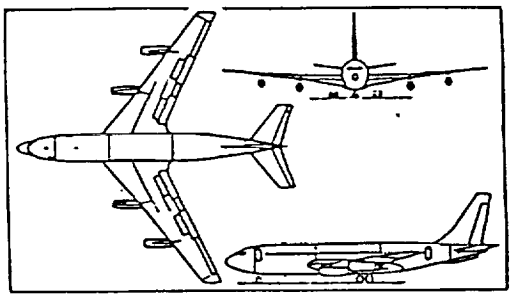

Figure 6. Boeing 720

Boeing 727. This three engine transport has a swept engine and a T-tail. From a level flight trimmed condition, throttles moved in concert produced about 0.5 deg/sec in pitch, and throttles moved differentially produced 3 deg/sec roll response. Electric trim was required to damp the phugoid sufficiently for a landing on a "field." Without the trim extensive practice was required (over 2 hours).

When two pilots divided the control task by axis, they could successfully land the aircraft but not on a runway. Considerable care was required not to excite the dutch roll and phugoid modes. Pilots found this unnatural and especially difficult when approaching touchdown. Level 3 ratings require some sort of stability augmentation for safe flight.

Boeing 720. This four engine jet transport has a low wing with 35 degrees of sweep. Gross attitude control in both the longitudinal and lateral axes was possible without the use of electric trim. If pilots split the tasks and used electric trim, a runway landing could be made.

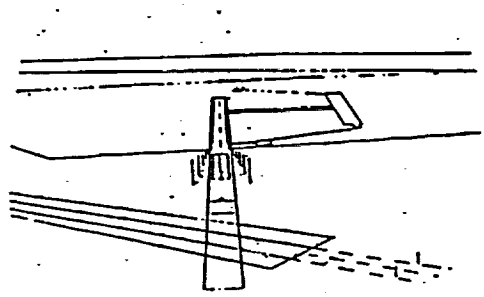

Figure 7. Simulation Visual

An augmentation system to control flight path angle, γ, was developed to convert conventional pilot control inputs into throttle motions. Using this system a single pilot could successfully land the aircraft with practice on a simulated runway. There still was a tendency for pilot-induced oscillations (PIO) near the ground, especially in the lateral axis, and control inputs for stability were requied to be very small to avoid exciting the oscillatory modes.

Control Law Development

An ideal propulsion-only flight control system (POFCS) would provide acceptable handling qualities in the event of any type of flight control malfunction. Essentially, however, the implemented control law must perform three functions. First, it must use the control power of the engines, in concert with the stability derivatives of the aircraft, to provide longitudinal and lateral flight path control under a variety of flight control failures throughout the flight envelope. This is difficult to achieve when the aircraft is far from a trimmed condition, or when the aircraft must descend rapidly under conditions of low thrust.

Second, the control law must allow pilot inputs and pilot-directed configuration changes without exciting large oscillations of the dutch roll or phugoid. Pilots who are trying to perform a high gain task with a low bandwidth control , such as landing an aircraft, must relearn how to generate lead compensation. There are no handling qualities specifications to cover this situation. The pilot must accept watching the throttles move with stick input and must resist the natural tendency to pull power off during the flare. Such a control law must be integrated with actual pilot inputs at each step during its development.

Finally, the engine time constants must be fast enough to control any oscillatory mode which could preclude a successful landing. Other relatively fast modes, such as the short period, must be stable. This condition simply states that the configuration with failed controls, at points in the flight envelope from landing to cruise conditions, must be stabilizable (the uncontrollable poles must be stable).[4]

Boeing 720 Control Law The baseline control law for the four engine jet transport, for both the longitudinal and the lateral axis, was developed by trial and error in the flight simulator at NASA Dryden. The augmentation control law for each axis was developed from a baseline aircraft configuration (gear-up, flaps-up, 10,000 ft pressure altitude, 160 knots, 190,000 lbs). For this baseline Level 2 pilot ratings were recorded for each axis given the task of landing on a runway. The baseline gains were

$$\{K_q, K_\theta, K_\gamma, K_p, K_\phi, K_\beta\} = \{-4, 0, -1, 0.5, 0.5, 1.0\}$$

where other potential gains, such as K_r, were tried but not kept in the baseline since the pilots noted no significant improvement in aircraft response.

Ten configurations were then flown with the above set of baseline gains and the results are summarized in Table 1. The worst ratings, those for configurations 5, 8, and 9, were for those configurations farthest from the baseline weight of 190,000 lbs. The poor rating (8) for configuration 3 can be considered an anomaly based on pilot comments of full stick throw and starting in too close. Otherwise, pilot comments for poorly rated configurations indicate the problem to be severe lateral oscillations that cannot be damped predictably by pilot inputs.

Table 1. Cooper-Harper Ratings for Boeing 720 Simulation to Touchdown
Baseline: 190000 lbs, 10000 ft, gear-up, flaps-up, 160 knots, light turbulence
$\{K_q, K_\theta, K_\gamma, K_p, K_\phi, K_\beta\} = \{-4, 0, -1, 0.5, 0.5, 1.0\}$

#	CONFIGURATION Altitude ($ft \times 10^3$)	Weight ($lb \times 10^3$)	Speed (knots)	Gear/ Flaps	Pilot Rating	Comments
1.	4	140	160	Up/Up	5-6	Landed long; needed small input
2.	4	190	160	Up/Up	4-5	OK!
3.	10	190	160	Up/Up	8	In too tight; kept hitting full stick throw; no control power could not get back from 30° bank; excited phugoid
4.	10	140	160	Up/Up	6	Kept VVI above 500 fpm to keep control power; OK!
5.	4	140	160	Up/50°	9,7	Crashed! Initial excitation caused undampable dutch roll. Second try better but could not get in loop safely.
6.	4	190	160	Up/50°	7	Could not get in control loop safely laterally; pulsed inputs.
7.	4	190	130	Up/50°	5	Small inputs required; excellent control; could damp roll.
8.	4	140	130	Up/50°	8	Controlled crash off of runway!; open loop only; very difficult to damp dutch roll; pulsed inputs did not help.
9.	4	140	130	Down/50°	7	Controlled touchdown off runway; same comments as #8.
10.	4	190	130	Down/50°	5	Excellent! Same comments as #7.

Classical Analysis. A linearized model of configuration 1 of Table 1 is shown in Figure 8. A two dimensional root locus for the lateral modes of response, varying K_p and K_ϕ, is illustrated in Figure 9. Note the difficulty in selecting these gains using conventional analysis. The lateral response mode has a lateral phugoid in addition to a dutch roll mode. Families of plots of these two pairs of complex roots show that varying either gain pushes one set of roots into the right-half plane. This effect of varying configurations exacerbates this tendency.

Normally, given conventional flight controls, the pilot could compensate for this type of mild and slow instability. Throttles-only control, however, even with an augmented system, make such compensation extremely difficult for the pilot.

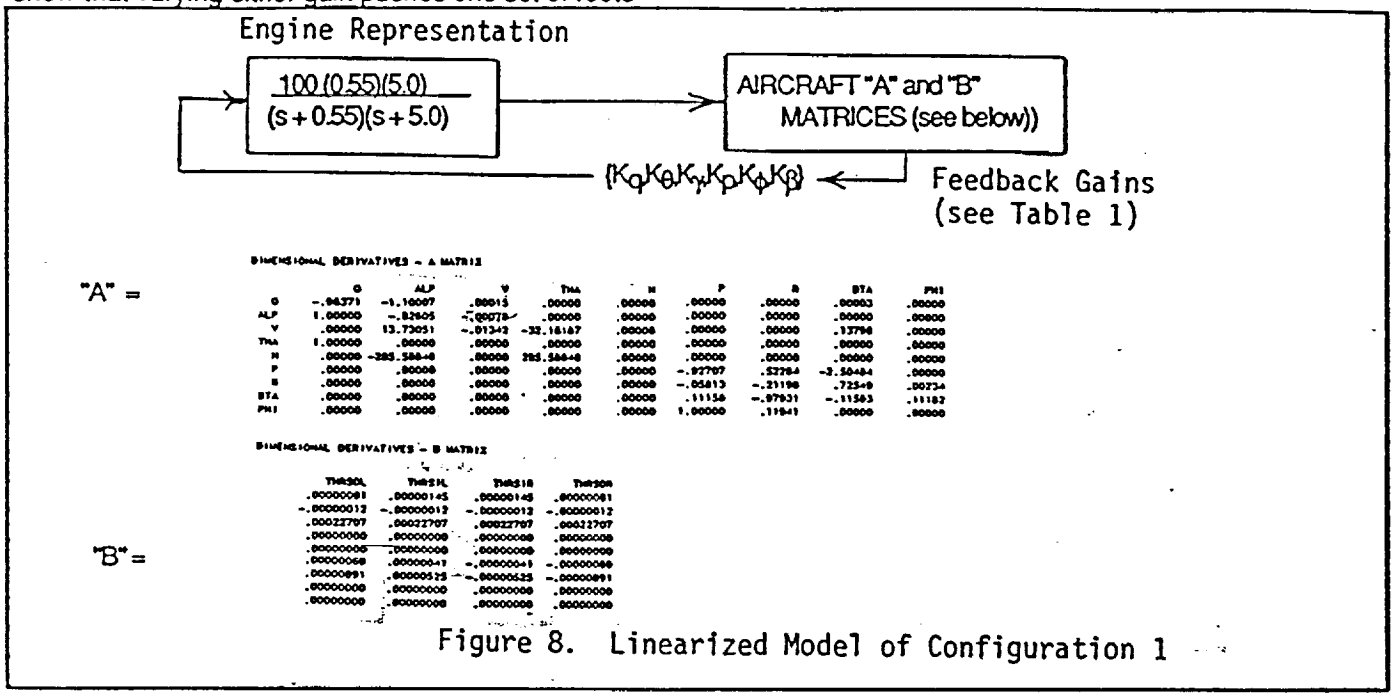

Figure 8. Linearized Model of Configuration 1

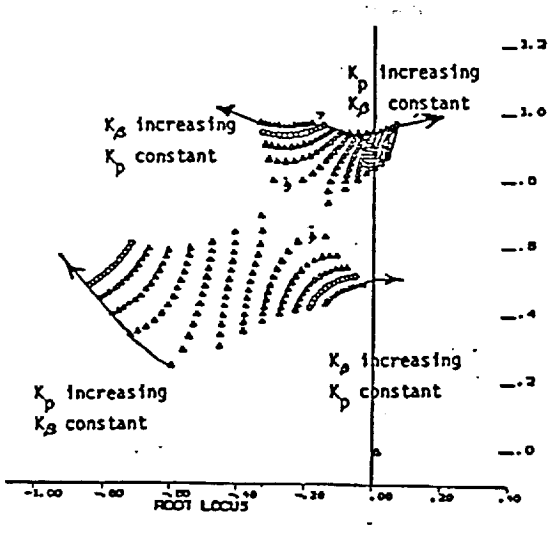

Figure 9. Lateral Root Locus

Optimal Control Analysis. An optimal control law was developed by Azzano for the linearized system shown in Figure 10. In his development a pilot command is directly translated into a single state-variable command. All four throttles were independently controlled, taking advantage of the vertical offset of the engines to allow pitching moments independent of airspeed change.

The design condition for the optimal controller was 4000 ft altitude, 160000 lbs, 175 knots, gear-up, and flaps-up. The engine lag was modeled as a second order system. Azzano's final design, incorporating many limiters, is shown in Figure 11.

$$A = \begin{bmatrix} -.89 & -.98 & .00011 & 0 & 0 & & & & & \\ 1 & -.79 & -.00065 & 0 & 0 & & & & & \\ 0 & 13 & -.012 & -32 & .00006 & & & — & & \\ 1 & 0 & 0 & 0 & 0 & & & & & \\ 0 & -312 & 0 & 312 & 0 & & & & & \\ & & & & & -.99 & .55 & -3.0 & 0 & 0 \\ & & & & & -.053 & -.21 & .76 & .0021 & 0 \\ & & — & & & .11 & -.98 & -.11 & .10 & 0 \\ & & & & & 1 & .11 & 0 & 0 & 0 \\ & & & & & 0 & 1.01 & 0 & 0 & 0 \end{bmatrix}$$

$$B = \begin{bmatrix} .000051 & .00012 & .00012 & .000051 \\ -.000009 & -.000009 & -.000009 & -.000009 \\ .020 & .020 & .020 & .020 \\ 0 & 0 & 0 & 0 \\ 0 & 0 & 0 & 0 \\ .000068 & .000040 & -.000040 & -.000068 \\ .00080 & .00047 & -.00047 & -.00080 \\ 0 & 0 & 0 & 0 \\ 0 & 0 & 0 & 0 \\ 0 & 0 & 0 & 0 \end{bmatrix}$$

Mode	Weight
Short Period	1
Phugoid	10
Dutch Roll	200
Spiral	.5
Roll	1

Design LQR Weights

$$K = \begin{bmatrix} q & \alpha & V & \theta & p & r & \beta & \phi \\ 594 & -467 & 2.6 & 780 & 93.9 & 584 & 91.6 & 125 \\ 1750 & -1290 & 2.1 & 2345 & 55.3 & 344 & 54.0 & 73.4 \\ 1750 & -1290 & 2.1 & 2345 & -55.3 & -344 & -54.0 & -73.4 \\ 594 & -467 & 2.6 & 780 & -93.9 & -584 & -91.6 & -125 \end{bmatrix}$$

Figure 10. Matrices for LQG Model

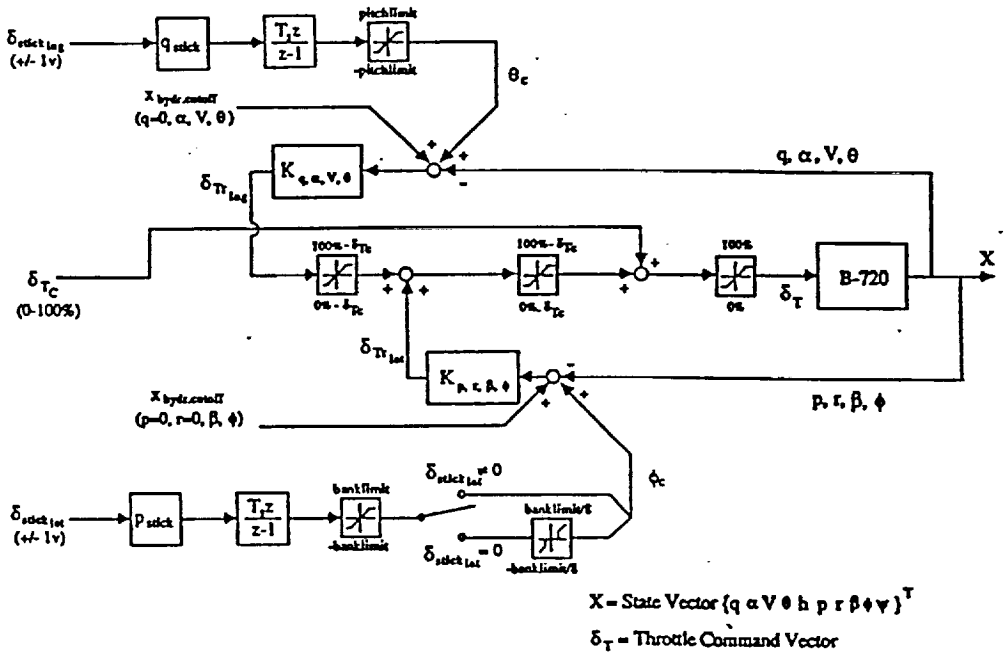

Figure 11. Linearized LQG Model for configuration 1 at 175 knots

Although open- and closed-loop responses of the ground simulator and the linear system matched reasonably well for small inputs, pilots found the optimally-designed augmentation system difficult to use in a few key areas. Pilots described returning to level flight coming out of a turn as unpredictable and velocity change as 'mysterious'. The flare maneuver was not responsive enough. They typically complained of a "wandering bank angle" and had a tendency to excite pilot induced oscillations even when the controller gains were reduced by changing the weights on the cost function.

The augmentation system designed using optimal control theory performed poorly when other failed configurations were tested. This was expected for this type of controller.

Conclusions

The results of in-flight operation using simulated failed flight controls for a variety of different aircraft show that the throttles can be effective low bandwidth controllers. When throttle controllability is a problem, electric pitch trim and/or rudder input may be required for safe flight. Pilot learning is rapid, but performance during high gain tasks such as touchdown is not predictable and requires augmentation. The pilot has difficulty generating lead compensation for a low bandwidth, lightly damped control system.

Ground simulation of a Boeing 720 four-engine jet transport showed that a simple augmentation system could assist the pilot. Problems were apparent, however, when the failed configuration being flown deviated from the design failed configuration, with pilot rating being most sensitive to aircraft weight and center of gravity.

Classical analysis highlighted the problem to be two lightly damped lateral modes which became unstable if either the roll rate or the beta feedback gains were increased from a nominal setting. Flight off of the design condition exacerbated the problem. The pilot found it difficult to control the off-design flight configuration in the lateral mode.

An augmentation scheme designed using optimal control was successful under pilot control but required many limiters and adjustments of design weights. The performance away from design condition was not acceptable.

Work is in progress to use quantitative feedback theory to build a simple compensator for the failed flight control configurations which will be more robust with respect to off-design conditions.

Acknowledgment

All of this work was made possible by the support of technical personnel at NASA Dryden, especially Bill Burcham, Glenn Gilyard, and Joe Conley. Use of the simulation facility was vital to the completion of this investigation.

References

1. MIL-STD-1797A, "Flying Qualities of Piloted Vehicles", limited distribution, ASD/ENES, Wright-Patterson AFB, Ohio, 30 Jan 1990.

2. Burcham, F., Fullerton, G., Gilyard, G., Conley, J. and J. Stewart, "A Preliminary Look at Propulsion-Enhanced Flight Controls Research," NASA Dryden internal document, 1990.

3. Gilyard, G., Conley, J., Le, J., and W. Burcham, "A Simulation Evaluation of a Four-Engine Jet Transport Using Engine Thrust Modulation for Flight Path Control," 27th Joint Propulsion Conference (to be presented), June 24-26, 1991, Sacramento, CA.

4. Kwakernaak, H. and R. Sivan, Linear Optimal Control Systems, John Wiley and Sons, 1972.

5. Azzano, C.P., "A Preliminary Look at Optimal Multi-Variable Design of Propulsion-Only Flight Controllers for Jet Transport Aircraft," NASA Dryden internal document, Sept 21, 1990.

6. Roskam, J., Airplane Flight Dynamics and Automatic Flight Controls, Roskam Aviation and Engineering Corp., Ottawa, Kansas, 1979.

7. McRuer, D., Ashkenas, I., and D. Graham, Aircraft Dynamics and Automatic Control, Princeton University Press, 1973.

Pilot-in-the-Loop Analysis of Propulsive-Only Flight Control Systems

by

Hwei-Lan Chou
Daniel J. Biezad

Cal Poly State University
San Luis Obispo, CA 93407

ABSTRACT

Longitudinal control system architectures are presented which directly couple flight stick motions to throttle commands for a multi-engine aircraft. This coupling enables positive attitude control with complete failure of the flight control system. The architectures chosen vary from simple feedback gains to classical lead-lag compensators with and without prefilters. Each architecture is reviewed for its appropriateness for piloted flight. The control systems are then analyzed with pilot-in-the-loop metrics related to bandwidth required for landing. Results indicate that current and proposed bandwidth requirements should be modified for throttles only flight control. Pilot ratings consistently showed better ratings than predicted by analysis. Recommendations are made for more robust design and implementation. The use of Quantitative Feecback Threory for compensator design is discussed. Although simple and effective augmented control can be achieved in a wide variety of failed configurations, a few configuration characteristics are dominant for pilot-in-the-loop control. These characteristics will be tested in a simulator study involving failed flight controls for a multi-engine aircraft.

NOTATION

q	pitch rate (deg/sec)
α	perturbed angle of attack (deg)
u	perturbed velocity (ft/sec)
θ	perturbed pitch angle (deg)
h	altitude change-down (ft)
γ	perturbed flight path angle (deg)
Γ	glide slope deviation angle (deg)
G_{in}^{out}	transfer function (s)
(a)	short form for (s+a)
(ζ, ω_n)	short form for $s^2 + 2\zeta\omega_n s + \omega_n^2$
Kq	pitch rate feedback gain
K_γ	gamma loop feed back gain
$\delta_{\Gamma c}$	throttle command (%)
z	thrust (lbs)
δ_s	stick input (full deflection=1 unit)
P	quadruple state-space representation
M_u	dimensional speed derivative
M_α	static stability dimensional derivative

INTRODUCTION

Work at NASA Dryden has shown that compensated thrust modulation coupled to flight stick motion provides a positive degree of flight controllability in the event of complete failure of the flight control system. Feedback control laws developed empirically had dramatically improved the pilot ratings from Level 3 to Level 2 for the simulated approach and landing of a Boeing 720 with failed flight controls[1-3] . Initial work on the modeling of these control systems showed that relatively simple feedback architectures, as well as those based on optimal control theory, could ease the piloting task for throttles-only flight unless moderate turbulence was encountered.[4-5]

The main thrust of research reported here has been to investigate the effect of throttles-only flight control on the flying qualities of multi-engine aircraft. Analytical system surveys are accomplished to explain this improvement from a handling qualities point of view. The pilot-in-the-loop metrics used in the investigation are primarily related to bandwidth criteria as reported in the literature. [6]

Previous work was extended by developing classical compensator designs with and without prefiltering to further improve the piloted ratings. The design goal was to find a robust controller for throttle-only control under various approach and landing flight conditions. Designs obtained from optimal control theory showed performance sensitivity to configuration changes[5].

All work assumes that the aircraft configuration has a positive M_u dimensional derivative and positive stability ($M_\alpha < 0$). System surveys follow, then the design architectures are analyzed. An expanded Appendix describes the aircraft configurations.

THROTTLES-ONLY SYSTEM SURVEYS

The basic system model as shown in the Appendix has four variations of configuration. The engine and bare airframe state-space models, called quadruples[7], were derived from perturbations of the full non-linear equations of motion about trim. Transfer functions used in design were then approximated with low order fits over the frequency range of effective throttle control.

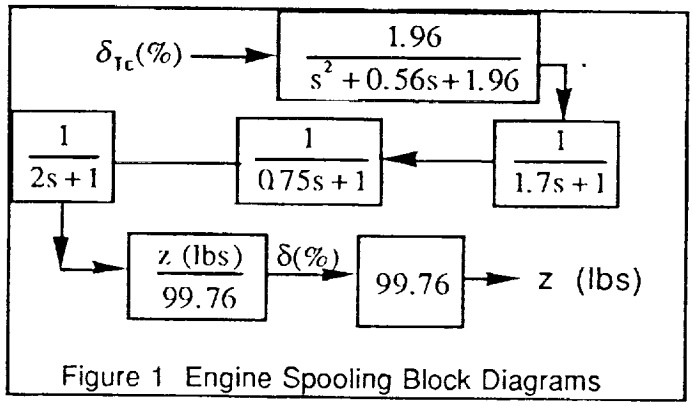

Figure 1 Engine Spooling Block Diagrams

Engines. The spool-up and spool-down engine dynamics for the B-720 engine are shown in Figure 1. The empirical transfer function developed is given in short form notation by

$$G^{z(lbs)}_{\delta_{Tc}(\%)} = \frac{275}{(0.55)(5)}$$

The above equation is illustrated in Fig. 2 over low frequency ranges up to 1.0 rad/sec.

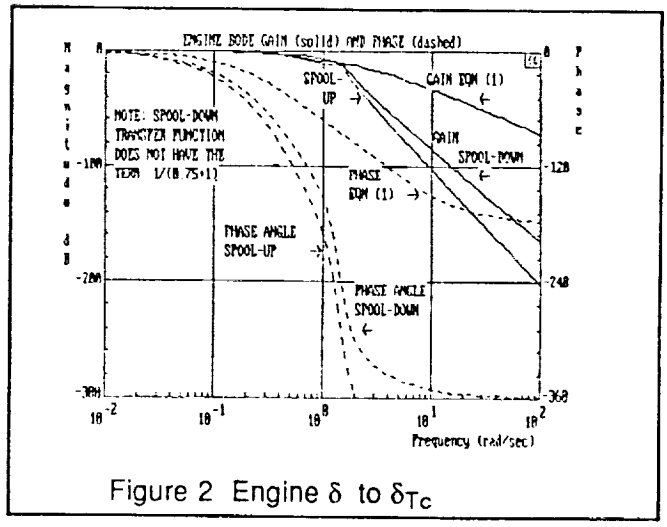

Figure 2 Engine δ to δ_{Tc}

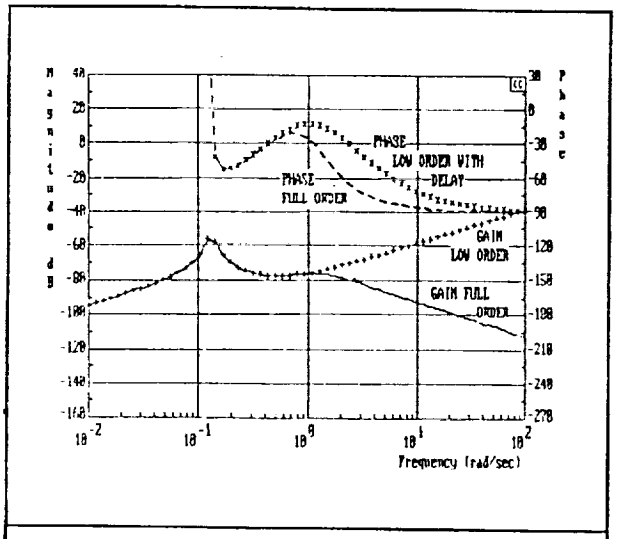

Figure 3 Pitch Rate to Thrust Bode

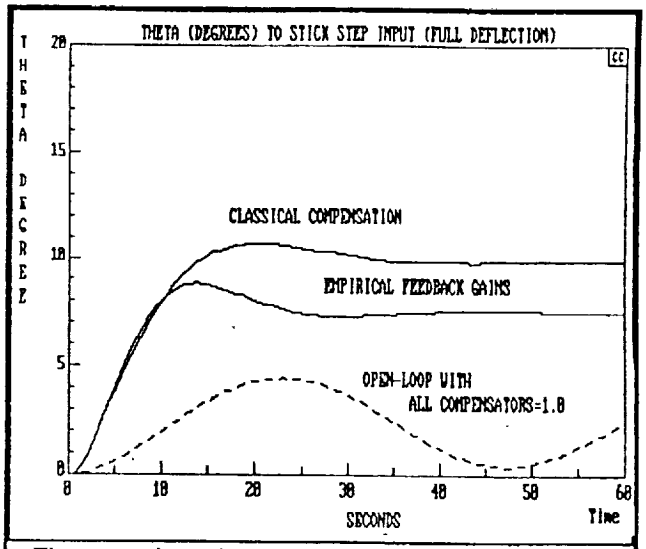

Figure 4 Longitudinal Time Responses

Bare Airframe. It is apparent from the engine bode diagrams that severe bandwidth attenuation occurs beyond frequencies of 1 rad/sec. It may not be possible, therefore, to increase the closed-loop bandwidth beyond 1 rad/sec within the range of available thrust.

This can be seen in the pitch rate "q" to thrust "z" transfer function of the bare airframe shown in Figure 3. The full-order thansfer function $G_{z(lbs)}^{q(deg/sec)}$ shows that 80 db of gain must be added to yield a crossover frequency beyond 1 rad/sec. This corresponds to 10,000 lbs of full thrust from each engine, which would not be practical for approach and landing.

A low order fit to $G_{z(lbs)}^{q(deg/sec)}$ is also depicted in Figure 3 and is very accurate near the phugoid frequency. Piloted flight of the unaugmented aircraft was consistently Level 3. The main difficulties were the lightly damped phugoid and the low bandwidth throttle control. The open-loop response of pitch angle to a full deflection step stick input is shown in Figure 4 with all compensation set to unity (see Appendix).

The accuracy of the low order fit near the phugoid frequency means that, to a first order approximation[9], the phugoid frequency and damping are found from

$$2\zeta\omega_n = -X_u + \frac{M_u(X_\alpha - g)}{M_\alpha}$$

$$\omega_n^2 = \frac{-g(Z_u - \frac{M_u}{M_\alpha}Z_\alpha)}{U_o}$$

and for conventional transport aircraft can be shown to be roughly proportional to M_u.

It should be strongly noted here for the classic case of M_u=0 and for negative values of M_u (Mach tuck) that the aircraft cannot be practically flown with throttles alone unless rotational control in pitch is added. Difficulties will also be encountered as M_α becomes small (aft cg location). Both of these cases require the addition of an effective rotational controller about the pitch axis. This may be achieved using differential inboard and outboard thrust, provided the inboard engines are a different distance from the aircraft xy-plane than the outboard engines. These configuration characteristics determine the innate capability for throttles-only piloted control.

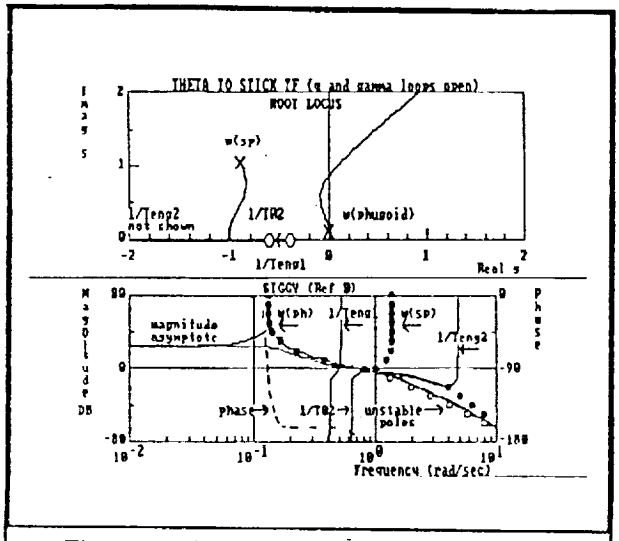

Figure 5 Pitch Angle System Survey

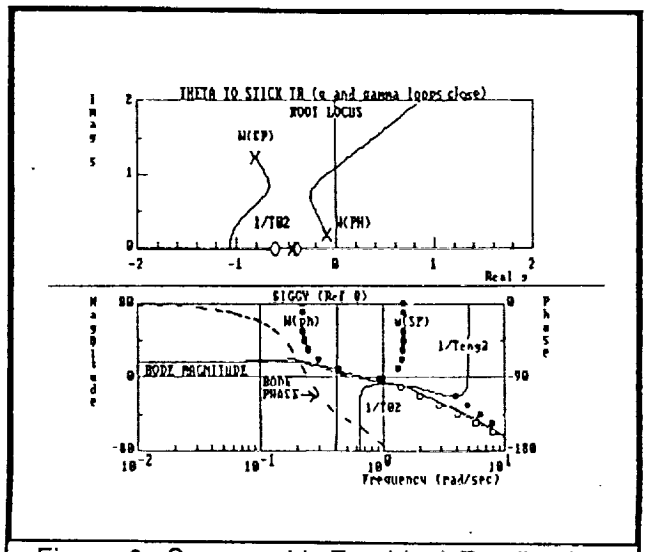

Figure 6 Survey with Empirical Feedback

FEEDBACK ARCHITECTURES

The generic feedback architecture is given in the Appendix. An effort was made in the designs to keep the structure simple, and so in all cases the flight path compensation was unity. The open-loop pitch angle to stick root locus, Bode, and "Siggy" plots[8] are shown in Figure 5. They are characterized by excessive resonance at ω_{nph}, low phase and gain margins, low crossover frequency, and large phase angle roll-off. The open-loop (OL) system is

$$G^{\theta(\deg)}_{\delta_s(\text{units})} \overset{\text{loops}}{\underset{\text{open}}{=}} \frac{8.32(0.4)(0.61)}{(.0039,0.13)(0.65,1.38)(0.55)(5.0)}$$

The root locus of the open-loop system makes it apparent that any feedback is limited by the phugoid roots going unstable.

Empirical Feedback. This longitudinal control law was developed by trial and error in the simulator at NASA Dryden with a pilot in the loop. It is given by

$$\{G^{\gamma_{in}(\deg)}_{\delta_s(\text{units})}, G^{\delta_{Tc}(\%)}_{e_\theta(\deg)}, K_q, K_\gamma, G^{\theta_{in}(\deg)}_{\gamma(\deg)}\} = \{10,10,4,1,1\}$$

The system survey for this structure is shown in Figure 6.

It can be seen that the q and γ feedback loops removed the resonance at the phugoid frequency along with the rapid phase drop. The gain and phase margins, however, are still low. The q loop closure caused the increase in phugoid damping, and the γ loop closure provided an additional 70% increase in settling time. The empirical feedback essentially cancelled the modified engine mode at -0.397 as shown below.

$$G^{\theta(\deg)}_{\delta_s(\text{units})} \overset{\text{loops}}{\underset{\text{closed}}{=}} \frac{8.42(0.4)(0.61)}{(0.518,0.244)(0.517,1.5)(0.397)(5.16)}$$

Classical Feedback Design. Classical compensation was designed to address the low gain and phase margins and to increase system bandwidth within the practical limits of the throttle command. The compensation chosen was

$$\{G^{\gamma_{in}(\deg)}_{\delta_s(\text{units})}, G^{\delta_{Tc}(\%)}_{e_\theta(\deg)}, K_q, K_\gamma, G^{\theta_{in}(\deg)}_{\gamma(\deg)}\} =$$

$$\{8,14\frac{(S+0.55)}{(S+0.65)},4,\frac{(S+0.65)}{(S+1.3)},1\}$$

The survey for this system is similar to Figure 6 and not repeated here.

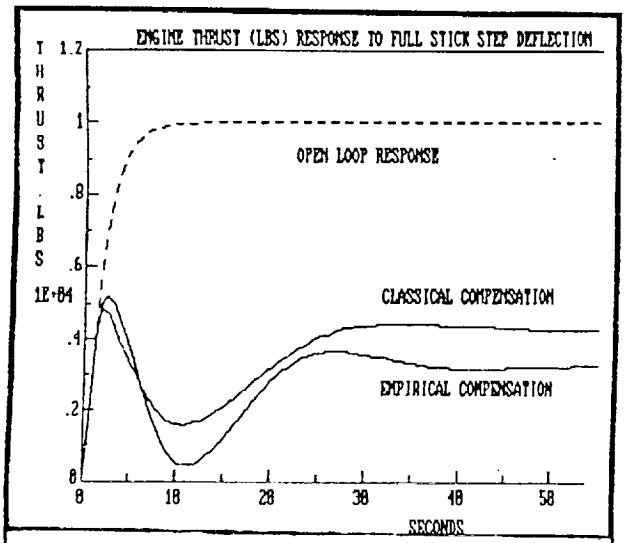

Figure 7 Comparison of Commanded Thrust

The classical design improved the empirical one primarily by increasing the phase margin of the pitch angle to stick transfer function from 13 to 26 degrees. The crossover frequency remained near 0.98 rad/sec.and the steady state performance increased 10%.

The improvement in phase margin made the controller more robust when used to fly the other configurations. The empirical controller was also surprisingly robust when used to fly the other configurations. A complete discussion of this is found in Reference 9.

Further improvements in bandwidth could be achieved only by substantially raising the compensator gain. This resulted in excessive control (thrust). A comparison of the thrust response to a full stick step deflection for the different feedback architectures is given in Figure 7. It was assumed that the throttle command could be moved instantaneously. A throttle actuator would introduce an additional lag.

Compensators currently being designed using Quantitative Feedback Theory are having similar difficulty meeting reasonable limits on control activity when the design closed-loop bandwidth is near 1 rad/sec. A design procedure is being developed to determine the achievable closed-loop bandwidth for a set of configurations given a bandwidth limit on a primary controller.

CONCLUSIONS

Bandwidth requirements on pitch to stick response should reach 3 rad/sec for acceptable pilot ratings[6]. Augmented throttles-only flight could not reach beyond 1 rad/sec, and received acceptable Level 2 ratings unless moderate turbulence was applied to the simulation. Work in progress at Systems Technology Inc. is establishing bandwidth limits for large, landing aircraft, and these limits will be used to design future compensators. Within the limits set by key configuration variables M_u and M_α , simple classical compensators that increase the phase margin result in acceptable pilot ratings for throttles-only flight.

ACKNOWLEDGMENT

This work was made possible by NASA Grant NCC 2-711. The authors are grateful for technical support from Mr. Glenn B. Gilyard at NASA Dryden.

REFERENCES

1. Burcham, F., Fullerton, G., Gilyard, G., Conley, J. and J. Stewart, "A Preliminary Look at Propulsion-Enhanced Flight Controls Research," NASA Dryden document, 1990.
2. Gilyard, G., Conley, J., Le, J., and W. Burcham, "A Simulation Evaluation of a Four-Engine Jet Transport Using Engine Thrust Modulation for Flight Path Control," 27th Joint Propulsion Conference , June 24, 1991, Sacramento, CA.
3. Azzano, C.P., "A Preliminary Look at Optimal Multi-Variable Design of Propulsion-Only Flight Controllers for Jet Transport Aircraft," NASA Dryden TR, Sept 21, 1990.
4. Biezad, D.J., "The Propulsive-Only Flight Control Problem," NAECON , Vol 2, pp494-500, Dayton, Ohio, May 20-24, 1991.

5. Biezad, D.J. and C.P. Azzano, "Designing Low Bandwidth Propulsive-Only Flight Controllers", AIAA Guidance, Navigation, and Control Conference, Paper #91-2628CP, pp 267-275, August 12-14, 1991, New Orleans, La.
6. Hoh, Roger H. and David G. Mitchell, Flying Qualities of Relaxed Static Stability Aircraft--Volume 1, FAA/CT-82/130-I, Sept, 1982.
7. Thompson, Peter M., Program CC Version 4 Reference Manual: Volume 1, Systems Technology, Inc., November 1988.
8. 15. McRuer, D., Ashkenas, I., and D. Graham, Aircraft Dynamics and Automatic Control, Princeton University Press, 1973.
9. Biezad, D.J., Chou, Hwei-Lan, "Low Bandwidth Robust Controllers for Flight," NASA INTERIM REPORT, June-November 1991.

APPENDIX: B-720 CONFIGURATIONS

The B-720 piloted simulation can be represented by the following block diagram:

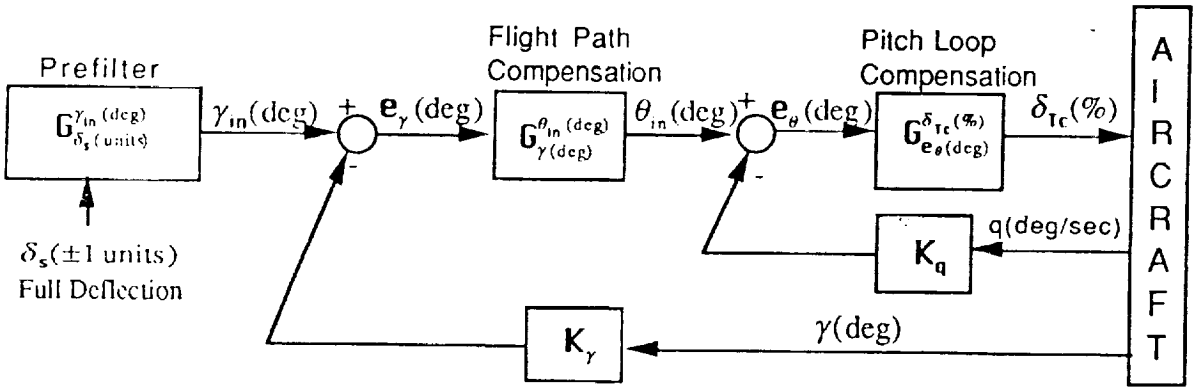

The "aircraft" above represents both the engine and the bare airframe dynamics. The engine is approximated by a transfer function and the bare airframe dynamics are represented mathematically by a single quadruple, **Pa/c**, shown as follows.

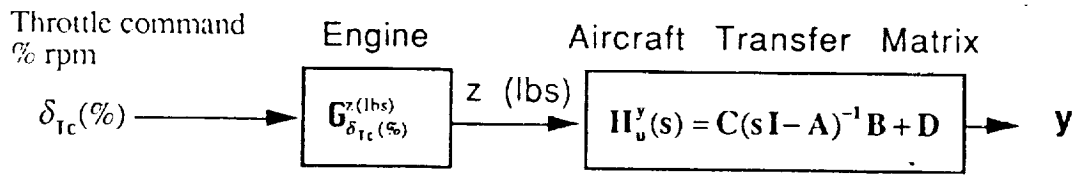

$$P_{a/c} = \left[\begin{array}{c|c} A & B \\ \hline C & D \end{array}\right] \overset{\text{throttle inputs equal}}{=} \left[\begin{array}{c|c} A & B_1(\text{column}) \\ \hline C & D = 0 \end{array}\right]$$

$$x = [q(\text{deg/sec}) \mid \alpha(\text{deg}) \mid v(\text{kts}) \mid \theta(\text{deg}) \mid h(\text{ft})]^T$$

$$y = [n_{\text{pilot g's}} \mid n_{\text{fcs g's}} \mid q \mid \alpha \mid v \mid \theta \mid h \mid \gamma(\text{deg})]^T$$

The thrust control depends on whether four engines receive independent or identical commands:

$$\mathbf{u} = \left[z_{\text{outbd left}}(\text{lbs}) \,\vdots\, z_{\text{inbd left}}(\text{lbs}) \,\vdots\, z_{\text{inbd right}}(\text{lbs}) \,\vdots\, z_{\text{outbd right}}(\text{lbs}) \right]^{T}$$

$$\mathbf{u}_1 = z(\text{lbs}) \qquad \text{[used when all throttles have same command]}$$

Note when all four throttles are given the same command from the pilot stick input the **B** matrix becomes a single column. Each row value in this column matrix $\mathbf{B}_1$ is equal to the sum of the corresponding row elements in the full order **B** matrix representing four engines. The open-loop configuration then becomes **P=Pa/c*Pe**, where **Pe** is the quadruple form of the engine transfer function, $G^{z(\text{lbs})}_{\delta_{th}(\%)}$. The quadruples for four different configurations were obtained as described in Reference 9.

The flight conditions for each of the configurations are summarized in the table below.

Configuration Summary - Gear Up

Config. Number	Weight (lbs)	Altitude (Ft MSL)	Airspeed (Knots)	Flaps (%)	CG % MAC
1	140,000	4,000	160	0	20.85
2	140,000	4,000	145	30	20.85
3	160,000	4,000	175	0	20.85
4	140,000	4,000	155	30	20.85

The transfer functions were obtained from the quadruples using System Technology's CC Program[7]. These aircraft transfer functions are listed here with each respective row of numbers designating the corresponding configuration transfer function values. The nominal configuration, number 1, is represented by values in each row 1 below.

$$N^{q(\text{deg/sec})}_{z(\text{lbs})} = N^{q(\text{deg/sec})}_{z(\text{lbs})} / \Delta_{long}$$

$$N^{\gamma(\text{deg})}_{z(\text{lbs})} = N^{\gamma(\text{deg})}_{z(\text{lbs})} / \Delta_{long}$$

$$N^{q(\text{deg/sec})}_{z(\text{lbs})} = \begin{array}{lllll} 3.07\text{E-}04 & (0) & (-1.17\text{E-}05) & (0.40)\ (.61) & \text{Conf \#1} \\ 3.02\text{E-}04 & (0) & (1.36\text{E-}06) & (0.797,\ 0.568) & \text{Conf \#2} \\ 2.57\text{E-}04 & (0) & (0.292) & (0.644) & \text{Conf \#3} \\ 2.59\text{E-}04 & (0) & (2.68\text{E-}06) & (0.819,\ 0.508) & \text{Conf \#4} \end{array}$$

$$N^{\gamma(\text{deg})}_{z(\text{lbs})} = \begin{array}{llll} 3.63\text{E-}05 & (0) & (0.203) & (0.370,\ 3.008) \quad \text{Conf \#1} \\ 2.36\text{E-}05 & (0) & (0.303) & (0.476,3.51) \quad \text{Conf \#2} \\ 2.77\text{E-}05 & (0.167) & (0.351\ ,\ 3.038) & \text{Conf \#3} \\ 1.91\text{E-}05 & (0) & (\quad 1) & (0.460\ ,\ 3.426) \quad \text{Conf \#4} \end{array}$$

$$\Delta_{long} = \begin{array}{lll} (1.438\text{E-}05) & (3.918\text{E-}02,0.130) & (0.652,1.382) \quad \text{Conf \#1} \\ (1.101\text{E-}05) & (7.423\text{E-}02,0.147) & (0.596,1.375) \quad \text{Conf \#2} \\ (3.949\text{E-}02,0.118) & (0.649,1.301) & \text{Conf \#3} \\ (1.878\text{E-}05) & (7.190\text{E-}02,0.138) & (0.588,1.279) \quad \text{Conf \#4} \end{array}$$

Application of QFT to the Problem of Failed In-Flight Controllers During Approach and Landing of a B-720 Aircraft

Hwei-Lan Chou
Daniel J. Biezad

Cal Poly State University
San Luis Obispo, CA 93407

Abstract

Previous studies by NASA Dryden have shown the use of throttles for emergency flight control to be extremely difficult, especially for landing. Flight control using only the throttles to achieve safe landing for a large jet transport airplane, the Boeing 720, is investigated using Quantitative Feedback Theory. Results are compared to an augmented control developed in a previous study. The controller corrected unsatisfactory open-loop characteristics by increasing system bandwidth and damping, but improving the control bandwidth substantially proved very difficult. The pitch controller is robust in conditions of no or moderate turbulence. The roll controller performed well in conditions of no turbulence, but is sensitive to moderate turbulence. Handling qualities of the augmented control for approach and landing were evaluated by piloted simulation flights.

Notation

TOFC	Throttle-Only Flight Control
QFT	Quantitative Feedback Theory
C_{mu}	Velocity-pitch rate derivative
$C_{l\beta}$	Sideslip-roll coupling derivative
q	pitch rate (deg/sec)
γ	flight path angle (deg)
β	angle of sideslip (deg)
φ	bank angle (deg)
θ	pitch angle (deg)
z	thrust (lbs)
ω_i	natural frequency
ζ	damping ratio
δ_{Tc}	stick input(full deflection=1 unit)
K_q	pitch rate feedback gain
K_γ	flight path angle feedback gain
K_β	sideslip angle feedback gain
K_φ	bank angle feedback gain
G_{in}^{out}	transfer functions
(a)	short form of (s+a)
$[\zeta, \omega]$	short form for $s^2 + 2\zeta\omega s + \omega^2$
c.g.	center of gravity

Introduction

Through throttle manipulations, engine thrust has been found useful in providing some controllability for multiengine aircraft in emergency situations with severe or complete flight control system failures. This paper focuses on a particular application, a simulation augmented control developed by NASA for Boeing-720 aircraft Throttles-Only Flight Control (TOFC) [1-2]. NASA has found the use of throttles feasible for emergency flight control for a range of airplanes, and their analyses for a variety of aircraft are available in the literature [3-6]. This controller was implemented on a high fidelity B720 flight simulator and obtained generally good pilot ratings by increasing the bare airframe Dutch-roll and phugoid damping. The primary aim of this study is to present an alternative control design technique based on Quantitative Feedback Theory(QFT) to further improve the Dutch-roll damping and to increase controller bandwidth for better handling qualities.

The QFT technique [7] was chosen because of the insights it provides throughout its design process. It allows designers to specify a desired closed-loop frequency response with a desired control bandwidth and damping characteristic. It shows why the desired performance may not be achieved within the given control actuation and rate limits.

In this paper a QFT augmented throttle-only flight path controller for approach and landing is presented. Complete details of the aircraft model and justification for TOFC are not included, but the reader is reminded that "trimming" must be possible and "controllability" must exist. Augmented control design using QFT is presented in a summary fashion. The full justification and step by step procedure may be found in Reference 8.

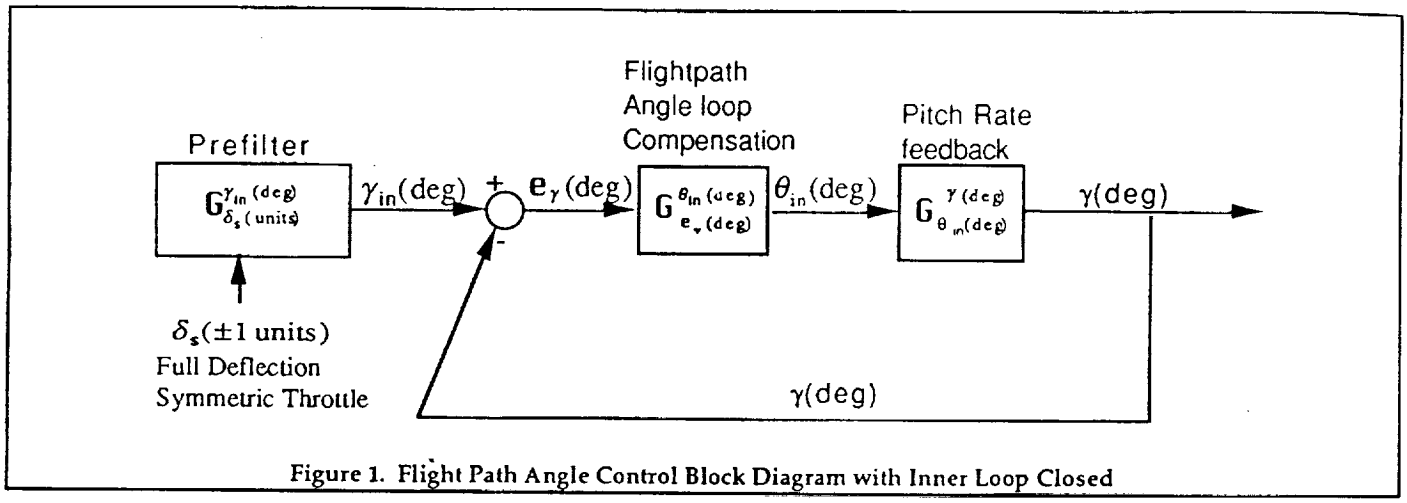

Figure 1. Flight Path Angle Control Block Diagram with Inner Loop Closed

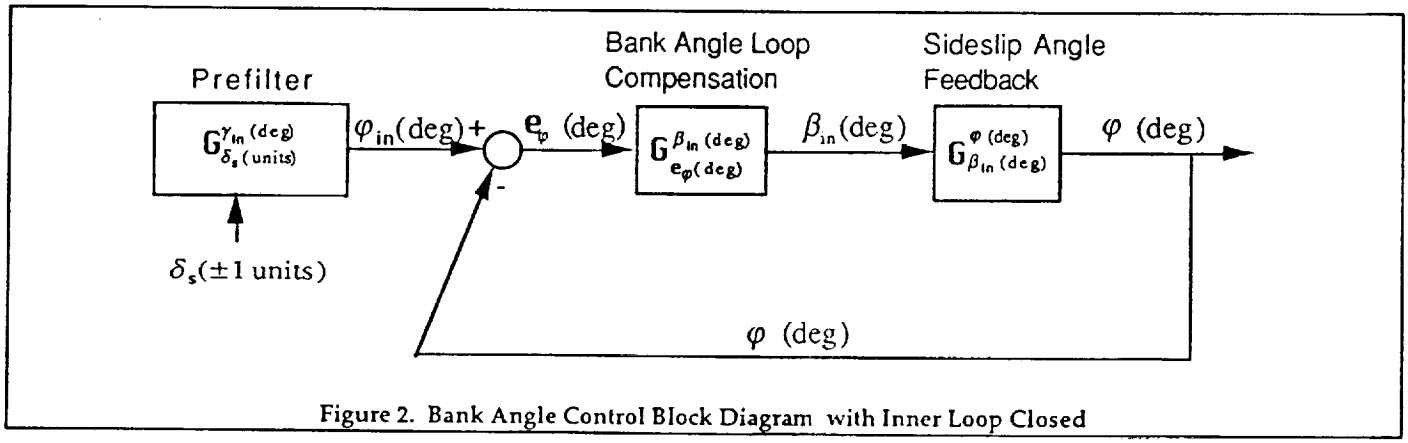

Figure 2. Bank Angle Control Block Diagram with Inner Loop Closed

B-720 Linear Model

The empirical transfer function developed for the engines is given in short form notation by

$$G^{z(lbs)}_{\delta_{T_c}(\%)} = \frac{275}{(.55)(5)}$$

Severe bandwidth attenuation occurs beyond frequencies of 1 rad/sec. For this application his prevented the increase the closed-loop bandwidth beyond 1 rad/sec within the range of available thrust (see Ref. 6).

Four configuration variations for the B-720 were considered as described in the Appendix. They are characterized in both the longitudinal and lateral axes by excessive resonance, low phase and gain margins, low crossover frequency, and large phase angle roll-off.

QFT Controller Design

To apply QFT, the aircraft model is rearranged in a unit feedback form as shown in Figures 1 and 2. The inner pitch rate and sideslip loops were closed using Kq=60 and $K\beta = 4$, which were the settings for the original simulation augmentation scheme.

Performance Specification

QFT allows designers to specify a desired closed-loop frequency response with an upper bound B_U, a lower bound B_L, and a tolerance δ_R specified to obtain robust performance. The maximum M_m is also given to obtain a desired system damping.

Table 1. QFT Performance Specification

Freq.(r/s)	0.1	0.3	0.5	0.7	1.0	2.0	5.0
Bu(dB)	17.0	17.0	17.3	-16.0	-4.0	20	-13.0
BL(dB)	16.8	-15.0	12.3	4.6	-12.4	7.1	-23.0
δ_R (dB)	0.2	2	5	8.4	8.4	9.1	15.0

The performance specification shown in Table 1 are the desired closed-loop responses for both the γ - and φ - loops. These two feedback loops are piloted open-loop systems. Additional specifications are ususallly given for piloted systems, such as a desired control bandwidth of 2 rad/sec. (see Ref. 9 for transport aircraft landing requirements) and a k/s slope near the crossover frequency. These added requirements promote good pilot handling qualities.[10]

Design Constraints

Four configurations were used to study the approach and landing of B-720 throttle-only flight control as summarized in Table 2 and in the Appendix. Configuration 1 was used as the nominal confiuration for control design.

Table 2. Flight Configurations for B-720 (Gear Up)

Conf	Weight (lbs)	Alt (Ft) (MSL)	A/S (Kts)	Flaps (%)
1	140,000	4,000	160	0
2	140,000	4,000	145	30
3	160,000	4,000	175	0
4	140,000	4,000	155	30

The performance bounds constraint is a curve on the Nichols Chart that shows the performance tolerance, δ_R, from Table 1 at each specified frequency. Satisfying the tolerance constraint guarantees that the variation of the system response due to plant uncertainties will be no greater than δ_R. There is a performance bound for each frequency.

U contours are also shown on the Nichols Chart. The U contour is a M-circle that has the magnitude of M_m, with part of the circle stretched for uncertainty at high frequencies. By having the open-loop frequency response not penetrate the U contour, the system's damping will be guaranteed no less than the damping selected for M_m as a design constraint.

For inner-loop transfer functions $G^{\gamma}_{\theta_{in}}$ and $G^{\phi}_{\beta_{in}}$, the parameter variation given by the four configurations can be expressed minimums and maximums. There are tradeoffs between plant parameter variations and performance. The wider the parameter variation, the more restricted the constraints; consequently, more compensation is required. In this application, due to the engine response limits, the performance specification will have to be relaxed because there is not enough control power to provide all the compensation that is required to meet specifications.

The minimum and maximum values of transfer functions, $G^{\gamma}_{\theta_{in}}$ and $G^{\phi}_{\beta_{in}}$, form the uncertainty template. The QFT control package [11] allows the designer to input maximum and minimum plant parameter variations, but due to the software's limitation of handling the quantity of uncertainties, some of them were averaged. These variations are listed in Figures 3 and 4.

The $G^{\gamma(deg)}_{\theta_{in}(deg)}$ of the nominal configuration(config. 1) is:

$$G^{\gamma(deg)}_{\theta_{in}(deg)}\ \text{config. 1} = \frac{.01(.203)[.37,\ 3.01]}{(.562)\,[.624,\ .111]\,[.441,\ 1.57]\,(5.25)}$$

and the min. and max. $G^{\gamma(deg)}_{\theta_{in}(deg)}$ are:

$$G^{\gamma(deg)}_{\theta_{in}(deg)}\ \text{min.} = \frac{.0053\ (.162)\,[.35\ ,\ 3.01]}{(.40)\,[.42\ ,\ 1.48]\,[.66\ ,\ .01]\,(5.19)}$$

$$G^{\gamma(deg)}_{\theta_{in}(deg)}\ \text{max.} = \frac{.01\ \ (.28)\,[.46,\ 3.43]}{(.58)\,[.45\ ,\ 1.57]\,[.92\ ,\ .14]\,(5.24)}$$

Figure 3. Longitudinal Mode Parameter Variation

The $G^{\phi(deg)}_{\beta_{in}(deg)}$ of the nominal configuration(config. 1) is:

$$G^{\phi(deg)}_{\beta_{in}(deg)}\ \text{nominal} = \frac{.09\,[.47\ ,\ 3.65]}{(.98)\,[.81\ ,\ .15]\,[.26\ ,\ 1.07]\,(5.02)}$$

and the min. and max. of $G^{\phi(deg)}_{\beta_{in}(deg)}$ are:

$$G^{\phi(deg)}_{\beta_{in}(deg)}\ \text{min.} = \frac{.06\,[.45\ ,\ 3.65]}{(.98)\,[.60\ ,\ .15]\,[.24\ ,\ .93]\,(5.01)}$$

$$G^{\phi(deg)}_{\beta_{in}(deg)}\ \text{max.} = \frac{.09\,[.61\ ,\ 4.33]}{(1.03)\,[1.0\ ,\ .20]\,[.29\ ,\ 1.09]\,(5.02)}$$

Figure 4 Lateral Mode Parameter Variation

Controller Design Technique

Poles/zeros/gain compensation will be required to reshape the open- loop transfer functions from $G^{\gamma}_{\theta_{in}}$ and $G^{\phi}_{\beta_{in}}$. On the Nichols Chart, gain raises the transfer function curve, a zero bends the curve to the right, and a pole bends the curve to the left. The compensation selected forms the controller, G_c. $G^{\gamma}_{\theta_{in}}$ and $G^{\phi}_{\beta_{in}}$ after reshaping, become respectively $L^{\gamma}_{e\gamma}$ and $L^{\phi}_{e\phi}$, the open-loop transfer functions of the flight path angle and bank angle feedback loops, where $L^{\gamma}_{e\gamma} = G^{\theta_{in}}_{e\gamma} * G^{\gamma}_{\theta_{in}}$ and $L^{\phi}_{e\phi} = G^{\beta_{in}}_{e\phi} * G^{\phi}_{\beta_{in}}$. $L^{\gamma}_{e\gamma}$ and $L^{\phi}_{e\phi}$ should be kept on and above the Bo($j\omega_i$), for each frequency, ω_i, on $L^{\gamma}_{e\gamma}$ and $L^{\phi}_{e\phi}$ to assure robust performance. $L^{\gamma}_{e\gamma}$ and $L^{\phi}_{e\phi}$ must also not penetrate the U contour in order to obtain the desired damping. In this application the additional constraint existed which required the controller to be physically realizable (zeros not outnumbering poles).

Longitudinal Flight Path Angle Controller

Transfer function $G^{\gamma}_{\theta_{in}}$ and its performance bounds, Bo($j\omega_i$), and U contour are displayed on a Nichols Chart in Figure 5. Since all the frequency points for $G^{\gamma}_{\theta_{in}}$ are below their corresponding Bo($j\omega_i$).reshaping is required. Pure gain compensation first raises the curve until it touches the U contour as shown in Figure 6($G^{\theta_{in}}_{\gamma}$ =16). Compensation is then added to avoid the U contour while satisfying all the Bo($j\omega_i$) constraints. Note that no realizable poles/zero compensation could be found to do this. A zero at .1 rad/sec, for example, pulls the whole $G^{\gamma}_{\theta_{in}}$ curve to the right of the U contour. But then a pole at any location would make the $G^{\gamma}_{\theta_{in}}$ curve penetrate the U contour. Since a compensator with only one zero is physically ununrealizable for this application, the compensator, G_c, for the flight path angle feedback loop, $G^{\theta_{in}}_{e_\gamma}$, is a pure gain of 16. The performance bound, hence the system robustness, was left unsatisfied.

The frequency response of the close-loop transfer function, $T^{\gamma}_{\gamma_{in}}$, where

$$T^{\gamma}_{\gamma_{in}} = L^{\gamma}_{e\gamma} / (1 + L^{\gamma}_{e\gamma}) = (G^{\theta_{in}}_{e\gamma} * G^{\gamma}_{\theta_{in}}) / (1 + G^{\theta_{in}}_{e\gamma} * G^{\gamma}_{\theta_{in}})$$

is shown in Figure 7. It can be seen in Figure 7 that δ_T, the spread between T_{max} and T_{min}, has exceeded the δ_R over the frequency range .1 to .7 rad/sec. This is because $L^{\gamma}_{e\gamma}$ did not satisfy the performance bounds over that frequency range. The frequency plot of the close-loop response after adding a prefilter is shown in Figure 8. A pure gain prefilter of 6 proved most effective in increasing the bandwidth and in meeting the prescribed specification.

Lateral Bank Angle Controller

Transfer function $G^{\phi}_{\beta_{in}}$ and its performance bounds, Bo($j\omega_i$), and U contour were similarly analyzed on a Nichols Chart. $G^{\phi}_{\beta_{in}}$ was not only below all the Bo($j\omega_i$) but also penetrated the U contour. A controller, $G^{\beta_{in}}_{e\phi}$ =(s+.15)/(s+1.5), was added to $G^{\phi}_{\beta_{in}}$ to reshape it. $L^{\phi}_{e\phi}$ is shown on a Nichols Chart in Figure 9 and the frequency plot of the close-loop transfer function, $T^{\phi}_{\phi_{in}}$, where $T^{\phi}_{\phi_{in}} = L^{\phi}_{e\phi} / (1 + L^{\phi}_{e\phi}) = (G^{\beta_{in}}_{e\phi} * G^{\phi}_{\beta_{in}}) / (G^{\beta_{in}}_{e\phi} * G^{\phi}_{\beta_{in}})$, is shown in Figure 10 which shows the close-loop frequency response of $T^{\phi}_{\phi_{in}}$ after reshaping but with no prefilter applied yet. Sufficient gain is available here. A lead compensator of (S+1)/(S+2) is added to haunch up the severely deteriorated curve at frequencies over 1 rad/sec, and a lag compensator of (S+.25)/(S+.15) is added to steeper the gain curve at low frequencies to provide a smoother k/s curve for good pilot handling qualities. The close-loop response after adding the prefilter is similar to Figure 8, The prefilter selected is 15(S+.25)(S+1)/((S+.15)(S+2)).

Results and Discussion

For bank angle control using only the throttles, β feedback was found effective in increasing Dutch-roll damping. Bank angle feedback is crucial to lateral phugoid damping. Yaw rate feedback, on the other hand, increases Dutch-roll damping very little and actually decreases the lateral phugoid damping. Tables 4 and 5 compare the dynamic modes of the bare airframe with those from the augmented control implemented in a previous simulation study (References 1 and 2), and with those from the QFT implementation.

Table 3. Longitudinal Mode Comparison

	Density	Phugoid	Short Period	Engine	Pre-Filter	$G^{\theta_{in}}_{e_\gamma}$	$G^{\delta_{T_c}}_{e_\theta}$	K_γ	K_q
Bare Airframe	(1.4E-6)	(.04,.13)	(.65,1.4)	(.55)(5.2)	*	*	*	*	*
Simulation Augmented Control	(4.7E-6)	(.52,.24)	(.52,1.5)	(.4)(5.2)	10	1	10	1	4
QFT Augmented Control	(3.4E-6)	(.62,.32)	(.46,1.6)	(.3)(5.2)	6	16	1	1	60

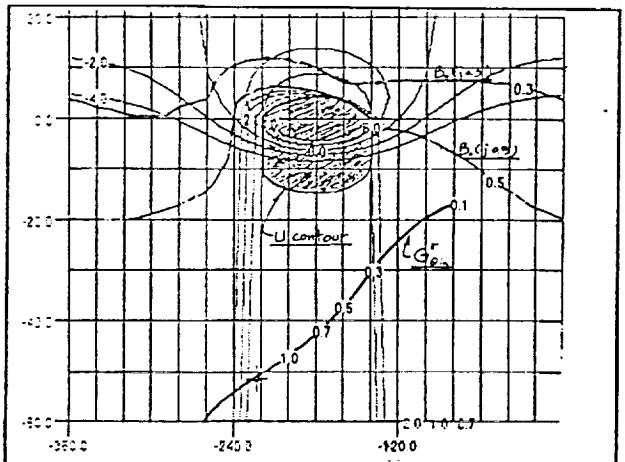

Figure 5.Transfer function $G^{\gamma}_{\theta_{in}}$, its performance bounds B(jw), and U contour on Nichols Chart

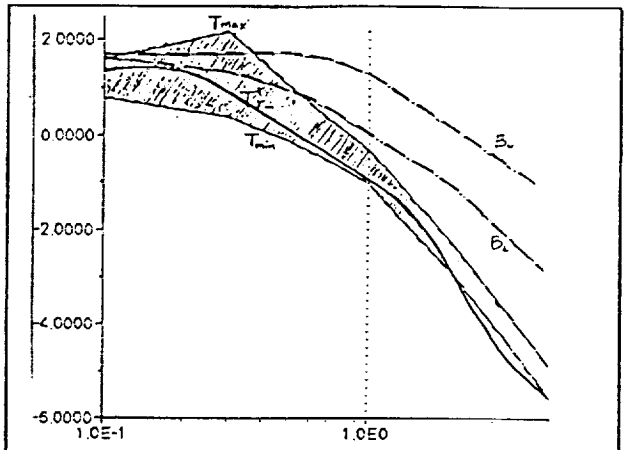

Figure 8. Frequency plot of the close-loop transfer function $T^{\gamma}_{\gamma_{in}}$ with prefilter

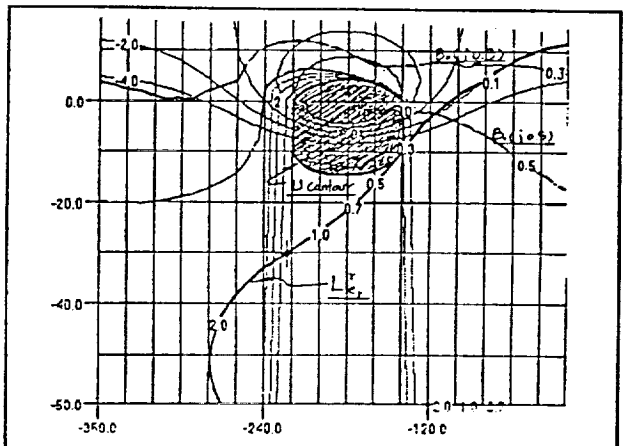

Figure 6. Open-loop transfer function, $L^{\gamma}_{\theta_{in}}$

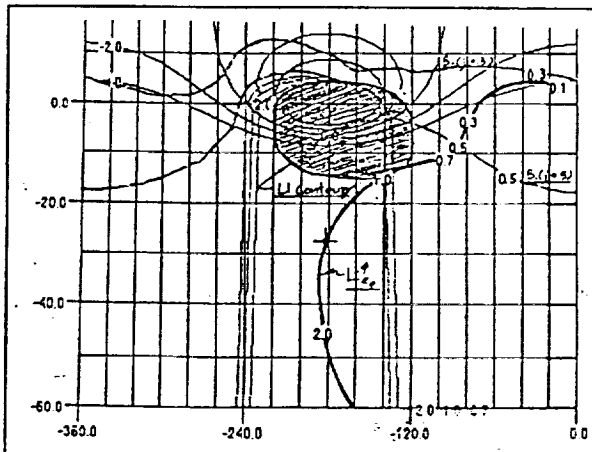

Figure 9. Open-loop transfer function, $L^{\phi}_{e\phi}$, on Nichols Chart

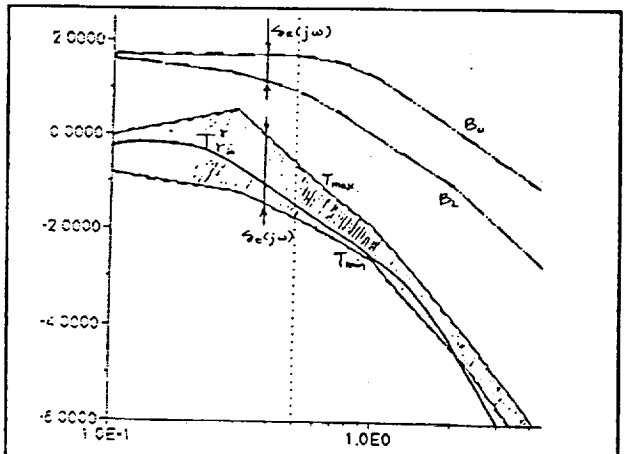

Figure 7. Frequency plot of the close-loop transfer function $T^{\gamma}_{\gamma_{in}}$ with no prefilter

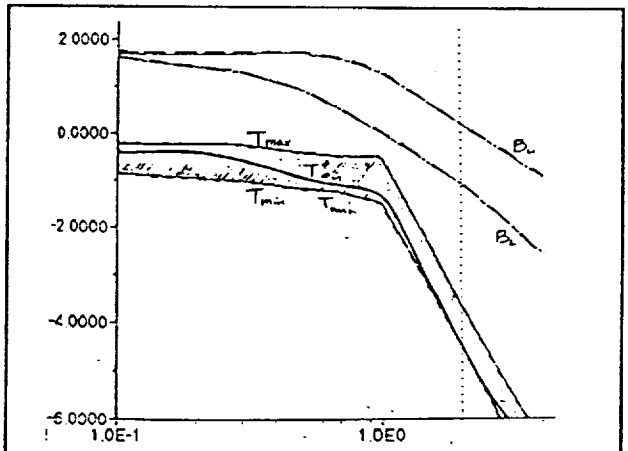

Figure 10. Frequency plot of the close-loop transfer function $T^{\phi}_{\phi_{in}}$ with no prefilter

Table 4 Lateral Mode Comparison

	Spiral	Dutch Roll	Roll	Engine	Pre-Filter	$G_{e_\phi}^{\beta}$	$G_{e_\beta}^{\delta_r}$	K_ϕ	K_β	K_p
Bare Airframe	(1.1E-4)	(.12,.99)	(1)	(.55)(5)	*	*	*	*	*	*
Simulation Augmented Control	(.73,.35)	(.15,.99)	(1)	(5)	40	1	1	.5	1	.5
QFT Augmented Control	(.39)	(.29,1.0)	(1.5)	(.45)(5)	$\frac{2.5(.25)}{(1.25)}$	1	1	$\frac{(.15)}{(1.5)}$	4	*

For longitudinal control, pure gain compensation was used. The short period mode has a frequency near 1.5 rad/sec, which is beyond the frequency that the throttles can control. Therefore, the primary concern was to increase phugoid damping and frequency. The short period damping decreased from .52 to .46 rad/sec while the phugoid damping and frequency increased from .52 to .62 and from .24 rad/sec to .32 rad/sec, respectively. This increase of response frequency can also be easily seen on the flight path angle response (not shown here).

For lateral control where pole/zero compensation was used, the Dutch-roll damping was almost doubled, from .15 to .29. The "simulation augmented controller" caused a lateral phugoid mode, [.73, .35], which combines the spiral and the slow engine mode. The QFT controller eliminated the lateral phugoid mode and resulted in higher damping for the Dutch roll mode (0.29 versus 0.15).

Turbulence Response

The response of the QFT flight path controller under intermediate turbulence was excellent. Since gusts were input, more than one simulation run was made to examine the tracking integrity under turbulence. Both controllers performed well, but the lateral QFT controller showed undue sensitivity to $K\beta$ during bank angle tracking.

During investigation of the bank angle tracking problem, it was found that the β being feedback in the simulation was the β at the c.g. instead of at the nose boom. The nose boom β was then modeled into the B-720 simulator, which improved the bank angle tracking under turbulence. The β at the nose boom has two extra terms, one a function of roll rate, the other a function of yaw rate. It was thought that the extra yaw rate term might have stabilized the bank angle tracking (the roll rate term was too small and was neglected.)

System response to configuration variations, for flight path control and for bank angle control, was very good. The robustness of the flight path control was improved by QFT. The Dutch-roll oscillation in the original simulation compensation was taken out by QFT compensation; however, the tracking did not improve.

Conclusions and Recommendations

For throttles-only pitch control using a QFT controller, the control bandwidth , tracking and control robustness were improved by QFT. For bank angle control, QFT has improved the Dutch-roll oscillation problem and performed well under no turbulence. However, the lateral phugoid tracking under intermediate turbulence did not perform well. Apparently a compromise is required between Dutch-roll and lateral phugoid mode damping. Further investigation is recommended for bank angle tracking under turbulence. The impact of system non-linearities, such as rate and thrust limits, was significant and resulted in a decrease in the bandwidth specification used in the QFT analysis.

Acknowledgment

This work was made possible by NASA Grant NCC 2-711. Thanks also goes to Mr. Glen Gilyard , Mr. Bill Burcham , and Jeanette Le at NASA Dryden for their technical support and guidance.

References

1. Burcham, F., Fullerton G., Gilyard, G., Conley, J. and J. Stewart, "A Preliminary Investigation of the Use of Throttles for Emergency Flight Control," NASA T.M. 4320, 1991.

2. Gilyard, G.B., Conley, J.L., Le, J., and F.W. Burcham, "A Simulation Evaluation of a Four-Engine Jet Transport Using Engine Thrust Modulation for Flight Path Control," AIAA-91-2223, 27th Joint Propulsion Conference, June 24-26, 1991, Sacramento, CA.

3. Azzano, C.P., "A Preliminary Look at Optimal Multi-Variable Design of Propulsion-Only Flight Controllers for Jet Transport Aircraft," NASA Dryden TR, Sept 21, 1990.

4. Biezad, D.J., "The Propulsive-Only Flight Control Problem," NAECON , Vol 2, pp494-500, Dayton, Ohio, May 20-24, 1991.

5. Biezad, D.J. and C.P. Azzano, "Designing Low Bandwidth Propulsive-Only Flight Controllers", AIAA Guidance, Navigation, and Control Conference, Paper #91-2628CP, pp 267-275, August 12-14, 1991, New Orleans, La.

6. Chou, Hwei-Lan and D.J. Biezad, "Pilot-in-the-Loop Analysis of Propulsive-Only Flight Control Systems," National Aerospace Electronics Conference, Vol. 2, pp 482-488, Dayton, Ohio, May 1822, 1992.

7. Horowitz,I. M. ,and Sidi,M., "Synthesis of feedback systems with large plant ignorance for prescribed time-domain tolerances" Int. J. Control, Vol.16, pp.287-309, 1972.

8. Chou, H.L., "Low Bandwidth Robust Controllers for Flight," Master's Thesis, Cal Poly State University, 1993.

9. Sarrafian, S.K., and Powers, B.G., "Application of Frequency Domain Handling Qualiities Criteria to the Longitudinal Landing Task." NASA Technical Memorandum, Aug. 1985.

10 MIL-STD-1797A, "Flying Qualities of Piloted Vehicles", limited distribution, ASD/ENES, Wright-Patterson AFB, Ohio, 30 Jan 1990.

11. Yaniv, O., "Multiple-input single-output (MISO) User Manual, Tel-Aviv University, 1991.

Appendix

Longitudinal Transfer Functions:

$$G^{q(\mathrm{deg/sec})}_{z(\mathrm{lbs})} = N^{q(\mathrm{deg/sec})}_{z(\mathrm{lbs})} / \Delta_{long}$$

$$G^{\gamma(\mathrm{deg})}_{z(\mathrm{lbs})} = N^{\gamma(\mathrm{deg})}_{z(\mathrm{lbs})} / \Delta_{long}$$

$$N^{q(\mathrm{deg/sec})}_{z(\mathrm{lbs})} = \begin{array}{|cccc|} \hline 2.36E-04 & (0) & (-1.17E-05) & (0.0) \quad (0.61) \\ 2.33E-04 & (0) & (1.4E-06) & (0.635, \ 0.563) \\ 1.976E-04 & (0) & (0.292) & (0.644) \\ 1.955E-04 & (0) & (2.68E-06) & (0.819, \ 0.508) \\ \hline \end{array}$$

$$N^{\gamma(\mathrm{deg})}_{z(\mathrm{lbs})} = \begin{array}{|cccc|} \hline 2.796E-05 & (0) & (0.203) & (0.370, \ 3.008) \\ -1.819E-05 & (0) & (0.364) & (2.255) \quad (-4.452) \\ 2.130E-05 & (0.167) & (0.351, & 3.038) \\ 1.470E-05 & (0) & (0.261) & (0.460, \ 3.426) \\ \hline \end{array}$$

$$\Delta_{long} = \begin{array}{|cccc|} \hline (1.438E-05) & (3.918E-02, & 0.130) & (0.652, \ 1.382) \\ (1.101E-05) & (7.423E-02, & 0.147) & (0.596, \ 1.375) \\ (3.949E-02, & 0.118) & (0.649, & 1.301) \\ (1.878E-05) & (7.190E-02, & 0.138) & (0.588, \ 1.279) \\ \hline \end{array}$$

Lateral Transfer Functions:

$$G^{\beta(\mathrm{deg})}_{z(\mathrm{lbs})} = N^{\beta(\mathrm{deg})}_{z(\mathrm{lbs})} / \Delta_{lat}$$

$$G^{\phi(\mathrm{deg})}_{z(\mathrm{lbs})} = N^{\phi(\mathrm{deg})}_{z(\mathrm{lbs})} / \Delta_{lat}$$

$$N^{\beta(\mathrm{deg})}_{z(\mathrm{lbs})} = \begin{array}{|ccc|} \hline -1.58E-03 & (-.0805) & (.927) \\ -1.59E-03 & (-.0922) & (.904) \\ -1.43E-03 & (-.0723) & (.981) \\ -1.44E-03 & (-.0879) & (.940) \\ \hline \end{array}$$

$$N^{\phi(\mathrm{deg})}_{z(\mathrm{lbs})} = \begin{array}{|cc|} \hline 3.19E-04 & (.468, \ 3.65) \\ 2.15E-04 & (.611, \ 4.17) \\ 2.89E-04 & (.447, \ 3.96) \\ 2.04E-04 & (.593, \ 4.33) \\ \hline \end{array}$$

$$\Delta_{lat} = \begin{array}{|cccc|} \hline (.0001) & (1.01) & (.116, & 1.05) \\ (.006) & (1.05) & (.067, & 0.93) \\ (.0028) & (1.06) & (.114, & 1.08) \\ (.0065) & (1.09) & (.060, & .944) \\ \hline \end{array}$$